St. John's University

St. John's Scholar

2020

aGAL ANTIGEN AND RUTINOSE GLYCOSIDES AS MODEL COMPOUNDS FOR THE DESIGN OF CLASSICAL AND CONFORMATIONAL GLYCOMIMETICS

Dhwani Ashish Mehta

αGAL ANTIGEN AND RUTINOSE GLYCOSIDES AS MODEL COMPOUNDS FOR THE DESIGN OF CLASSICAL AND CONFORMATIONAL GLYCOMIMETICS

A thesis submitted in partial fulfillment

of the requirements for the degree of

MASTER OF SCIENCE

to the faculty of the

DEPARTMENT OF GRADUATE DIVISION

of

COLLEGE OF PHARMACY AND HEALTH SCIENCES

at

ST. JOHN'S UNIVERSITY

New York

by

Dhwani Ashish Mehta

Date Submitted _____   Date Approved _____

_____   _____
Dhwani Ashish Mehta   Dr. Carlos Sanhueza Chavez

ABSTRACT

αGAL ANTIGEN AND RUTINOSE GLYCOSIDES AS MODEL COMPOUNDS FOR THE DESIGN OF CLASSICAL AND CONFORMATIONAL GLYCOMIMETICS

Dhwani Mehta

αGal or Galili epitope (αGal(1→3)βGal(1→4)GlcNAc) is a natural trisaccharide associated with cell-surface glycoproteins of certain mammalian and non-mammalian cells. The saccharide is not expressed by humans and anti-αGal antibodies account for ~1% of the total circulating antibodies in sera as a result of our constant exposition to the antigen from food and intestinal flora. Our interest in αGal relies on its involvement in a variety of pathologies including red meat allergy, hyperacute xenotransplant rejection, and parasitic and bacterial infections. In particular, we have an interest in developing structurally simple glycomimetics for engaging in high-affinity binding αGal-recognizing receptors such as the human anti-αGal IgG antibody and the *Clostridium difficile toxins* TcdA and TcdB in order to develop αGal based vaccine adjuvants and novel anti-infective therapies respectively. This communication presents our progress towards the synthesis of fluorinated αGal analogues as glycomimetics for their further applications to these goals. Apart from the role of carbohydrates in immune response, energy storage and as structural building blocks they are also involved in various other biological activities and many processes including cell-cell communication, immune response, fertilization, protein recycling, infection, among many others. The success of protein-carbohydrate interactions is conditioned to the fulfillment of conformational requirements imposed by

the recognition site in the protein over the, inherently flexible, carbohydrate ligand. Hence, the study of the conformational preferences of saccharides is fundamental for the understanding of protein-carbohydrate interactions. In the second half of this thesis, we describe the results of the conformational study of rutinose (αRha(1$\rightarrow$6)βGlcOR) glycosides. In particular, we centered our study on how the nature of the aglycone substituent can modulate the conformational equilibria around the interglycosidic linkage. Given the inherent flexibility of the (1$\rightarrow$6) linkage, the hydrophobic nature of the rhamnose moiety, and the simplicity of the NMR spectra, rutinose constitutes a convenient model saccharide for performing these studies. The spectroscopic evidence gathered suggest the existence of an effect that could be used in the rational design of *conformational mimetics* of bioactive carbohydrates.

ACKNOWLEDGEMENT

TABLE OF CONTENTS

LIST OF TABLES

LIST OF FIGURES

LIST OF SYNTHETIC SCHEMES

ABBREVIATIONS

$(CH3)_2C(OCH3)_2$	2,2-Dimethoxypropane
$(EtO)_3CCH_3$	1,1,1-triethoxyethane
$(Ph)_3CCl$	Triphenylmethyl chloride
Ac_2O	Acetic Anhydride
ACN	Acetonitrile
AcOH	Acetic Acid
APC	Antigen Presenting Cell
BF_3Et_2O	Boron Trifluoride etherate
BnBr	Benzyl Bromide
BnOH	Benzyl Alcohol
BzCl	Benzoyl Chloride
CbzCl	Benzyl Chloroformate
$CDCl_3$	Chloroform-d
COSY	Correlated spectroscopy
CSA	Camphor Sulfonic acid
DAST	Diammonium sulfur trifluoride
DBU	1,8-Diazabicyclo[5.4.0]undec-7-ene
DCM	Dichloromethane
DMF	N,N-Dimethylformamide
Et_2O	Diethyl ether

Et$_3$SiH	Triethylsilane
EtOAc	Ethyl acetate
g	Gram
Gal	Galactose
gg	gauche-gauche
Glc	Glucose
GlcNAc	Glucose-N-acetylamine
gt	gauche-trans
HSQC	Heteronuclear single quantum correlation
IgE	Immunoglubulin E
IgG	Immunoglubulin G
IgM	Immunoglobulin M
K$_2$CO$_3$	Potassium Carbonate
Kd	Dissociation Constant
M^{-1}	Per mole
MeCN	Acetonitrile
MeOD	Methanol-d
MeOH	Methanol
mg	Milli gram
MHC	Major Histocompatibility Complex
mL	Milli Litre

mmol	Milli mole
MsCl	Mesyl Chloride
$NaBH_4$	Sodium Borohydride
NaF	Sodium Fluoride
NaH	Sodium Hydride
$NaHCO_3$	Sodium Bicarbonate
NaOMe	Sodium Methoxide
NH_2NH_2	Hydrazine
NIS	N-iodo succinimide
NOESY	Nuclear Overhauser effect Spectroscopy
Pd	Palladium
$PhC(OMe)_2$	Benzaldehyde dimethyl acetal
PhCHO	Benzaldehyde
Py	Pyridine
Rha	Rhamnose
rt	Room temperature
TBAF	Tert-butyl ammonium Fluoride
TcdA	Clostridium difficile Toxin A
TcdB	Clostridium difficile Toxin B
Tf_2O	Triflic anhydride
TFA	Trifluoro acetic acid

tg	Trans-gauche
TLC	Thin Layer Chromatography
TMSOTf	Trimethylsilyl methanesulfonylanhydride
TolSH	Tolylmercaptan
μL	Micro Litre

CHAPTER 1

SYNTHESIS OF αGAL GLYCOMIMETICS FOR APPLICATIONS IN IMMUNOLOGY AND ANTI-INFECTIVE THERAPIES

1. INTRODUCTION

1.1.   Biological roles of carbohydrates and their potential in biomedicine

Carbohydrates are complex molecules which are ubiquitous in all living systems. The biological function of saccharides is vast, and it is not restricted to their classical roles of energy storage and structural units. The structural complexity of carbohydrates confers them a unique capacity to codify biological information. In fact, the molecular recognition of sugars by protein receptors is a key step in many biological processes including cell-cell communication, pathogenesis, immune response, cell differentiation, modulation of protein and lipid function, among many others.[1] Carbohydrates are structurally diverse polymers giving a large number of isomers for a given sequence. Compared with peptides composed by equal number of monomers, there are more combinations possible for sugars given the polyfunctional nature of the respective monomers. While the structure of peptide polymers is restricted to linear architectures, with amide bond formation limited to α-amine and the carboxylic acid, saccharides can generate linear and branched polymers containing glycosidic bonds that can be presented in several configurations. The higher structural diversity that can be found in carbohydrate polymers arises from the

possibility to make glycosidic bonds with at least three different hydroxyl groups; the creation of a new stereogenic center that can generate two types of anomers; and, in the case of pentoses and hexoses, the possibility to form pyranose and furanose rings. In addition, oligosaccharides are typically more flexible than proteins and peptides and can generate several conformational families adding more complexity to their solution structures.[2]

Glycans associated with cell surface glycoconjugates are typically recognized by protein receptors leading the initiation of biological functions.[3] Among the processes that include protein-carbohydrate interactions as part of the signaling cascade are cell adhesion, as in the case of white cell recruitment in inflammation; the physical stabilization of tissue interfaces, as in the case of dystroglycan and muscular integrity; the initiation of infection, as in the case of viral and bacterial toxin fusion with cell membranes; etc. During the last decades, an increasing interest in obtaining pure and structurally well-defined glycans has gained significance in the biological sciences and has stimulated the search for effective and high-yielding synthetic methods for preparing complex glycans and enabling the study of carbohydrate function. The success of these efforts is testified by the birth of a new paradigm about the function of glycans where these biomolecules are regarded as molecular codifiers of biological information, a paradigm also known as the *glycocode*.[3]

1.2.   Carbohydrate antigens

An area of special interest is the study of the role of glycans in immune response. The surface of most prokaryotic and eukaryotic cells is heavily decorated with a *glycocalyx*

made primarily of protein- and lipid-conjugated glycans in addition to polysaccharides.[4] The structure of these glycans are part of the *molecular signature* of organisms such as bacteria, archaea, protozoa. Strain classifications are normally based on the structure of the glycocalyx. This dense superficial layer of carbohydrates, constitute a first line of recognition that is involved in innate and adaptive immune responses.[5] Compared with proteins, carbohydrate antigens are more difficult to obtain in the laboratory since the structure of glycans is not encoded directly in the genome and their isolation from cells is, in general, a tedious and cost-ineffective process.[6] Hence, the need for efficient synthetic methods aimed to prepare complex carbohydrate antigens is imperative for advancing in the study of carbohydrate immunology and for the future development of carbohydrate-based immunotherapies. The structural complexity of carbohydrate antigens, and glycans in general, represents an appealing challenge to the synthetic chemist. Currently, synthetic methodology for preparing any existing glycosidic linkage is available, however, there is still a need for cost-effective methods with the potential to generate bioactive glycans on a mass scale. This problem does not seem to be easily addressable given the inherent relationship between structural complexity and synthetic cost. An attractive alternative towards this objective is the design of structurally simple glycomimetics capable to elicit the same, or equivalent, function of complex glycans. In the case of antigens, a glycomimetic should be capable to elicit cross-reactive antibodies directed to more complex carbohydrate antigens.[7]

1.3. α-Gal or *Galili epitope*

A remarkable carbohydrate antigen is αGal, also known as the Galili epitope. αGal is found associated with cell surface glycoconjugates of various protozoal parasites such as *Trypanosoma cruzi* (Chagas disease)[8-10], *Plasmodium falciparum* (Malaria),[11] and *Leishmania spp*. (Leishmaniasis),[8, 12] and various bacterial species including pathogenic *Mycobacterium tuberculosis* (Tuberculosis),[13] and *Clostridium difficile* (diarrhea and colitis). In addition, recent findings has connected the αGal antigen with tick-bite associated red meat allergy where exposure to αGal glycoconjugates from tick bites[9, 14] elicit hypersensitization to this antigen resulting in allergy to the consumption of red meat products. This condition has recently been renamed as αGal syndrome.

αGal or *Galili epitope*, a name given to both the Gal-α-1,3-Gal disaccharide and Gal-α-1,3-Gal-β−1,4-GlcNAc trisaccharide[12], is a naturally occurring carbohydrate and it is associated with cell-surface glycoproteins of certain mammalian and non-mammalian cells.[15, 16] The αGal epitope (Gal-α-1,3-Gal) is a common type-2 terminus glycan abundantly synthesized on lipids and proteins of non-primate mammals and New World monkeys through glycosylation *via* α(1,3)-galactosyl transferase.[17, 18] The epitope is however found to be absent in humans, apes and Old World monkeys.[19] In these organisms the gene encoding for α(1,3)-galactosyl transferase is silenced as a consequence of a hypothetical natural selection event carried out by a viral infection over early hominids.[16, 20, 21] α(1,3)-galactosyl transferase is responsible for catalyzing the α-galactosylation on the position 3 of terminal galactose acceptors. Typical substrates of

this enzyme are glycoproteins and glycolipids ended by lactose (Gal-β-1,4-GlcNAc-R) and *N*-acetyl lactosamine (Gal-β-1,4-GlcNAc-R).[14] The inactivation of the α(1,3)-galactosyl transferase gene in humans, ancestral Old World monkeys and apes is a unique event in mammalian evolution as it was followed by production of large amounts of the natural anti-αGal antibody against the eliminated αGal epitope.[9] Our system is, however, exposed to αGal epitopes from food intake (red meats) and natural bacterial flora. This constant exposure leads to development of immune response against αGal. Structure of some major naturally occurring glycans displaying αGal epitopes is presented in figure 1.1
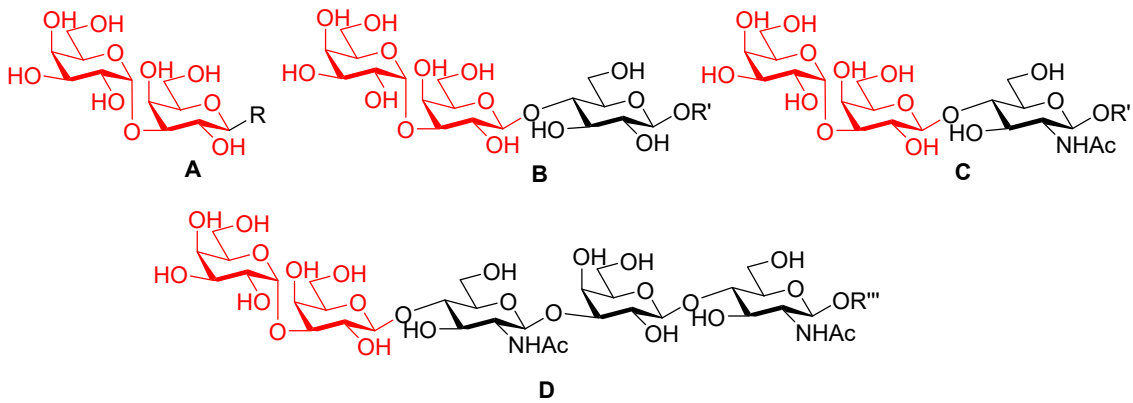
Figure 1.1. Major α gal epitopes: A: αGal disaccharide epitope (Gal-α-1,3-Gal-OR), B: isoglobotriaose (Gal-α-1,3-Galβ1,4-Glc-OR'), C: αGal xenoantigen Gal-α-1,3-Gal-β−1,4-GlcNAc-OR', D: Pentaose Galili antigen (Gal-α-1,3-Gal-β-1,4-GlcNAc-β−1,3-Gal-β−1,4-Glc-OR)

1.4. Anti-αGal Antibody

Normal bacterial flora populating the gastrointestinal tract such as *Escherichia coli*, and bacteria of the genus *Serratia*, *Salmonella*, and *Klebsiella* express surface glycoconjugates displaying αGal. This results in a constant exposure to αGal epitopes leading to a steady production of anti-αGal antibodies by B cells residing in the lymphoid tissue lining the

gastrointestinal tract. Circulating anti-αGal antibody accounts for the most abundant type of immunoglobulin in human blood and [9, 12, 19, 22, 23] about 1% of B cells produce anti-αGal antibodies[17] being IgG, IgM and IgA the predominant isotypes in serum whereas IgA and, to a lesser extent, IgG are the predominating isotypes in human secretions such as colostrum, milk, bile, and saliva. Human anti-αGal antibody is encoded by several heavy-chain genes primarily of the VH3 immunoglobulin gene family.[17, 19] Since the anti-αGal antibody production is constant along lifetime, anti-αGal is an attractive target for studying the immunology of carbohydrate and glycomimetic antigens and can be harnessed for a variety of biomedical applications.[9]

Our interest in αGal lies in the opportunity that this antigen offers for developing carbohydrate-based drugs for a variety of biomedical applications including immunotherapies for allergy and neglected parasitic diseases, and the development of adjuvants for boosting the efficacy of vaccines.

1.5.   Binding site of α-Gal epitope (anti-gal antibody binding pocket)

The epitope recognized by the anti-αGal antibody is the Gal-α-1,3-Gal disaccharide and the binding affinity is dependent on the nature and number of the subsequent saccharides. The affinity of the free trisaccharide Gal-α1,3-Gal-β-1,4-GlcNAc is found to be ~7-fold higher compared with the disaccharide epitope.[17] The inhibition of >80% of anti-αGal antibody is achieved by an αGal-disaccharide concentration of approximately 3.3 mM whereas that of αGal-trisaccharide Gal-α 1,3-Gal-β-1,4-Glc and Gal-α1,3-Gal-β-1,4-GlcNAc-OR' is 1.0 mM. The association affinities of the trisaccharide and disaccharide

were found to be 6×10^6 M^{-1} and 5×10^5 M^{-1} respectively.[24] The recognition of αGal epitopes by anti-αGal antibodies is primarily effected *via* direct polar contacts with hydroxyl groups located in the terminal galactose units (αGal disaccharide epitope) and, to a lesser extent, with polar contacts with hydroxyls situated in the third sugar. Thus, the nature of the antigen recognized by anti-αGal is an αGal-containing trisaccharide fragment.[9, 19]

1.6.   Biomedical relevance of the αGal antigen and the anti-αGal antibody

αGal antigen and the anti-αGal antibody have an outstanding, yet underexplored, potential for developing therapies aimed to modulate immune responses. Since the epitope is expressed in several pathogenic microorganisms, it is an attractive antigen for developing broad-spectrum vaccine candidates by designing constructs that increase the concentration of anti-αGal immunoglobulins with a correlated protective effect. In fact, evidence suggest a correlation between low anti-αGal titers with major susceptibility to infectious diseases produced by αGal expressing pathogens such as tuberculosis and malaria. On the other hand, the elevated titers of anti-αGal antibodies in normal human sera provides the opportunity to develop vaccine adjuvants based on αGal *via* engagement of the circulating anti-αGal IgG and promotion of T helper cell mediated immune response. Furthermore, the involvement of αGal in red meat allergy stimulates the design of small molecule-based therapies for preventing allergic reactions. In the next paragraphs, we describe the potential applications of this unique carbohydrate antigen that we are interested in exploring.

αGal as vaccine adjuvant

The immunogenicity of a vaccine can be increased by including components that promote a stronger immune response. Such components are defined as *adjuvants* and are added to the vaccines as part of the formulation. An alternative strategy for boosting the efficacy of a vaccine by inducing a specific immune mechanism is the targeted delivery of the antigen to antigen-presenting cells (APC), such as dendritic cells and macrophages. Given the high concentration of anti-gal IgG antibody, it is reasonable to hypothesize that antigens tagged with α gal epitopes are susceptible to be recognized by anti-gal IgG and be subsequently endocytosed by APCs[19, 25]
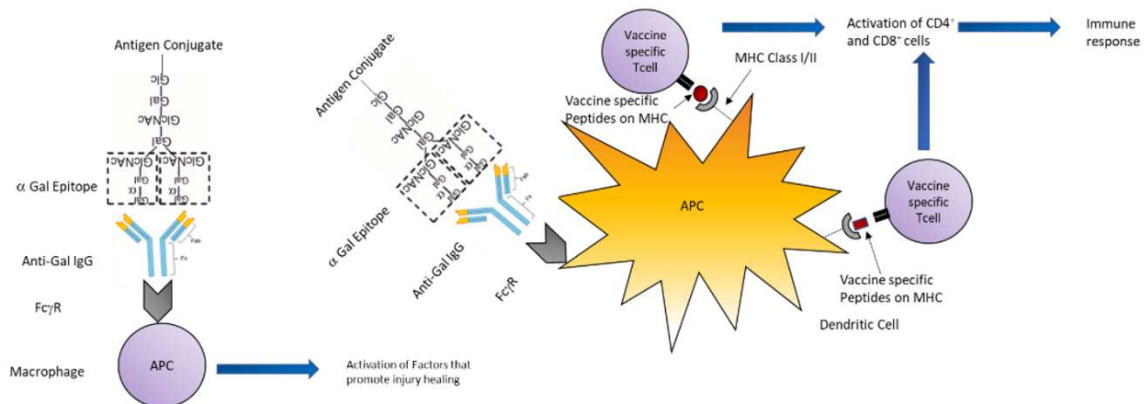
Figure 1.2. Targeting of vaccine candidate to antigen-presenting cell (APC) by the natural anti-Gal antibody.

Figure 1.2 describes the hypothesized antigen-antibody interaction for increasing the efficacy of a vaccine candidate presenting the αGal epitope. Once the vaccine formulation carrying the αGal epitope, or αGal-mimetic, is administered into the system it is presumed to interact with anti-αGal IgG. The antigen-antibody complex so formed, known as immune complex, can be endocytosed by antigen presenting cells for further

presentation of the antigens as major histocompatibility complex-conjugates (MHC).[19] The internalization of the immune complexes by APC is accomplished via interaction between the Fc portion of immune-complexed anti-αGal antibody and Fcγ receptors (FcγR) on the antigen presenting cell. The APC's then migrate to regional lymph nodes where they present the MHC-conjugated antigens.[9] This further leads to activation of specific CD4$^+$ and CD8$^+$ T-cells thus, leading to generation of long memory immune response. Our interest in this area is focused in study the potential use of the αGal antigen as vaccine adjuvant and the discovery of αGal glycomimetics able to elicit the same or equivalent adjuvant effect.

αGal antigen for the development of vaccine candidates against parasitic diseases

αGal epitopes has been found in the cell surface of several human parasites such as *Trypanosoma cruzi* (Chagas disease),[10] *Leishmania spp* (leishmaniasis),[12] *Plasmodium falciparum* (malaria), and evidence suggest its expression in *Mycobacterium tuberculosis* (tuberculosis).[14,26, 13, 27] It has been shown that high levels of anti-αGal IgM and IgG isotypes provides resistance to the acquisition of *Plasmodium falciparum* or *Mycobacterium tuberculosis* infections[11,13] providing the basis for future developments on αGal-based vaccine candidates directed to these pathogens.

anti-αGal antibody mediated 'autoimmune like' phenomena in Chagas disease and Leishmaniasis.

Chagas disease and leishmaniasis are marked by 10–30 fold higher anti-Gal titers compared with uninfected individuals.[9, 10, 12] αGal epitopes are present on the cell surface

of *T. cruzi* and *Leishmania spp.* predominantly as glycoinositolphospholipids and lipophosphoglycans[9] and anti-αGal binding of these epitopes induces complement-mediated lysis of the pathogens contributing to lower parasitemia.[8] However, this protection is not complete and escaping parasites penetrate into various tissues were they are protected. The intracellular parasites continue to produce, and release, αGal-containing glycoconjugates stimulating the immune system to produce anti-αGal antibody which, in turn, interacts with the anti-αGal glycoconjugates concentrated in the tissue. This interaction leads to a localized 'autoimmune-like' inflammatory reactions characterized by the infiltration of macrophages and lymphocytes which results in cardiomyopathy, hepatomegaly, and megacolon, which are characteristic symptoms of acute and chronic Chagas disease and Leishmaniasis.[8, 9]

Hence, we hypothesize that neutralization of circulating anti-αGal can mitigate the chronic inflammation undergone by patients of leishmaniasis and Chagas disease. Such anti-αGal neutralization could be achieved by competitive αGal-based inhibitors.
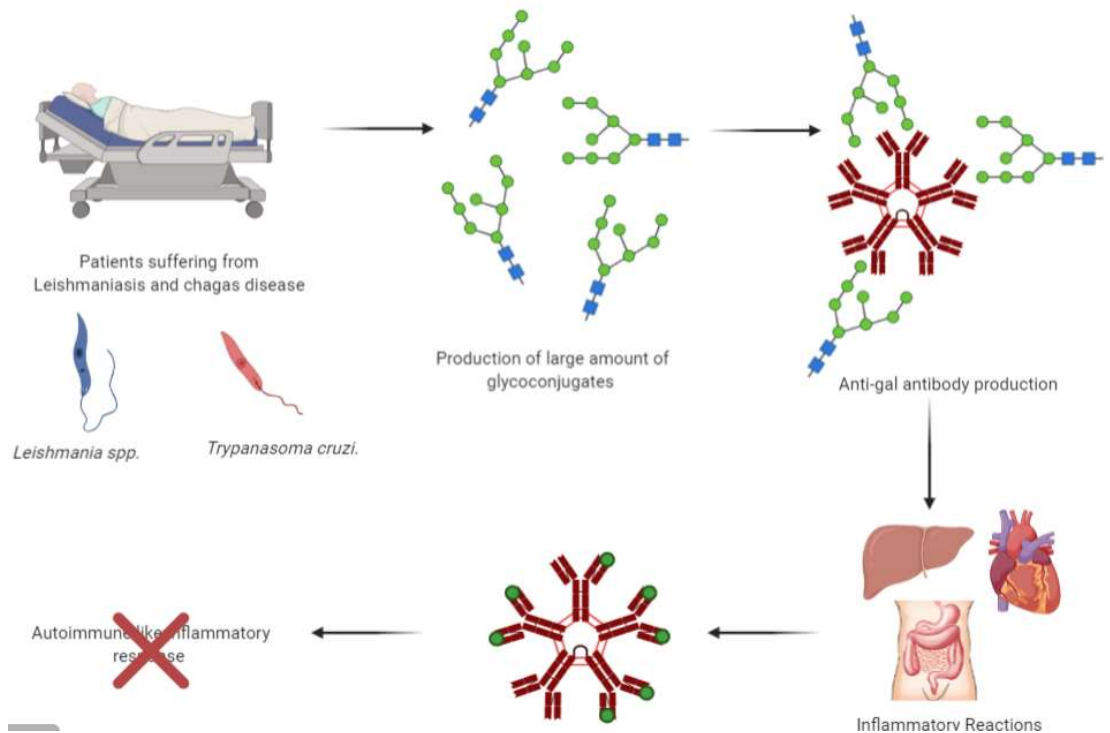
Figure 1.3: Diagrammatic representation of reduction of anti-Gal mediated 'autoimmune like' phenomena in Chagas' disease and Leishmaniasis using αGal epitopes/ αGal epitope mimetics

Red meat allergy and αGal antigen

Red meat allergy is the clinical manifestation of the hypersensitization to αGal as a result of an IgE response to the antigen. The origin of this hypersensitization has been linked to tick bites where the proposed allergen could be a salivary glycoconjugate expressing the epitope. Red meat allergy has been connected with the bites of different tick species around the world. In the US, the lone star tick (A*mblyomma americanum*), the vector that also transmits Lyme disease, is accounted for most of the reported cases. It is hypothesized that exposure to the αGal allergen from ticks induces the isotype switch of anti-αGal IgG to anti-αGal IgE.[28] After a exposure to αGal allergen, anti-αGal IgE develops

and binds to basophils and mast cells generating an "αGal-sensitized" status of the individual. Ingestion of red meat, which is found to contain αGal epitopes, crosslink basophil and mast cell bound anti-αGal IgE triggering cell degranulation and release of histamine cytokines, leukotrienes among other pro-inflammatory components (figure 1.5 A). This results in the [29, 30]
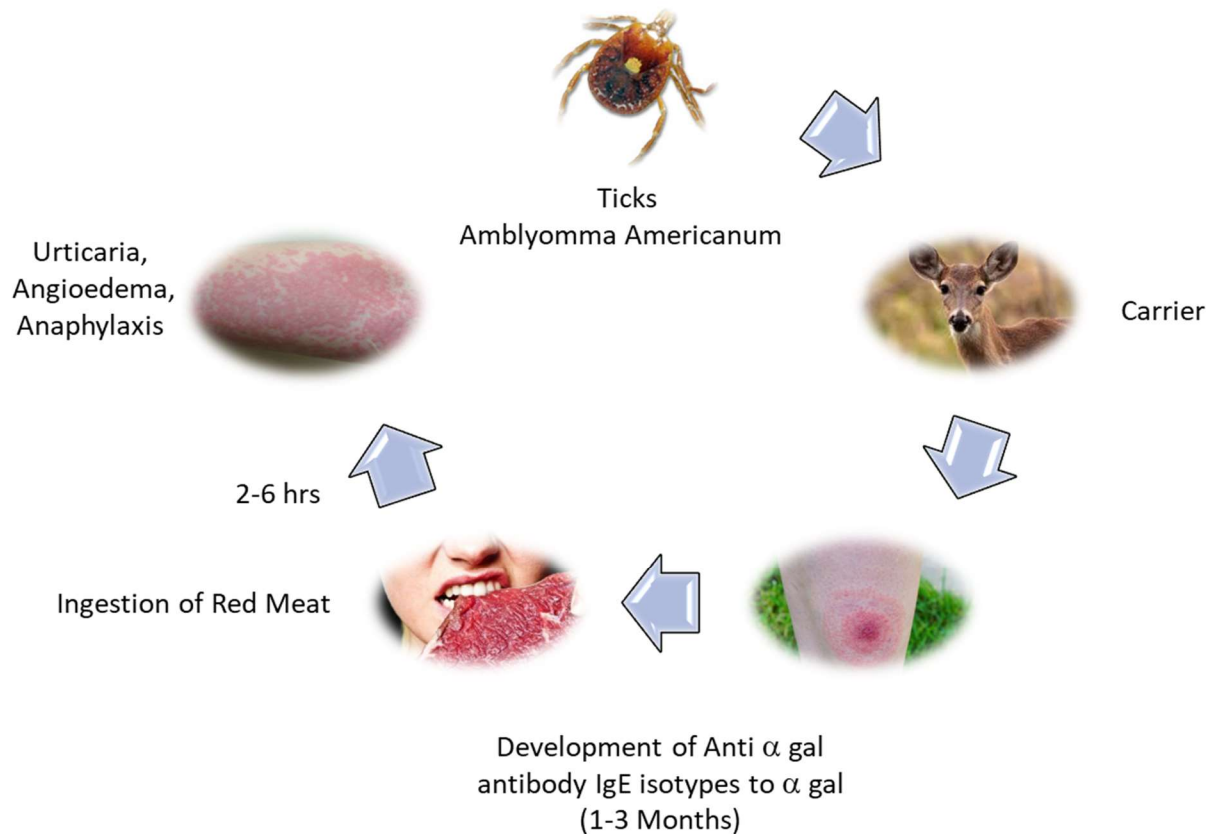
Figure 1.4. Summary of alpha-gal sensitization leading to clinical symptoms of red meat allergy.

Since the allergic reactions are triggered by the cross-linking of basophil or mast cell-bound anti-αGal IgE by the allergen, an opportunity to develop anti-allergy drugs appears by targeting the allergen/IgE interaction (figure 1.5 B). This strategy has proven successful

in *in vitro* and *in vivo* models of peanut and penicillin allergies[31, 32] and we hypothesize that this strategy based on IgE inhibitors can also be effective in preventing allergic reactions in patients with allergy to red meat.
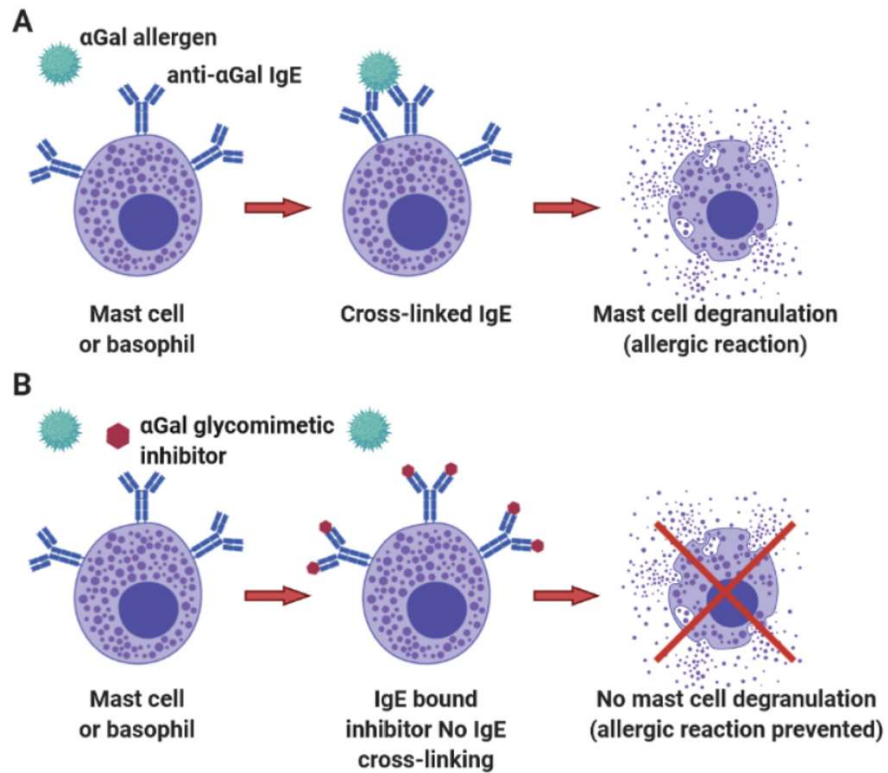
Figure 1.5. Mechanism of IgE-mediated allergic reaction (A) and inhibition of antigen/IgE interaction as a strategy for preventing allergic reactions in αGal sensitized individuals (B).

2. Discussion

The recognition of the αGal epitope by the circulating human anti-αGal IgG antibody has been partially characterized and information related to the structure of αGal and its affinity for the antibody is available. Peng et al.[16] determined the key functional groups in the Gal-α-1,3-Gal-β-1,4-GlcNAc trisaccharide (figure 1.6) that are critical for maintaining the affinity for the antibody, presumably because of the direct contact that these groups make with the receptor. The main structure-affinity relationships reported are summarized below:
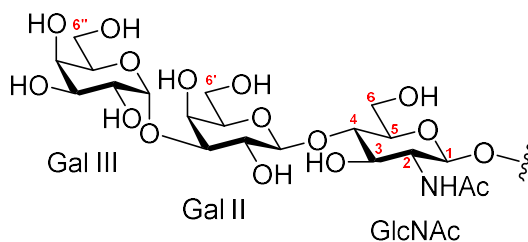
Figure 1.6. Structure of the αGal antigen Gal-α-1,3-Gal-β-1,4-GlcNAc and numbering system for carbohydrates**.** Numbers for the galactose moieties follows the same order that of GlcNAc, however, the distinction is made by adding single or double quotation marks for Gal II and Gal III respectively.

- Gal-$\alpha-$1,3-Gal (Gal(III)–Gal(II)) disaccharide binds with lower affinity than Gal$\alpha-$1,3-Gal-$\beta-$1,4-GlcNAc trisaccharide

- Replacement of GlcNAc by Glc leads to lower affinity

- Elimination of hydroxyl groups over C2, C3 and C4 in terminal galactose (Gal(III)) result in affinity loss

- Elimination of hydroxyl C6 on Gal(III) does not affect anti-αGal binding.

Based on these structure-affinity relationships we have designed αGal mimetic candidates for studying their affinities for the human anti-αGal antibody with the end goal of developing αGal-based immunoadjuvants and anti-αGal antibody inhibitors with applications in red meat allergy and Chagas disease autoimmune-like disorder. In addition, we also plan to evaluate the synthesized ligands as inhibitors of bacterial αGal receptors such as *Clostridium difficile* toxins TcdA and TcdB, as well as in the development of vaccine candidates for parasitic diseases.

Given that the epitope recognized by the antibody is primarily the Gal-α-1,3-Gal moiety of the αGal trisaccharide[28], we aim to prepare derivatives of this disaccharide as primary synthetic targets and perform iterative isosteric modifications for studying the effect over the affinity. We started our research by preparing analogues where hydroxyl groups C4 and C6 groups are replaced with fluorine, a standard hydroxyl isostere. The structure of the proposed αGal mimetics is shown in figure 1.7. The glycomimetic candidates have been designed including an amino functionalized aglycone for their further bioconjugation to protein carriers, in order to generate substrates for immunization studies as well as for allowing the immobilization to sensor chips for performing affinity studies by localized surface plasmon resonance (LSPR).
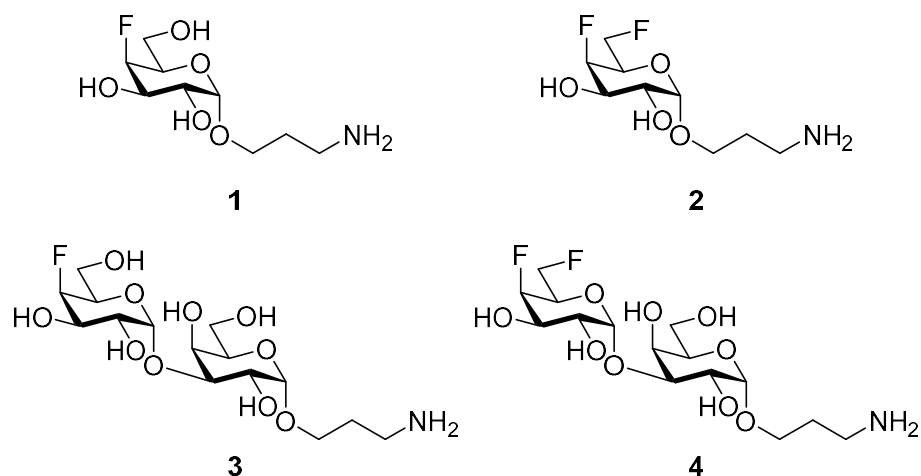
Figure 1.7. Structure of the target fluorinated αGal analogues

Scheme 1.1 and Scheme 1.2 shows the retrosynthetic analysis followed for designing the synthetic route for the target αGal mimetics **1**, **2**, **3** and **4**. A key step for generating the C4 fluoro galactose core is the C4 epimerization of glucose. The C4 fluoro galactose donors **22** and **27** will allow the access to the monosaccharide **1** via coupling with a 3-aminopropanol aglycone and to the disaccharide **3** via coupling with the galactose acceptor **34**.

To prepare C4 and C6 fluorinated analogues of αGal, we should start by defining the route for generating the key C4 fluoro-galactose monosaccharide. The C4 epimerization of glucose via S_N2 substitution of the equatorial hydroxyl is an attractive strategy proven effective by different authors.[33-36] Another aspect to consider is the appropriate selection of protecting groups for directing the stereoselectivity of the glycosylation reactions to be performed using the synthesized donors. Given that the inter-glycosidic configuration of αGal disaccharide is α (the oxygen atom from the acceptor galactose is axially connected to the donor) we should then select non-participating protective groups as

substituent of the C2 hydroxyl. In addition, the selection of the solvent for running the glycosylation reactions should also be made considering the desired stereoselectivity.
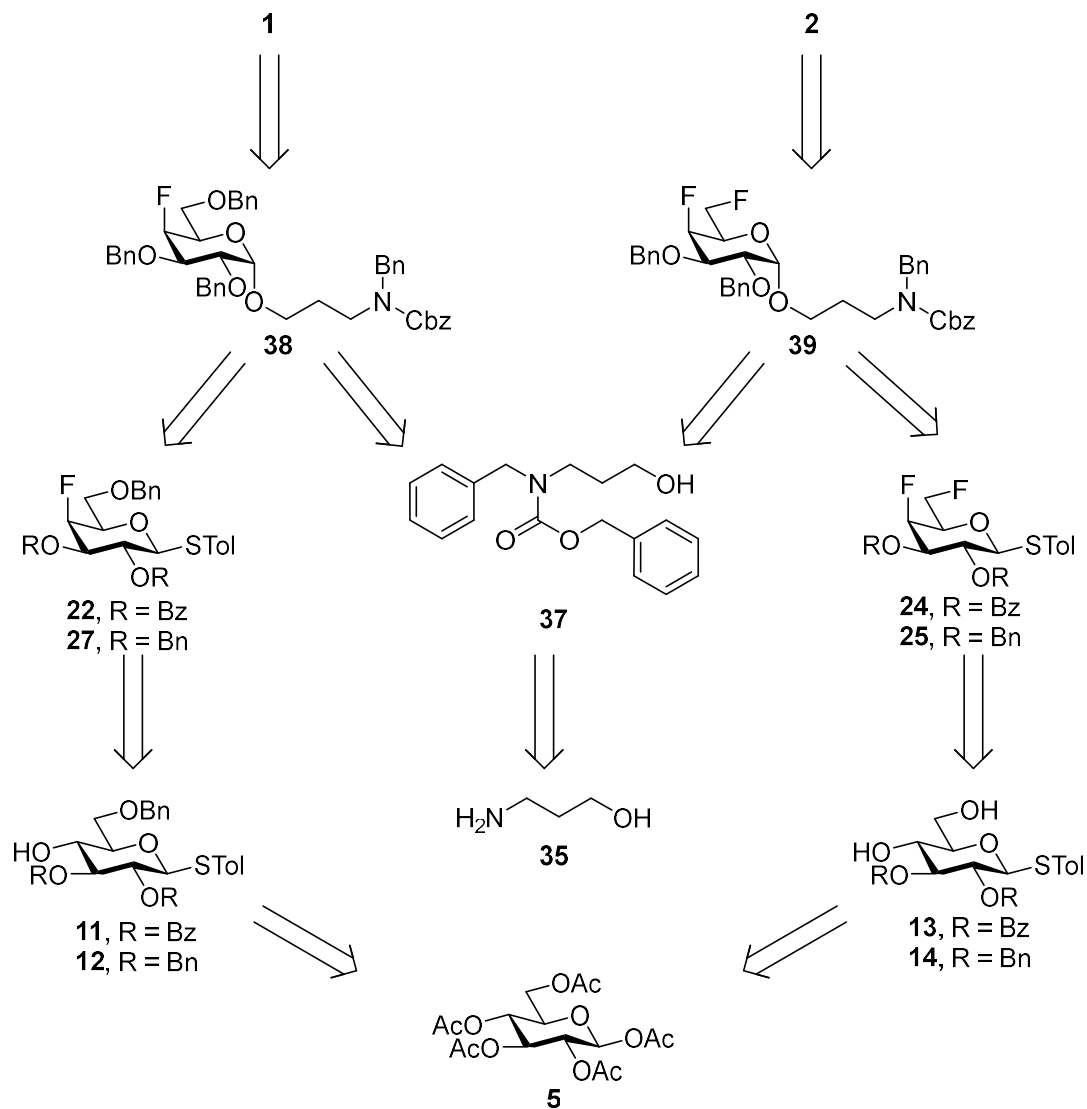
Scheme 1.1. Retrosynthetic analysis of α-Gal derivatives **1** and **2**.
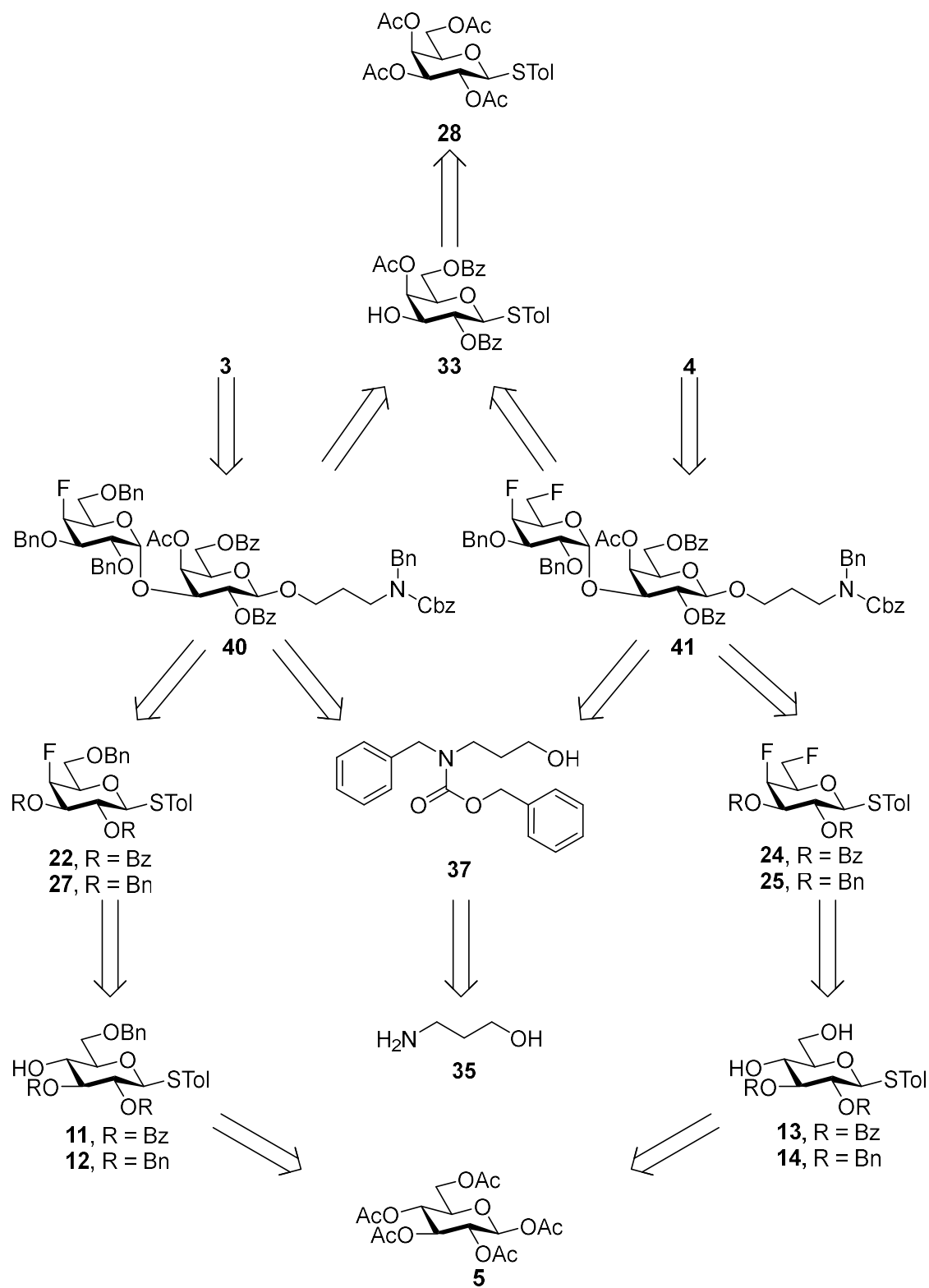
Scheme 1.2. Retrosynthetic analysis of α-Gal derivatives **3** and **4**.

2.1. Synthesis of fluorinated galactosyl thioglycoside donors
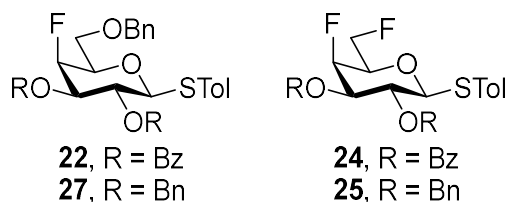
Figure 1.8. Structure of the fluorinated galactosyl donors to be used in this work

The preparation of the C4 monofluoro and C4, C6 difluorogalactose donors **22, 27, 24** and **25** started from commercially available glucose penta-acetate **5** (scheme 1.3). The first step consisted in the formation of the respective thioglucosyl donor by glucosylation reaction of tolylmercaptan in DCM catalyzed by BF_3Et_2O at room temperature.[34] This procedure afforded the thioglycoside donor **6** in 92% yield. Subsequently, the acetyl protecting groups of **7** were removed under typical transesterification conditions by treatment with NaOMe (catalytic amount) in MeOH at rt.[35] The respective tetraol **7** was formed quantitatively. The hydroxyl groups on C4 and C6 were selectively protected as 4,6-benzylidene acetal by the treatment of **7** with $PhC(OMe)_2$ and CSA in dry DMF.[34, 35] This procedure afforded the key benzylidene **8** in 95% yield.
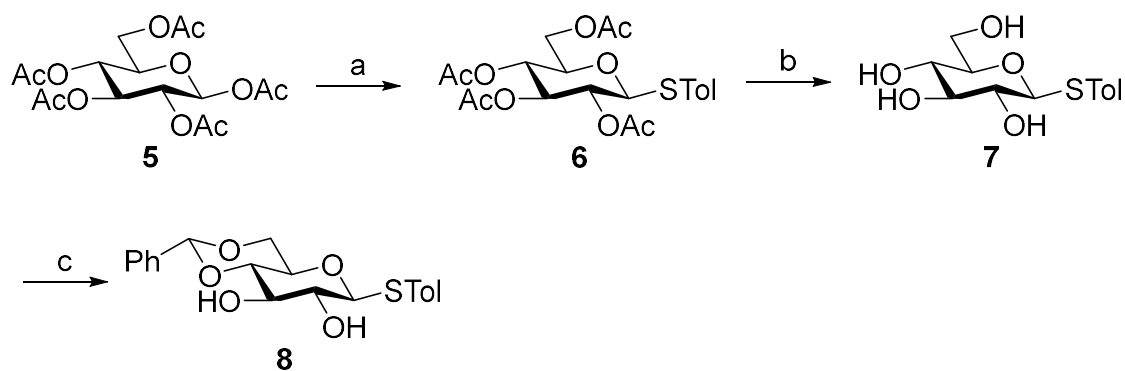
Scheme 1.3 Synthesis of benzylidene intermediate **8**: a) TolSH, BF$_3$Et$_2$O, CH$_2$Cl$_2$, 0°C; b) NaOMe, MeOH, rt; c) PhC(OMe)$_2$, CSA, DMF, rt.

Given the strategic value of having an intermediate with the positions of interest, C4 and C6, orthogonally protected, and considering literature reports related to the effect of sugar protecting groups over the efficiency of the C4 epimerization reactions [37-39], we decided to prepare two types of intermediates from **8** bearing ether and ester protecting groups. The installation of the benzyl (ether) protecting groups on C2 and C3 was accomplished by the treatment of **8** with NaH in dry DMF followed by the addition of BnBr.[40] This procedure furnished the benzyl protected intermediate **9** in 86% yield. Benzoyl (ester) protected intermediate **10** was obtained in 65% yield from the treatment of **8** with BzCl in pyridine.
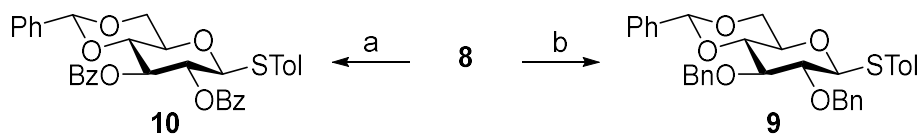
Scheme 1.4 Protection of hydroxyls C2 and C3 as ether **9** and ester **10.** a) BzCl, Py, DCM, rt; b) NaH, BnBr, DMF, 0°C to rt.

The preparation of the C4 hydroxyl derivative **11** was performed by the regioselective opening of the benzylidene ring on benzoyl adduct **10** under reductive conditions with Et$_3$SiH in TFA.[41] This procedure afforded the C4 hydroxyl adduct **11** in 70% yield. It is important noting that the regioselectivity of this reaction is driven by the basicity of the C4 hydroxyl. Protonation of C4 hydroxyl promotes the opening of the benzylidene ring and subsequent formation of a hemiacetal oxonium ion which is reduced *in situ* to benzyl ether by the silane reagent (scheme 1.6).

Scheme 1.5. Benzylidene ring opening of **9** and **10**. a) Et$_3$SiH, TFA, DCM, b) TFA/H$_2$O (9:1)

Hydrolysis of the 4,6-benzylidene **10** in a TFA/H$_2$O (9:1) mixture, afforded the diol **13** in quantitative yield. The next step is one of the most critical which involves the C4-epimerization of glucose along with the substitution of the hydroxyl groups with fluorine atom to generate the subsequent C4 monofluorinated and the C4, C6 difluorinated thiogalactoside donors.

Scheme 1.6. Mechanism for the regioselective 4,6-benzylidene ring opening.

To generate a series of glycosyl donors and acceptors with orthogonal reactivity at the anomeric carbon, we decided to prepare the *O*-glycosides analogues **19** and **21**. The anomeric oxygen on these compounds will put at our disposition a more stable glycoside towards electrophilic fluorinating reagents such as DAST. In addition, these new substrates can be used in future one-pot assembly of oligosaccharides combined with the thioglycoside donors previously synthesized. The new compounds were prepared using the same synthetic route for the preparation of thioglucosides. We opted for benzyl alcohol as aglycone because of the simplicity of the benzyl group removal by Pd-catalyzed hydrogenolysis in addition to be a stable anomeric protecting group.
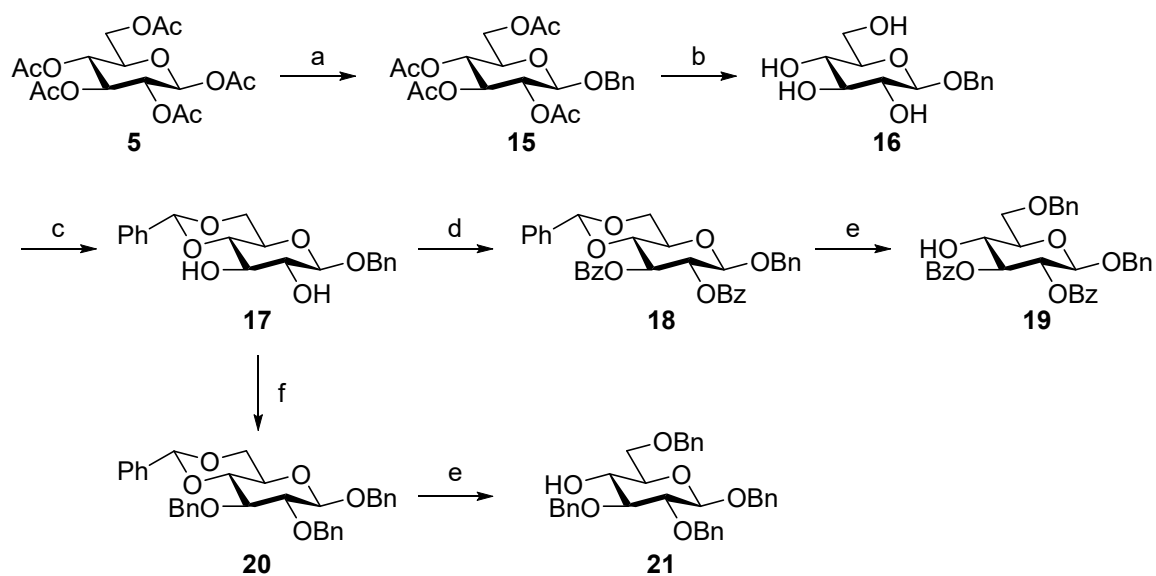
Scheme 1.7. Synthesis of benzyl *O*-galactosides **19** and **21**. a) BnOH, BF₃Et₂O, MeCN, 50-80⁰C; b) NaOMe, MeOH, rt; c) PhC(OMe)₂, CSA, DMF, rt; d) BzCl, Py, CH₂Cl₂, rt; e) Et₃SiH, TFA, DCM; f) NaH, BnBr, DMF, 0°C to rt.

We attempted the direct C4 fluorination of *O*-glycosides **19** and **21** by treating the substrates with DAST in DCM.[42] This procedure did not afford the desired fluorinated compounds and no reaction was observed for both ester **19** and ether **21** protected substrates.
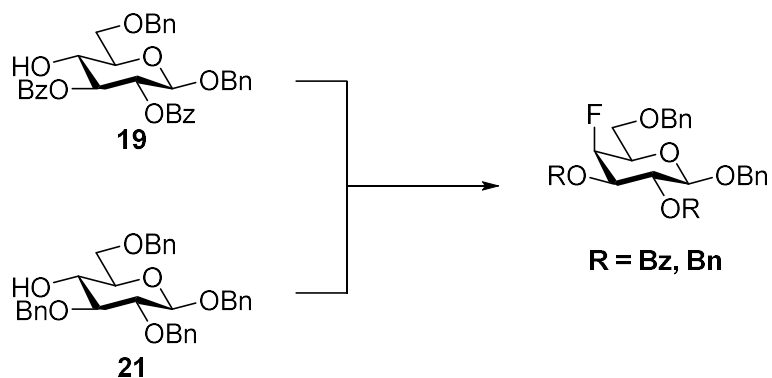
Scheme 1.8. Treatment of benzyl *O*-glucosides **19** and **21** with DAST.

After this result, we focused our attention in the thioglycoside donors and tested a two-step procedure involving the generation of a C4 triflate leaving group and its subsequent displacement by fluoride. The procedure starts with reacting a mono-deprotected sugar with Tf_2O and pyridine in DCM at -78°C for installing the respective triflate leaving group. After the reaction is completed, normally within 40 minutes, the system is diluted with organic solvent and washed with 1M $NaHCO_3$ and brine solution. The organic phase is subsequently concentrated and the crude triflate is re-dissolved in THF and reacted with TBAF. First, we explored this procedure on thioglucoside **11** in a small-scale reaction and the outcome probed positive, affording a compound with an ^{1}H NMR spectra (figure 1.8) consistent with the desired fluorinated adduct. The repetition of this procedure on a large-scale afforded the desired compound **22** in 76% yield.
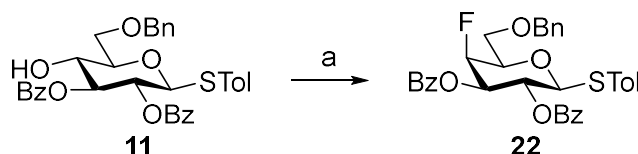
Scheme 1.9. Synthesis of C-4 fluoro thiogalactoside donor **22**. a) i. Tf_2O, Py, CH_2Cl_2, -78°C, 40 mins ii. TBAF, THF, rt, 30 mins

The installation of the fluorine atom in the sugar ring is confirmed by the splitting pattern of the proton connected to C4. H4 appears as a double doublet with a large coupling constant of 50.1 Hz (figure 1.8.), attributed to the two-bond coupling between H-4 and ^{19}F ($^2J_{H4-F}$), and a second constant of 2.1 Hz, assigned to the coupling with either H-5 or H-3. The third coupling constant expected for H-4 is too small to be detected by the equipment (400 MHz).
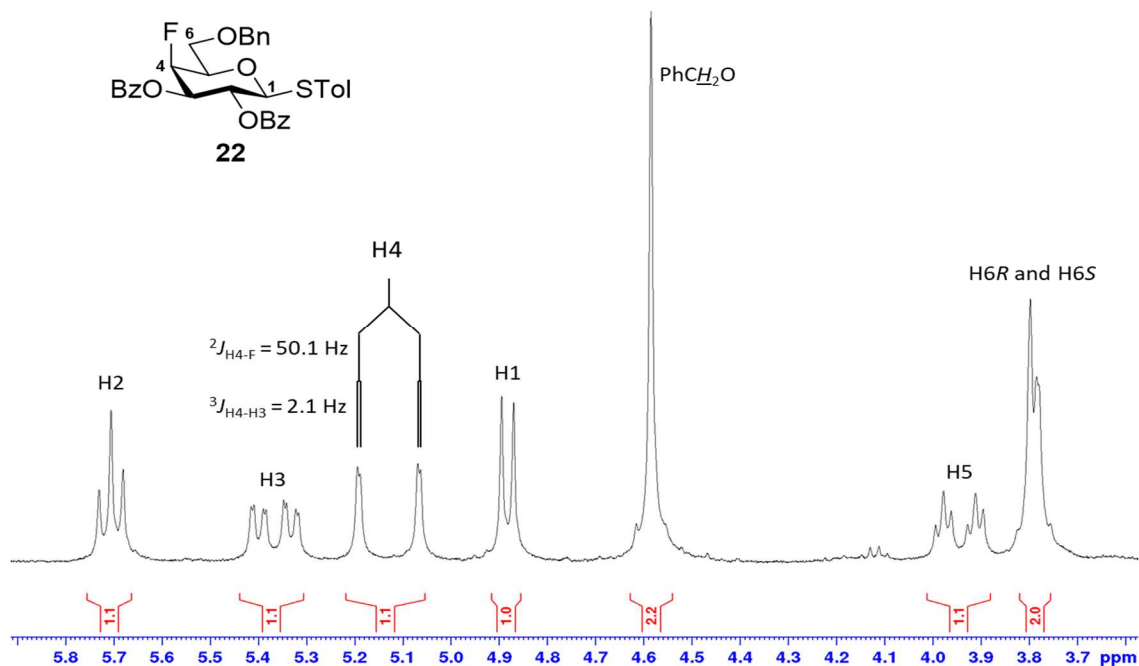
Figure 1.9. ^{1}H NMR spectra of sugar region of 4-Fluoro galactosyl thioglycoside **22.**

During our attempts to synthesize the C-4 fluoro derivative **22** in a large-scale, we found that the nature of the solvent used to dilute the triflate crude prior to the washing step can lead to the generation of major byproduct. If in this step EtOAc is used instead of DCM, the major isolated product is a non-fluorinated derivative with an inverted C-4 stereocenter. ^{1}H and ^{13}C NMR spectrum of this product is shown in Figure 1.9, Figure 1.10. and Figure 1.11. In the proton experiment, no large coupling constants are observed that can be assigned to coupling with fluorine. Assignments of the proton identities by COSY experiments revealed that H-4 appears as a double doublet with *J* values of 3.0 Hz and < 1.0 Hz, consistent with galactose configuration and confirming the inversion of the C4 stereocenter. In addition, the presence of a new acetyl group in the structure can be inferred from the signature signals in the ^{1}H NMR for the methyl group (2.20 ppm) and a

third carbonyl carbon in the ^{13}C spectra. Given that H-4 is the most de-shielded proton in the ^1H spectra, we propose that the new acetyl group is connected to C4 and the structure of the byproduct is that shown for compound **23.**
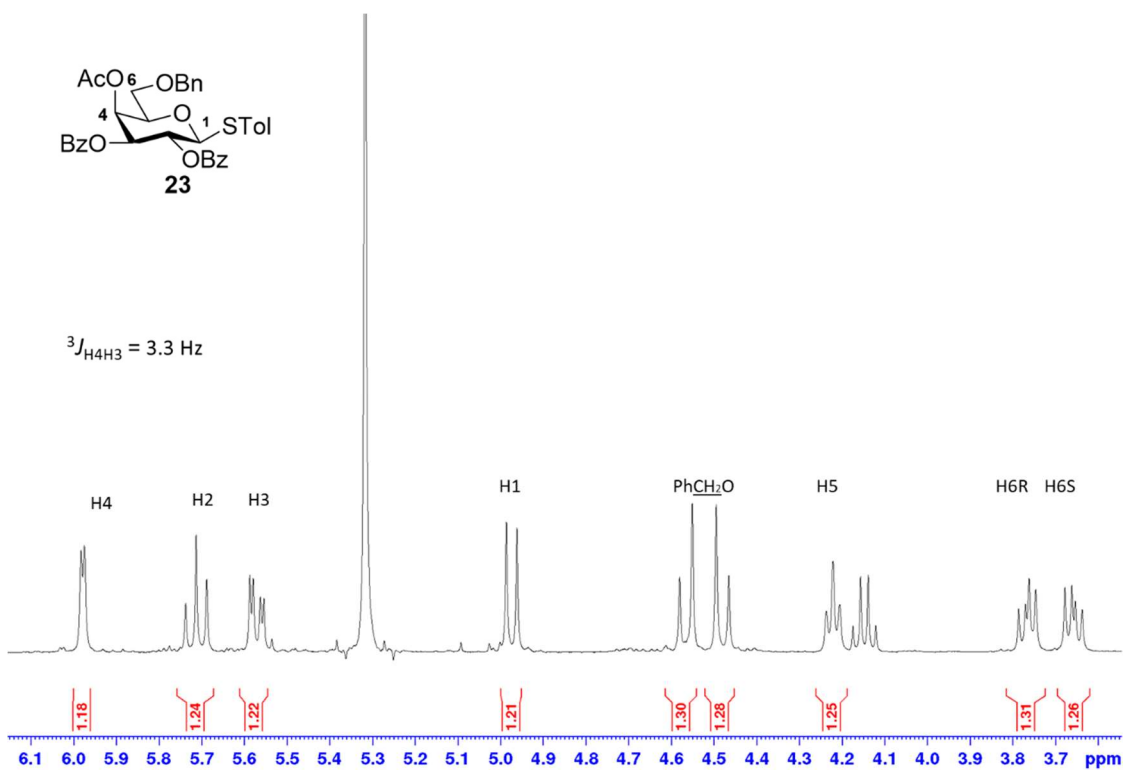
Figure 1.10. ^1H NMR spectra of sugar region of 4-*O*-acetyl galactosyl thioglycoside **23.**
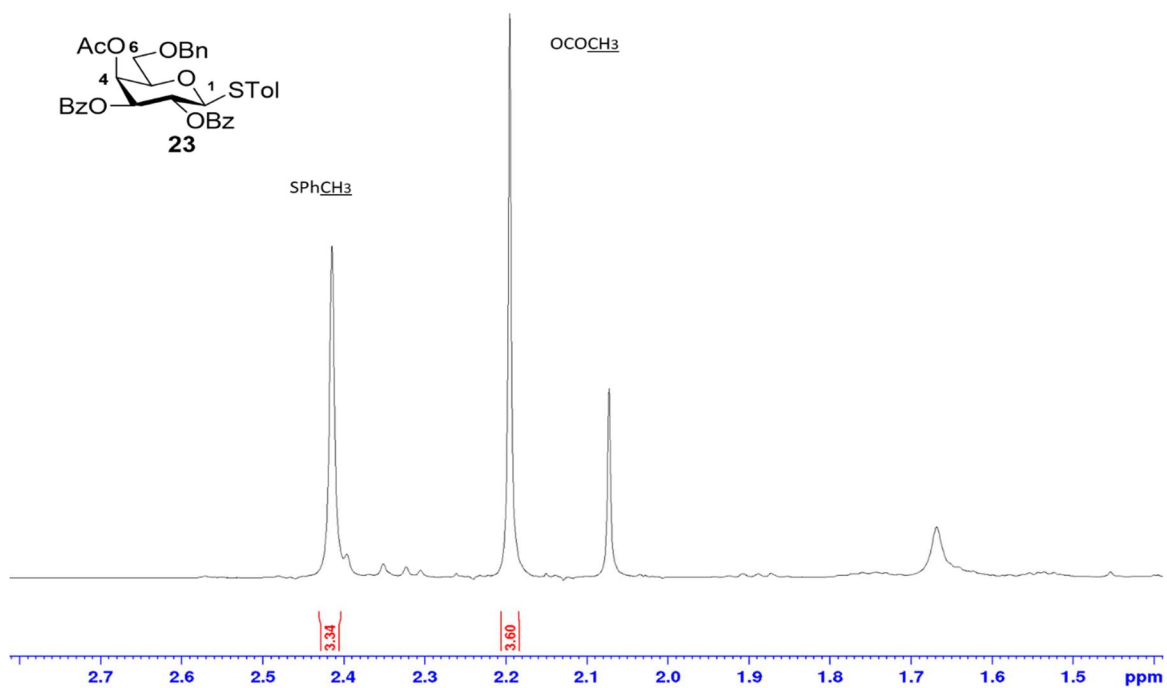
Figure 1.11. ¹H NMR spectra of 4-*O*-acetyl galactosyl thioglycoside **23.**
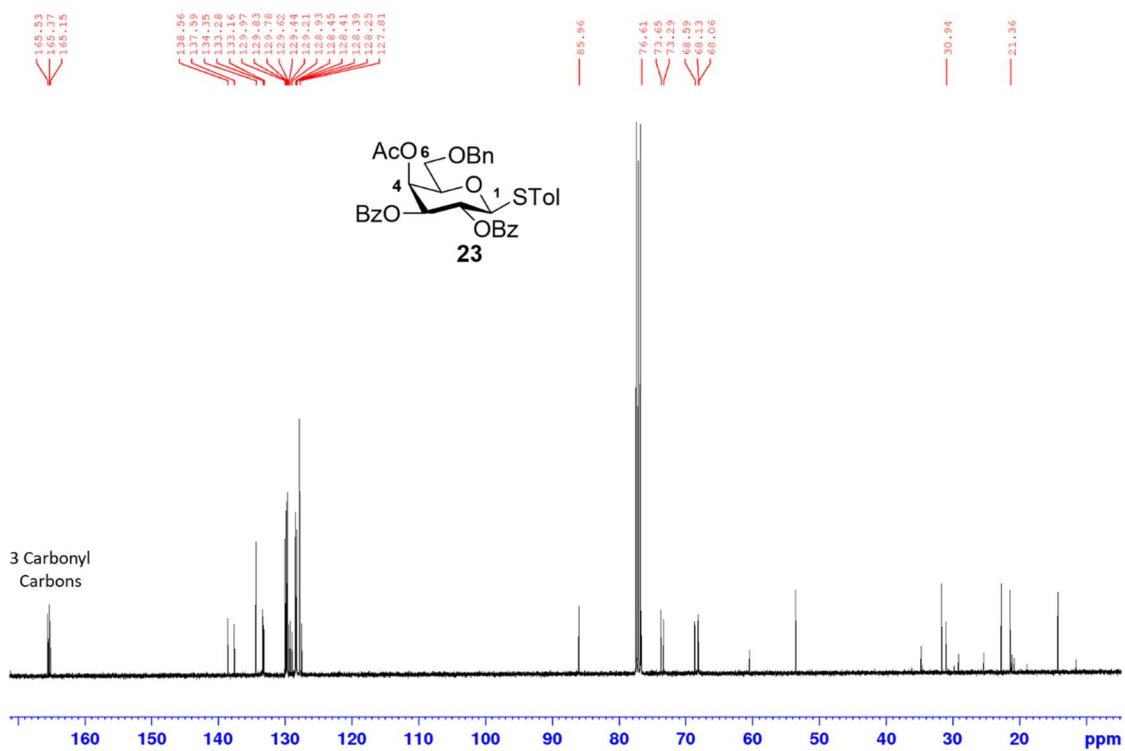
Figure 1.12. ¹³C NMR spectra of 4-*O*-acetyl galactosyl thioglycoside **23.**

A plausible mechanism for explaining the formation of this 4-*O*-acetyl galactose derivative

is shown in scheme 1.11. Since triflates are highly reactive leaving groups, its

displacement by the nucleophilic attack of the EtOAc carbonyl generates the intermediate

II that is subsequently attacked by a molecule of water for generating the acetate adduct

23 plus a molecule of ethanol.
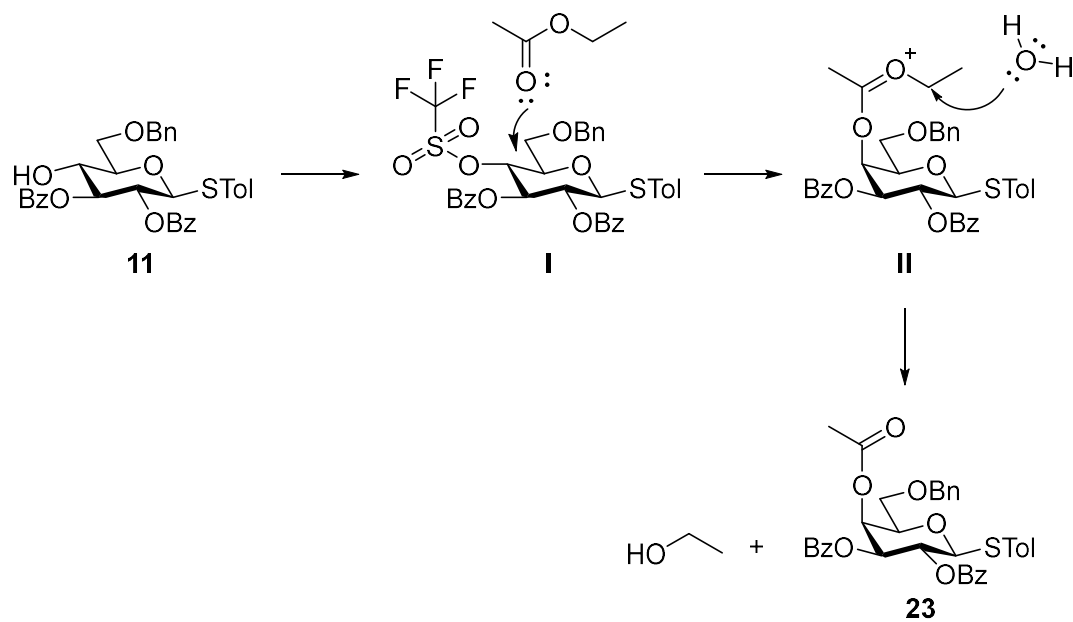
Scheme 1.10. Proposed mechanism for the formation of the 4-*O*-acetyl galactosyl thioglycoside **23**.

To explore an alternative method involving a less-reactive intermediate, we explored the

reaction using MsCl instead of Tf$_2$O given the lower reactivity of the mesylates, compared

with triflates, as leaving groups. Two test reactions were performed over the mesylate **13**

using TBAF and NaF as fluoride sources, but these attempts did not afford the desired compound even after 3 days of reaction.
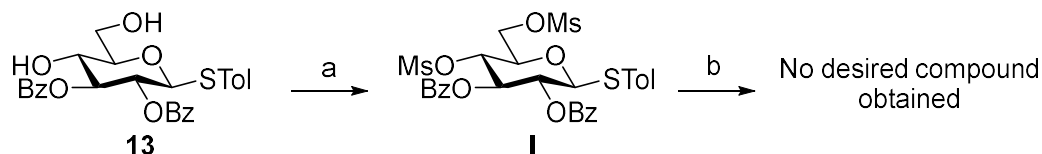
Scheme 1.11. Treatment of **13** with Mesylchloride, NaF and TBAF : a) MsCl 3.0 eq.,DCM, Pyridine, 24hrs; b) NaF, DMF, TBAF, 3 days

Given the positive result obtained for the Tf$_2$O/TBAF system, we continued our synthesis using this method for preparing the fluoro-galactose donors.

The target disaccharide core to be synthesized, αGal, connects two galactose residues via an α glycosidic bond. Then we should be careful with the nature of the protecting group positioned over C2, since this group can be decisive for the stereoselectivity of the glycosylation reaction. The substitution of C2 with esters, directs the selectivity of the glycosylation towards the formation of the β anomer as major product. This is because of the anchimeric assistance played by the carbonyl that leads to the formation of a reactive intermediate with the carbonyl occupying the axial plane, which leaves the equatorial plane available for a subsequent nucleophilic attach by the glycosyl acceptor. Ether protecting groups, in contrast, do not participate of this type of interaction and allows the nucleophilic attack from both equatorial and axial planes. Hence, the replacement of the benzyl protecting group on C2 by an ether, is necessary for favoring the α-selectivity of the donor **22** in glycosylation reactions.

Removal of the benzoyl protecting groups on **22** was performed by treatment with NaOMe in MeOH. The installation of the benzyl ethers was accomplished using NaH as a base and BnBr as benzyl source in DMF(Scheme 1.13).
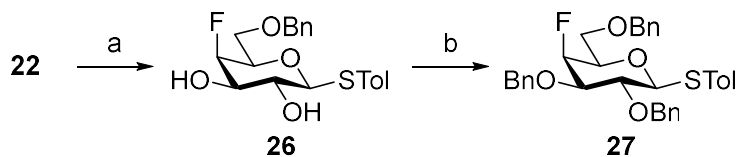
Scheme 1.12. Protecting group exchange for C-4 fluoro thiogalactoside **22.** a) NaOMe, MeOH, b) NaH, BnBr,DMF

Benzyl protected donor **27** was also prepared via fluorination of the alcohol **12** using the Tf$_2$O/TBAF system (scheme 1.14.).
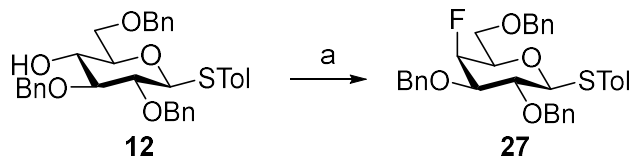
Scheme 1.13. Synthesis of fluorinated donor **27** via nucleophilic fluorination of alcohol **12.** a) i. Tf$_2$O, Py, DCM, ii. TBAF, THF

2.2. Synthesis of galactosyl acceptor/donor

Galactose acceptor **34** was prepared from tolyl thiogalactoside **28** as described in scheme 1.15. Compound **28** was subjected to acetyl group removal by treatment with NaOMe in MeOH. The *cis*-dihydroxyl groups on C3 and C4 in the resulting tetraol **29** were regioselectively protected as acetonide by treating it with 2,2-dimethoxypropane and CSA in DMF. The remaining hydroxyl groups on C2 and C6 were then protected as benzoate esters by treating the acetonide **30** with BzCl and pyridine in DCM. Hydroxyl groups on C3

and C4 were then deprotected by the hydrolysis of the acetonide ketal in TFA/H_2O (9:1).

The selective acetylation of the axial hydroxyl on C4 was accomplished in two steps. First, a hetero-orthoester from the diol **32** was formed by treating this intermediate with 1,1,1-triethoxyethane and TsOH in toluene. Then, the orthoester was hydrolyzed under mild conditions by adding AcOH and water to the system and heating to 40°C.

The 4-*O*-acetyl adduct **33** was then used as a donor in the glycosylation of *N*-benzyl-*N*-carboxybenzyl-3-aminopropanol **37**. The activation of the glycosyl donor with the NIS/TMSOTf system in the presence of 2 equivalents of the primary alcohol **37**, afforded the desired glycoside **34** in 89% yield. The possible disaccharide byproduct expected from the self-glycosylation on C-3 was not observed given the better nucleophilicity and higher concentration of the primary alcohol of the aglycone.
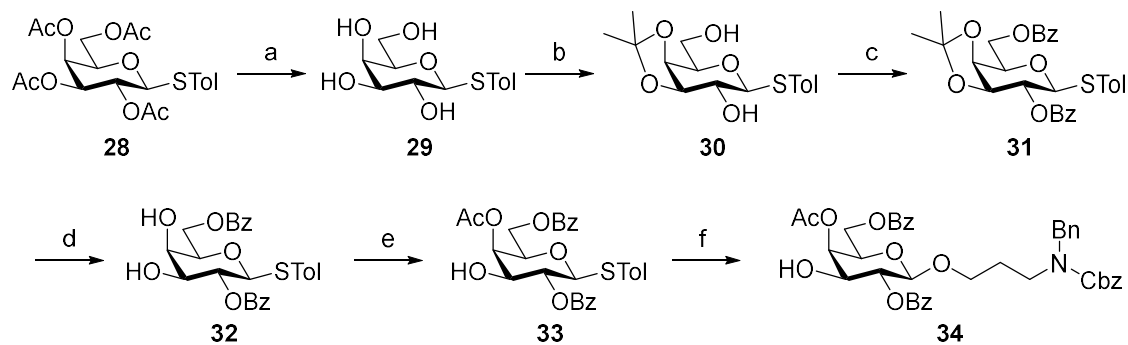
Scheme 1.14. Synthesis of acceptor **34.** a) NaOMe, MeOH, rt; b) $(CH_3)_2C(OCH_3)_2$, CSA, DMF rt; c) BzCl, Py, rt; d) TFA, H_2O, rt; e) $(EtO)_3CCH_3$, *p*-TsOH, Tol., rt. then AcOH, H_2O, 40°C; f) **37**, NIS, TMSOTf, MeCN, -20 to -30°C

2.3. Synthesis of *N*-benzyl-*N*-carboxybenzyl-3-amino propanol aglycone 25

The aglycone structure was selected based on the future applications of the αGal glycomimetics. Since our primary interest is the utilization of these ligands on immunological studies, this requires the availability of a reactive functional group for the conjugation of these substrates to protein or lipid carriers. Amines are among the most versatile and widely used functional groups for this purpose. The coupling of amines to carboxylic acids allows not only the direct attachment of ligands to protein carriers but also allows the installation of different functional groups, such as alkynes, azides, biotin, etc. for biorthogonal conjugation reactions. Therefore, we selected the amine group as the reactive functional group, and we installed it in our glycomimetic candidates as part of the aglycone chain. The *N*-protected aglycone **37** was prepared from 3-aminopropanol in two steps (Scheme 1.16.). First, the amine group is protected as benzyl amine *via* reductive amination of benzaldehyde. Then, the isolated product **36** is reacted with CbzCl and pyridine in DCM to install the second protecting group over the secondary amine. Both Cbz and Bn groups can be cleaved by Pd-catalyzed hydrogenolysis. The protected aglycone **37** was isolated in 98% from the two steps.
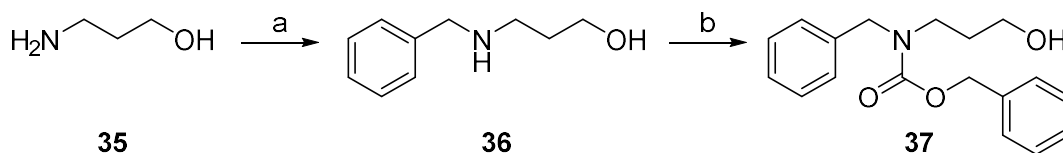
Scheme 1.15. Synthesis of *N*-protected aglycone **37.** a) i. PhCHO, MeOH, HC(OMe)$_3$, 0°C ii. NaBH$_4$, 0°C, 10 h, rt. b) CH$_2$Cl$_2$, K$_2$CO$_3$ Cbz-Cl, 0°C, 12 h

2.4. Synthesis of 4-fluoro galactosides

The presence of the fluorine atoms in the sugar rings have a deactivating effect on the reactivity of the donors towards activation given that the electronegativity of fluorine destabilizes the oxocarbenium intermediate generated during the activation. In contrast, benzyl ether protecting groups have an activating effect due to their electron donating character (scheme 1.17.). Therefore, when choosing an activating system for glycosylation reactions, attention must be paid to the reactivity of the donor and highly reactive activating systems should be selected for activating low reactivity (or disarmed) donors. With these considerations, we decided to select an activating system that will secure enough reactivity for activating our fluorinated donors and the NIS/TMSOTf combination was selected for promoting glycosylation using donor **22** (Scheme 1.19.).
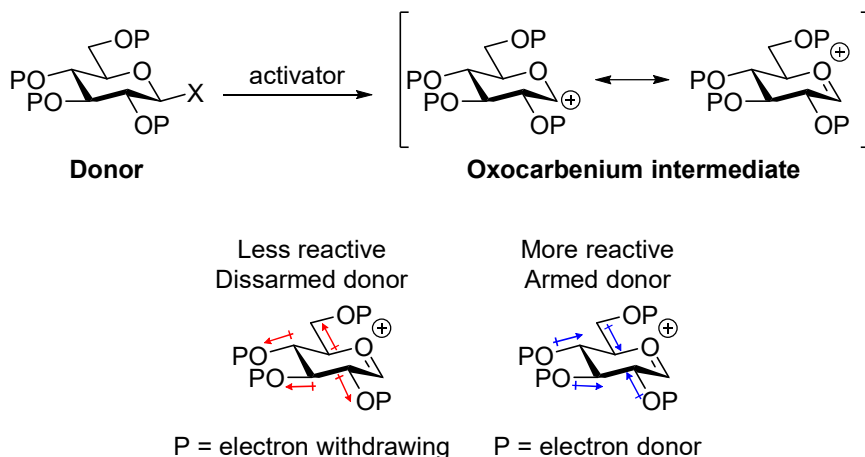
Scheme 1.16. The reactivity of glycosyl donors is determined by the stability of the oxocarbenium intermediate generated from the activation. Donors protected with electron-withdrawing substituents are less reactive and require more aggressive activating reagents.

The selection of the solvent is relevant for directing the stereoselectivity of the glycosylation reaction and the formation of axial (α) glycosides is normally favored if

ethereal solvents are used for running the reaction. Ethereal solvents, such as diethyl ether, dioxane, and tetrahydrofuran, can interact with the oxocarbenium intermediate by generating a transient covalent bond and occupying the equatorial position in the anomeric center. Consequently, a nucleophile will preferentially attack the α–plane leading to the respective α–glycoside (scheme 1.18.)
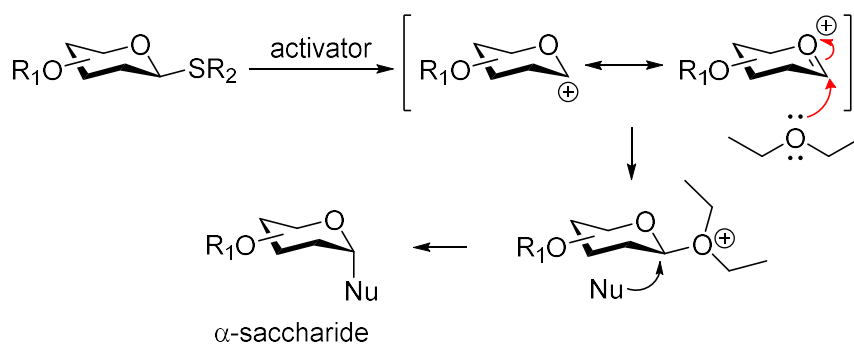
Scheme 1.17. Control of the stereoselectivity of glycosylation reactions by the solvent. Ethereal solvents favor the formation of α-linkages.

The synthesis of the α-glycoside **38** was accomplished by activating the donor **27** with NIS/TMSOTf in the presence of the primary alcohol **37** in Et$_2$O. We gladly observed that the product **38** was obtained in an excellent yield (85%) indicating that the NIS/TMSOTf combination is reactive enough for the efficient activation of the fluorinated donors and afforded, as expected, the α anomer as unique compound. The β stereoisomer was not observed in this process.

$$27 \quad + \quad 37 \quad \xrightarrow{a} \quad 38$$
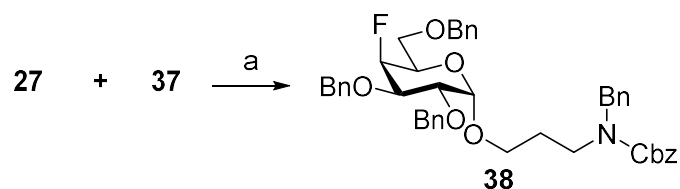
Scheme 1.18. Synthesis of glycosides **38**. a) NIS, TMSOTf, Et$_2$O, -30^{0}C, 30 min.

2.5. Synthesis of fluorinated analogues of αGal disaccharide

To generate the αGal disaccharide mono- and di-fluorinated cores **40** and **41**, we envisaged a strategy based on the glycosylation of **34** with the benzylidene-protected thioglucoside donor **9**. The center of this strategy is the preparation of the key intermediate **42** for enabling the synthesis of **40** and **41** *via* C4 epimerization/fluorination strategy. The activation of **9** with NIS/TMSOTf in Et$_2$O in the presence of the acceptor, afforded the respective glucose disaccharide **42** in 89% yield. We then attempted the regioselective reductive opening of the benzylidene ring on this substrate by treating it with Et$_3$SiH and TFA in DCM. The reaction outcome was a complex mixture of products not possible to resolve by chromatography.
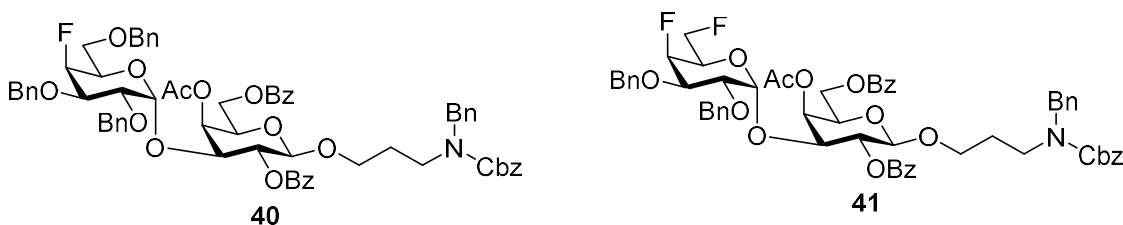
Figure 1.13. Structure of the target protected mono and di-fluorinated disaccharides **41** and **42.**
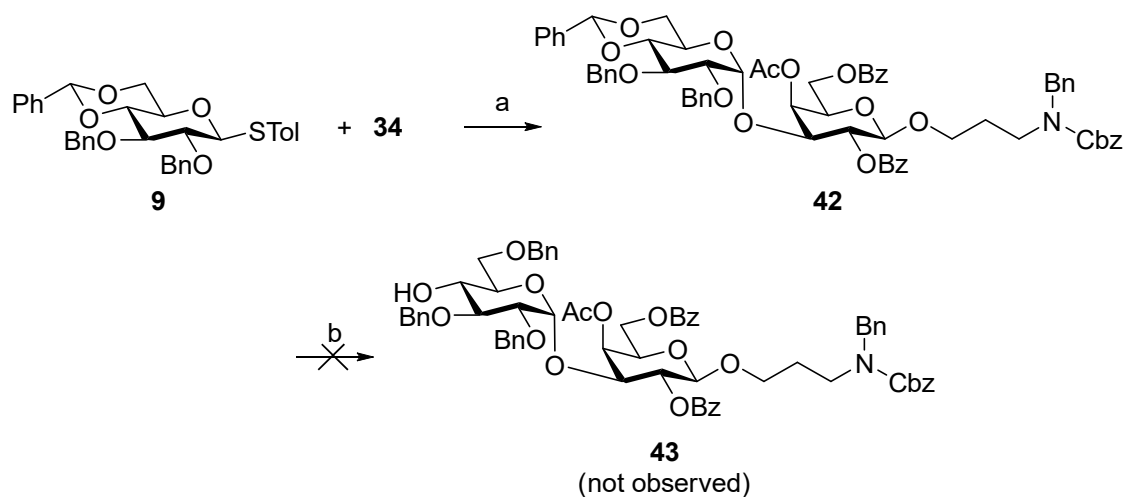
Scheme 1.19. Alternative route for synthesis of disaccharides **40** and **41.** a) NIS, TMSOTf, Et$_2$O, -20°C; b) Et$_3$SiH, TFA, DCM
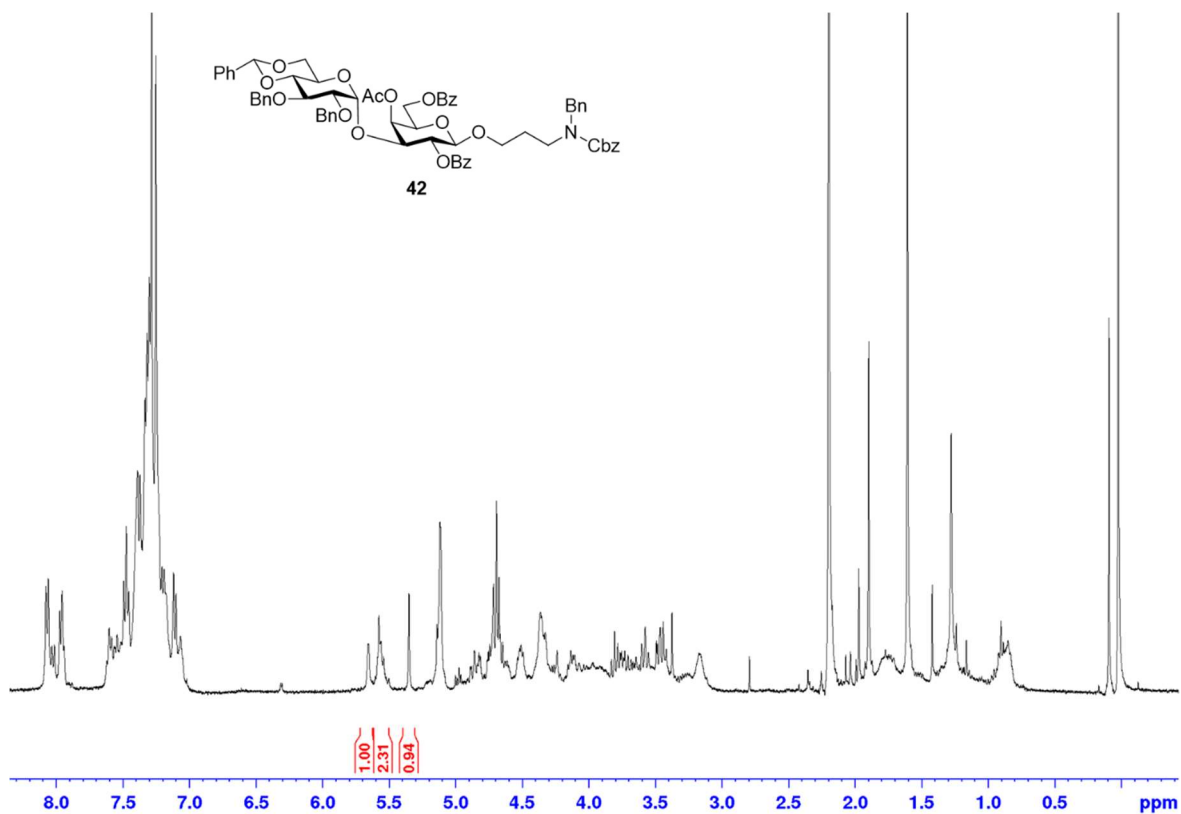
Figure 1.14. ^{1}H NMR (CDCl$_3$, 400 MHz) of disaccharide **42**

The glycosylation using fluorinated thioglycoside donors activated by the NIS/TMSOTf system proved effective for the high yield formation of glycosides and saccharides. The

reaction showed a high stereoselective control favoring the formation of the desired α glycosidic bonds. The use of Et_2O is assumed to contribute to the control of the stereoselectivity.

The results of this work have demonstrated that the stereoselective synthesis of fluorinated analogues of the αGal antigen is feasible when using fluorinated thioglycoside donors. The future work will be centered in using this methodology for preparing the remaining target analogues.

3. Future work

We will continue our research program by focusing on the synthesis of the remaining mono- and di-fluorinated monosaccharide **39** and disaccharides **40** and **41** by glycosylation of acceptors **24** and **25** respectively with **34.** Fluorination will be performed using two-steps procedures involving the generation of a C4 triflate leaving group and the subsequent treatment with fluoride using TBAF as fluorinating agent. (Scheme 1.21.)
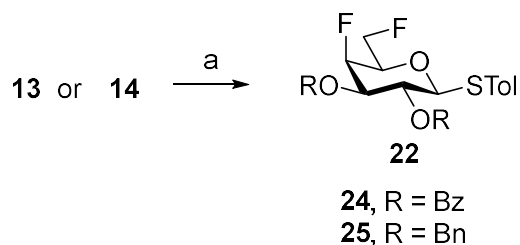
Scheme 1.20. Proposed synthesis of C4 fluoro thiogalactoside donor **24** and **25.** a) installation of triflate leaving group by treatment with Tf_2O/Py in DCM at -78^0C then TBAF in THF at rt.

The synthesis of the α-glycosides **39** will be attempted by using the activating system NIS/TMSOTf in Et_2O. (Scheme 1.22.)
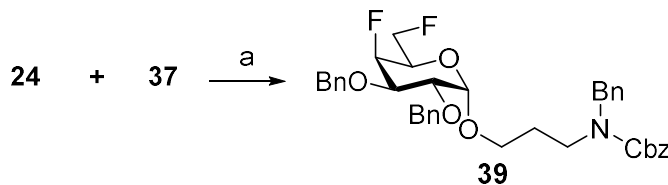
Scheme 1.21. Proposed synthesis of glycosides **39**. The activation of the difluorinated donor **24** will be performed by using the NIS/TMSOTf system in Et_2O at -20^0C.

αGal disaccharide analogues **40** and **41** will be prepared by glycosylation of acceptor **34** with donors **27** and **25** respectively (scheme 1.23.). The activation system to be used is NIS/TMSOTf and the reaction will be performed in Et$_2$O for inducing solvent-mediated α-stereoselectivity. The disaccharides **40** and **41** will be isolated and α/β selectivity of the disaccharides **40** and **41** obtained will be determined, respectively.
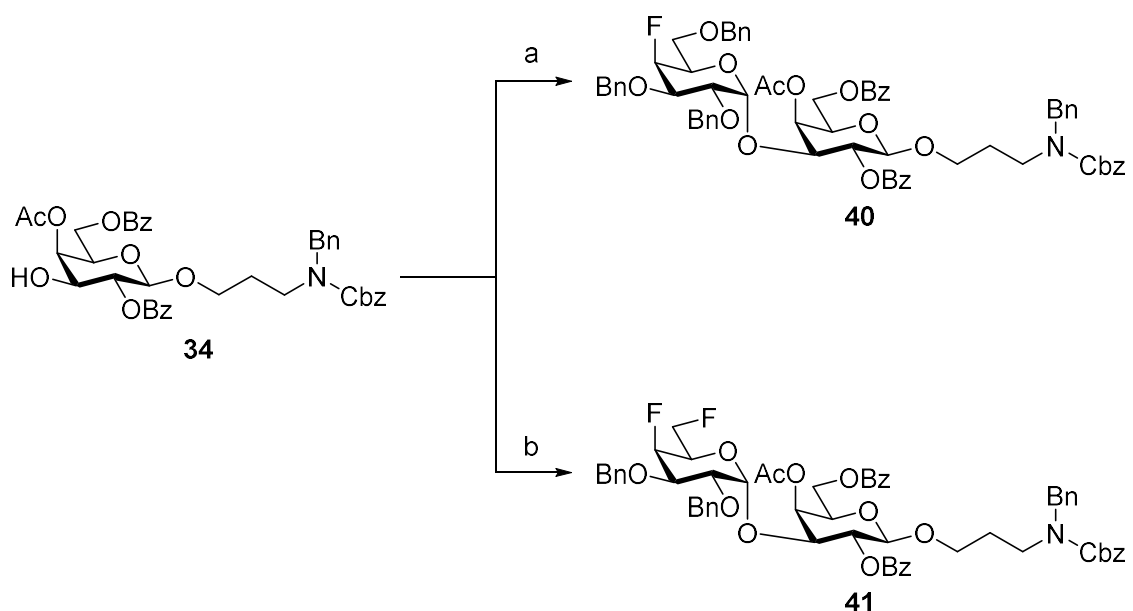
Scheme 1.22. Proposed synthesis of disaccharides **40** and **41**. a) **27**, NIS/TMSOTf, Et$_2$O, -20°C. b) **25**, NIS/TMSOTf, Et$_2$O, -20°C.

After completing the synthesis of all four protected fluorinated saccharides **38**, **39**, **40** and **41** the final step is the deprotection of the saccharides. Acetyl (Ac) and benzoyl (Bz) ester protecting groups will be removed by treatment with sodium methoxide in methanol or methanolic solution of ammonia. Benzyl ethers (Bn) will be cleaved by catalytic hydrogenolysis using Pd/C catalyst and hydrogen atmosphere. In this way, we expect to

obtain the corresponding fluorinated αGal mono and disaccharides **1**, **2, 3** and **4**. (Scheme 1.24.)
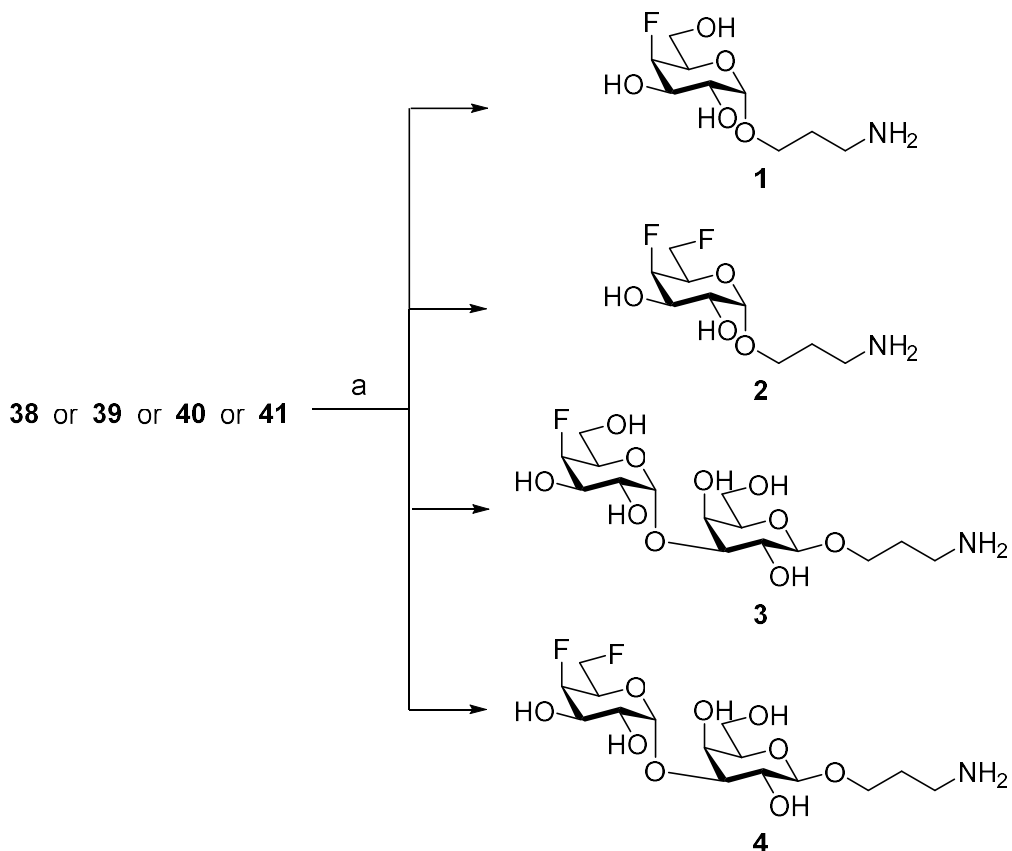
Scheme 1.23. Deprotection of ether and ester protected fluorinated αGal analogues **1-4**. Ester removal (Ac or Bz): NaOMe, MeOH, or NH_3 in MeOH; Benzyl ether removal: H_2, Pd/C, EtOH

The affinity of the synthesized αGal analogs for anti-αGal antibodies, and other receptors, will be determined as the respective dissociation constants (Kd) using the biophysical techniques of localized surface plasmon resonance (LSPR) and isothermal titration microcalorimetry (ITC).

4. Experimental Section

Commercially available carbohydrate starting materials were purchased from Carbosynth Ltd. All other commercial reagents and dry solvents were purchased from TCI, Across or Alpha Aesar. Chemicals and solvents were used without previous purification. Normal phase flash chromatography was done using SiliaFlash irregular silica gel F60, 40-63 μm, 60 Å (Silicycle) in glass columns and air pressure. NMR spectroscopy (^{1}H, ^{13}C, COSY, HSQC) were recorded in a Bruker Avance 400 spectrometer at St. John's University.

Procedures and experimental data of synthesized compounds
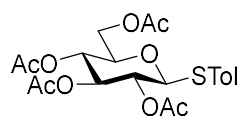
S-pTolyl-2,3,4,6-tetra-O-acetylglucoside (6): Glucose pentaacetate **5** (10.07 g, 25.7 mmol) and tolylmercaptan (6.38 g, 51.4 mmol) were dissolved in dry DCM (52.0 mL) and cooled to 0°C. BF$_3$Et$_2$O (3.17 mL, 25.7 mmol) was added dropwise and the solution was warmed to rt under stirring. After 5 hours of TLC shows total consumption of the starting material and the reaction was cooled to 0°C and quenched with triethylamine (4.0 mL). After 15 minutes of stirring at 0°C, the volatiles were removed in vacuum and the crude purified by flash chromatography using SiO$_2$ as stationary phase and EtOAc/Hexanes mixture (3:7) as eluent. Thioglycoside **6** (9.23 g, 19.6 mmol, 91.6%) was isolated as a waxy white solid. Compound identity was confirmed by comparison of ^{1}H and ^{13}C NMR spectra data with previously reported data. [43] ^{1}H NMR (CDCl$_3$, 400 MHz): δ 7.39(d, *J* = 8.1 Hz, 2H), δ 7.12 (d, *J* = 8.1 Hz, 2H), δ 5.20 (dd, *J* = 9.3 and 9.3 Hz, H-3), δ 5.02 (dd, *J* = 9.8 and 9.6 Hz, H-4), δ 4.93 (dd, *J* = 10.0 and 9.3 Hz, H-2), δ 4.63 (d, *J* = 10.0 Hz, H-1), δ 4.19 (dd, *J* = 4.8 and 2.7 Hz, H-6), δ 4.13 (dd, *J* = 6.3 and 11.3 Hz, H-

6'), δ 3.93 (m, *J* = 1.0, H-5), δ 2.35 (s, 3H), 2.09 (s, 3H), δ 2.08 (s, 3H), δ 2.01 (s, 3H), δ 1.98

(s, 3H). ^{13}C NMR (100MHz, CDCl$_3$) δ 132.8 ,128.6 , 84.8 , 73.9 , 67.2 , 61.0 , 19.6.
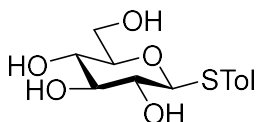
S-pTolyl glucoside (7): Thioglycoside **6** (12.1 g, 26.6 mmol) was dissolved in methanol (37.0 mL) and sodium methoxide (100 mg) was added. The suspension was stirred at r.t. for 24 hours which is enough time for the

trans-esterification reaction to be completed (shown by TLC analysis). The system was

then neutralized with Amberlyst IR-120+ resin followed by filtration. Methanol was

removed *in vacuo* with rotary evaporator and the crude dried under high vacuum in a

Schlenk line for 24 hours prior to use. Structure of tetraol **7** was confirmed by comparison

of its ^{1}H and ^{13}C NMR spectra with previously reported data.[44] ^{1}H NMR (CDCl$_3$, 400 MHz):

δ 7.48 (d, *J* = 8.2 Hz, 2H), δ 7.14 (d, *J* = 7.9, 2H), δ 4.52 (d, *J* = 9.8 Hz, H-1), δ 3.87(dd, *J* =1.6

Hz and 1.9 Hz, H-4), δ 3.67 (m, H-5), δ 3.38 (dd, *J* = 8.6 Hz and 8.6 Hz, H-3), δ 3.29 (m, H-6

and H-6'), δ 3.19 (dd, *J* = 9.6 and 8.8 Hz, H-2), δ 2.33 (s, 3H). ^{13}C NMR (100 MHz, MeOD) δ

137.4, 132.1, 129.8, 129.1, 88.3, 80.7, 78.3, 72.3, 69.9, 61.5, 48.2, 48.0, 47.8, 47.6, 47.4,

47.2, 46.9, 19.7.
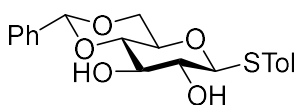
S-pTolyl-,4,6-benzylideneglucoside (8): *S-p*Tolyl glucoside (7)

(5.45 g, 18.1 mmol) and benzaldehyde dimethoxyacetal (4.05

mL, 27.1 mmol) are dissolved in dry DMF (36.2 mL) at r.t. followed by the addition of

camphorsulfonic acid (21.02 mg, 0.90 mmol). The reaction is stirred for 18 hours and

quenched by addition of Et$_3$N (2.0 mL). System is diluted with DCM, transferred to a

separation funnel, and washed with water. The organic layer is collected, dried over

Na$_2$SO$_4$, filtered and the volatiles removed *in vacuo*. Benzylidene adduct is purified by

flash chromatography using SiO_2 as stationary phase and EtOAc/Hexane (1:5) mixture as eluent. Chromatography afforded compound **8** (8.33 g, 25.4 mmol, 99%) as a waxy white solid. Compound identity was confirmed by comparison of ^{1}H and ^{13}C NMR spectra data with previously reported data.[45] ^{1}H NMR (CDCl$_3$, 400 MHz): ^{1}H NMR (400 MHz, CDCl$_3$) δ 7.52 – 7.44 (m, 4H), 7.42 – 7.34 (m, 3H), 7.14 (dd, J = 20.5, 7.6 Hz, 2H), 4.60 (d, J = 9.7 Hz, H-1), 4.40 (dd, J = 10.4, 4.2 Hz, H-4), 4.14 (dd, J = 7.1 Hz and 10 Hz, H-2), 3.87 (t, J = 8.6 Hz, H-6), 3.83 – 3.76 (m, H-3), 3.58 – 3.49 (m, H-6'), 3.45 (dd, J = 9.1 Hz and 10.0 Hz, H-5), 2.38 (s, 1H). ^{13}C NMR (101 MHz, CDCl$_3$) δ 206.9, 152.8, 138.9, 136.9, 133.7, 129.9, 128.3, 126.3, 125.6, 80.2, 77.4, 77.0, 76.7, 74.6, 72.5, 70.6, 68.6, 30.9, 21.2, 1.0.
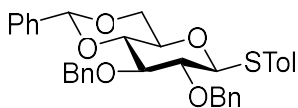
S-pTolyl-2,3-O-dibenzyl-4,6-benzylideneglucoside (9): S-pTolyl-4,6-benzylideneglucoside (8) (8.10 g, 24.8 mmol) is dissolved in dry DMF (124.0 mL) and cooled to 0°C with an ice-bath. Sodium Hydride (1.78 g, 74.4 mmol, 60% suspension in mineral oil) was added portion-wise and the resulting suspension was kept under vigorous stirring at 0°C for 20 minutes. Benzyl bromide (3.53 mL, 29.76 mmol) was then added, and the system allowed warming to r.t. After 2 hours TLC analysis shows total consumption of the starting alcohol and the predominance of one single spot. The mixture was cooled again to 0°C, quenched by MeOH (10.0 mL) addition and transferred to a pear-shaped flask for solvent is removed *in vacuo*. The crude was then purified by flash chromatography over SiO_2 and using EtOAc/Hexanes (1:4) mixture as eluent. Benzylated adduct **9** (0.14 g, 21.1 mmol, 86%) was isolated as a waxy white solid. Compound identity was confirmed by comparison of ^{1}H and ^{13}C NMR spectra data with previously reported data.[46] ^{1}H NMR (400 MHz, CDCl$_3$) δ 7.51 – 7.28 (m, 19H),

7.12 (d, *J* = 8.0 Hz, 2H), 4.97 – 4.74 (m, 4H), 4.69 (d, *J* = 9.6 Hz, H-1), 4.38 (dd, *J* = 10.2, 4.6 Hz, H-4), 3.84 (d, *J* = 8.8 Hz, H-6), 3.79 (d, *J* = 10.8 Hz, H-3), 3.68 (t, *J* = 9.2 Hz, H-6'), 3.49 (d, *J* = 8.9 Hz, H-2), 3.45 (d, *J* = 5.3 Hz, H-5), 2.34 (s, 3H). ^{13}C NMR (100 MHz, CDCl$_3$) δ 206.98, 133.0, 129.8, 128.4, 128.3, 128.2, 128.1, 125.9, 83.1, 77.3, 77.2, 77.0, 76.7, 60.4, 30.9, 14.2.
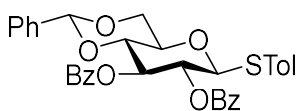
S-pTolyl-2,3-O-dibenzoyl-4,6-benzylideneglucoside (10): *S-pTolyl-4,6-benzylideneglucoside* (8) (1.02 g, 3.56 mmol) was dissolved in pyridine (11.9 mL) and benzoyl chloride (1.21 mL, 10.2 mmol) was added to the solution at r.t. After 8 hours of stirring TLC analysis shows total consumption of the starting material and the volatiles were removed *in vacuo*. Dibenzoylated adduct was then purified by flash silica gel chromatography using EtOAc/Hexanes mixture (1:4) as eluents. Compound **10** (1.35 g, 2.32 mmol 65%) was isolated as a white solid. Compound identity was confirmed by comparison of ^{1}H and ^{13}C NMR spectra with previously reported data.[47] ^{1}H NMR (CDCl$_3$, 400 MHz): δ 8.07-7.07 (m, Aromatic H's, 19H), δ 5.76 (dd, *J* = 7.3 and 9.6 Hz, H-3), δ 5.52 (s, 2H), δ 5.42 (dd, *J* = 9.8 and 9.3 Hz, H-2) , δ 4.95 (d, *J* = 9.9 Hz, H-1), δ 4.43 (dd, *J* = 5.2 and 4.6 Hz, H-5), δ 3.86 (m, H-4 and H-6), δ 3.72 (dd, *J*= 4.8 and 4.8 Hz, H-6'), δ 2.03 (s, 3H). ^{13}C NMR (101 MHz, CDCl$_3$) δ 206.9, 129.7, 128.1, 126.1, 79.6, 77.4, 77.1, 76.7, 40.2, 30.7, 19.2.
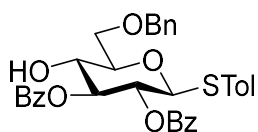
S-pTolyl-2,3-O-dibenzoyl-6-benzylglucoside (11): Benzylidene **10** (2 g, 3.4 mmol) and Et$_3$SiH (5.4 mL, 34.0 mmol) are dissolved in DCM (20.4 mL) at 0°C and TFA (2.62 mL, 34.0 mmol) is added. The reaction is allowed warming

to r.t and stirred for 5 hours which is enough time for reaction completion (TLC analysis shows total consumption of the starting benzylidene and the predominance of a high polarity spot). The mixture is then transferred to a pear-shaped flask and the volatiles removed *in vacuo*. The obtained crude is purified by flash chromatography using silica gel as stationary phase and EtOAc/Hex (3:7 mixtures as eluents. Alcohol **11** (1.33 mg, 2.27 mmol, 67%) was isolated as colorless syrup. Compound identity was confirmed by comparison of ^{1}H and ^{13}C NMR spectra data with previously reported data.[48] ^{1}H NMR (CDCl$_3$, 400 MHz): 8.11 (d, *J* = 7.1 Hz, 1H), 7.95 (m, 4H), 7.49 (m, 3H), 7.36 (m, 9H), 7.06 (d, *J* = 8.0 Hz, 2H), 5.44 (dd, *J* = 9.3 and 9.3 Hz, H-3), 5.39 (dd, *J* = 9.4 and 9.4 Hz, H-2), 4.86 (d, *J* = 9.5 Hz, H-1), 4.63 (d, *J* = 11.8 Hz, 1H), 4.59 (d, *J* = 11.8 Hz, 1H), 3.93 (dd, *J* = 9.3 and 9.3 Hz, H-4), 3.88 (m, 2H, H-6 and H-6'), 3.72 (ddd, *J* = 4.4, 4.4 and 9.2 Hz, H-5), 2.31 (s, 3H). ^{13}C NMR (100 MHz, CDCl$_3$) δ 167.2, 165.2, 138.4, 137.8, 133.7, 133.5, 133.4, 133.3, 130.2, 129.9, 129.8, 129.7, 129.4, 129.0, 128.5, 128.5, 128.4, 128.3, 127.8, 127.8, 86.3, 78.9, 77.9, 77.3, 77.0, 76.7, 73.8, 70.8, 70.2, 70.1, 30.9, 21.2.
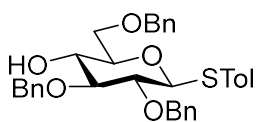
S-pTolyl-2,3,6-O-dibenzylglucoside (12): Benzylidene **9** (2 g, 3.4 mmol) and Et$_3$SiH (5.4 mL, 34.0 mmol) are dissolved in DCM (20.4 mL) at 0°C and TFA (2.62 mL, 34.0 mmol) is added. The reaction is allowed warming to r.t and stirred for 5 hours which is enough time for reaction completion (TLC analysis shows total consumption of the starting benzylidene and the predominance of a high polarity spot). The mixture is then transferred to a pear-shaped flask and the volatiles removed *in vacuo*. The obtained crude is purified by flash chromatography using silica gel as stationary phase and EtOAc/Hex (3:7 mixtures as eluents. Alcohol **6** (1.33 mg, 2.27 mmol,

67%) was isolated as colorless syrup. ^{1}H NMR spectra of this compound was consisted with previously published data[OBJ]
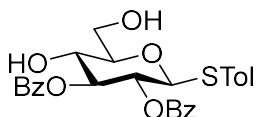
S-pTolyl-2,3-O-dibenzoylglucoside (13): 4,6-Benzylidene glucoside **10** (2.06 g, 3.54 mmol) was dissolved in a mixture of TFA/H_2O (9:1, 4.0 mL) at r.t. and stirred for 60 minutes. After that period TLC analysis shows complete consumption of the starting material. Then TFA and water were removed *in vacuo* with rotary evaporator and the crude diol was purified by flash chromatography with silica gel as stationary phase and EtOAc/Hex mixtures (1:1) as eluents. Compound **7** (1.24 g, 3.34 mmol, 60%) was isolated as a white solid. Compound identity was confirmed by comparison of ^{1}H and ^{13}C NMR spectra data with previously reported data.[OBJ]
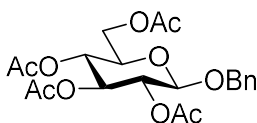
O-benzyl-2,3,4,6-tetra-O-acetylglucoside (15): Glucose pentaacetate **5** (10.07 g, 25.7 mmol) and Benzyl alcohol (5.34 ml, 51.4 mmol) were dissolved in dry Acetonitrile (77.1 mL) and BF_3Et_2O (1.58 mL, 12.85 mmol) was added dropwise and the solution was refluxed at 50 – 80⁰C under stirring. After 6 hours of TLC shows total consumption of the starting material and the reaction was cooled to 0°C and quenched with triethylamine (4.0 mL). After 15 minutes of stirring at 0°C, the volatiles were removed in vacuum and the crude purified by flash chromatography using SiO_2 as stationary phase and EtOAc/Hexanes mixture (3:7) as eluent. O-acetylglycoside **15** (7.55 g, 17.2 mmol, 75.15%) was isolated as a waxy white solid. Compound identity was confirmed by comparison of ^{1}H and ^{13}C NMR spectra data with previously reported data.[511] ^{1}H NMR (400 MHz, $CDCl_3$) δ 7.35 − 7.26 (m, 6H), 5.09 (dd, *J* = 9.3 Hz and 6.1 Hz, H-4), 5.03 (dd, *J* = 8.5 Hz and 9.5 Hz, H-3), 4.99 (dd, *J* = 9.3 Hz

and 7.7 Hz, H-2), 4.82 (d, J = 12.3 Hz, 1H), 4.56 (d, J = 12.3 Hz, 1H), 4.48 (d, J = 7.9 Hz, H-1), 4.21 (dd, J = 12.3, 4.7 Hz, H-6), 4.10 (dd, J = 12.3, 2.4 Hz, H-6'), 3.60 (ddd, J = 9.6, 4.6, 2.4 Hz, H-5), 2.04 (s, 3H), 1.95 (s, 3H), 1.94 (s, 3H), 1.93 (s, 3H). ^{13}C NMR (100 MHz, CDCl$_3$) δ 170.7, 170.3, 169.4, 169.3, 140.9, 136.6, 128.6, 128.5, 128.1, 127.8, 127.7, 127.0, 99.3, 77.3, 77.0, 76.7, 72.8, 71.8, 71.3, 70.7, 68.4, 65.4, 61.9, 20.8, 20.6, 1.0.
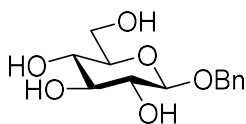
O-benzylglucoside (16): *O*-benzyl-2,3,4,6-tetra-*O*-acetylglucoside **15** (7.24 g, 15.9 mmol) was dissolved in methanol (30.0 mL) and sodium methoxide (100 mg) was added. The suspension was stirred at r.t. for 24 hours which is enough time for the trans-esterification reaction to be completed (shown by TLC analysis). The system was then neutralized with Amberlyst IR-120+ resin followed by filtration. Methanol was removed *in vacuo* with rotary evaporator and the crude dried under high vacuum in a Schlenk line for 24 hours prior to use. Structure of glucopyranoside **16** was confirmed by comparison of its ^{1}H and ^{13}C NMR spectra with previously reported data.[51] ^{1}H NMR (400 MHz, CDCl$_3$) δ 7.32 – 7.18 (m, 5H), 4.75 (d, J = 12.0 Hz, 1H), 4.49 (d, J = 11.4 Hz, 1H), 4.29 (d, J = 5.6 Hz, 1H), 3.71 (s, 2H), 3.51 (s, 1H), 3.35 (s, 2H), 3.13 (s, 1H). ^{13}C NMR (100 MHz, CDCl$_3$) δ 136.0, 127.4, 127.1, 76.3, 76.2, 75.9, 75.7, 70.3, 59.4, 20.0, 13.2.
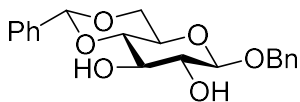
O-benzyl-4,6-benzylideneglucoside (17): *O*-benzylglucoside **16** (1.90 g, 7.0 mmol) and benzaldehyde dimethoxyacetal (1.57 mL, 10.5 mmol) are dissolved in dry DMF (14.0 mL) at r.t. followed by the addition of camphorsulfonic acid (81.30 mg, 0.35 mmol). The reaction is stirred for 18 hours and quenched by addition of Et$_3$N (2.0 mL). System is diluted with DCM, transferred to a separation funnel, and washed with water. The organic layer is collected, dried over

Na$_2$SO$_4$, filtered and the volatiles removed *in vacuo*. Benzylidene adduct is purified by flash chromatography using SiO$_2$ as stationary phase and EtOAc/Hexane (3:7) mixture as eluent. Chromatography afforded compound **17** (2.125 g, 6.17 mmol, 86%) as a waxy white solid. confirmed by comparison of ^{1}H and ^{13}C NMR spectra data with previously reported data. ^{1}H NMR (400 MHz, CDCl$_3$) δ 7.47 – 7.38 (m, Aromatic H's, 10H), 4.96 (d, *J* = 11.6 Hz, 1H), 4.65 (d, *J* = 11.6 Hz, 1H), 4.53 (d, *J* = 7.7 Hz, H-1), 4.39 (dd, *J* = 10.5, 5.0 Hz, 1H), 3.83 (m, 2H), 3.59 (m, 2H), 3.50 (m, 1H), 2.66 (s, 1H), 2.48 (s, 1H). ^{13}C NMR (100 MHz, CDCl$_3$) δ 206.9, 128.6, 128.4, 128.2, 126.7, 126.3, 102.1, 101.9, 80.6, 77.3, 77.2, 77.0, 76.7, 74.6, 73.2, 68.7, 66.5, 30.9.[51]
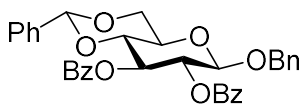
O-benzyl-2,3-O-benzoyl-4,6-benzylideneglucoside (18): 2,3-Diol **17** (1.01 g, 2.92 mmol) was dissolved in pyridine (4.67 mL) and benzoyl chloride (1.01 mL, 8.76 mmol) was added to the solution at r.t. After 8 hours of stirring TLC analysis shows total consumption of the starting material and the volatiles were removed *in vacuo*. Dibenzoylated adduct was then purified by flash silica gel chromatography using EtOAc/Hexanes mixture (2:3) as eluents. Compound **18** (1.68 g, 2.97 mmol 99%) was isolated as a white solid. Compound identity was confirmed by comparison of ^{1}H and ^{13}C NMR spectra with previously reported data. ^{1}H NMR (400 MHz, CDCl$_3$) δ 8.17 - 7.18 (m, 22H), 5.73 (dd, *J* = 9.6 Hz and 9.5 Hz, H-3), 5.56 (dd, *J* = 6.5 Hz and 10.5 Hz, H-2), 4.91 (d, *J* = 12.5 Hz, 1H), 4.82 (d, *J* = 7.8 Hz, H-1), 4.68 (d, *J* = 12.5 Hz, 1H), 4.46 (dd, *J* = 10.5, 4.9 Hz, -6H), 3.95 (dd, *J* = 9.3, 5.0 Hz,H-4), 3.91 (d, *J* = 5.0 Hz and 10.4 Hz,H-6'), 3.67 (m, H-5). ^{13}C NMR (100 MHz, CDCl$_3$) δ 165.2, 162.4, 136.8, 136.5, 134.5, 133.2, 133.1, 130.6, 129.9, 129.8, 129.4, 129.3, 129.0, 128.9, 128.4, 128.3, 128.2, 128.2,

127.9, 127.8, 126.7, 126.1, 101.5, 100.0, 78.8, 77.3, 77.2, 77.0, 76.7, 72.3, 72.1, 70.8, 68.7, 66.6.[52]
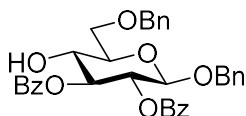
O-benzyl-2,3-O-benzoyl-6-O-benzylglucoside (19): Benzylidene **18** (0.952 g, 1.68 mmol) and Et$_3$SiH (2.68 mL, 34.0 mmol) are dissolved in DCM (20.4 mL) at 0°C and TFA (2.62 mL, 16.8 mmol) is added. The reaction is allowed warming to r.t and stirred for 5 hours which is enough time for reaction completion (TLC analysis shows total consumption of the starting benzylidene and the predominance of a high polarity spot). The mixture is then transferred to a pear-shaped flask and the volatiles removed *in vacuo*. The obtained crude is purified by flash chromatography using silica gel as stationary phase and EtOAc/Hex (3:7) mixtures as eluents. Alcohol **19** (0.60 g, 1.05 mmol, 63%) was isolated as colorless syrup.
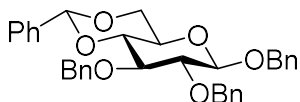
O-benzyl-2,3-benzyl-4,6-O-benzylideneglucoside (20): 2,3-Diol **18** (1.02 g, 2.96 mmol) is dissolved in dry DMF (14.8 mL) and cooled to 0°C with an ice-bath. Sodium Hydride (213 mg, 8.88 mmol, 60% suspension in mineral oil) was added portion-wise and the resulting suspension was kept under vigorous stirring at 0°C for 20 minutes. Benzyl bromide (0.421 mL, 3.55 mmol) was then added, and the system allowed warming to r.t. After 2 hours TLC analysis shows total consumption of the starting alcohol and the predominance of one single spot. The mixture was cooled again to 0°C, quenched by MeOH (10.0 mL) addition and transferred to a pear-shaped flask for solvent is removed *in vacuo*. The crude was then purified by flash chromatography over SiO$_2$ and using EtOAc/Hexanes (2:3) mixture as eluent. Benzylated adduct **20** (1.6 g, 2.97 mmol, 99%) was isolated as a waxy white solid. Compound identity

was confirmed by comparison of ^{1}H and ^{13}C NMR spectra data with previously reported data.[51]
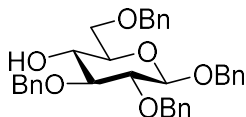
O-benzyl-2,3,6-O-benzylideneglucoside (21): Benzylidene **20** (0.707 g, 1.31 mmol) and Et$_3$SiH (2.092 mL, 13.1 mmol) are dissolved in DCM (4.3 mL) at 0°C and TFA (1.01 mL, 13.1 mmol) is added. The reaction is allowed warming to r.t and stirred for 5 hours which is enough time for reaction completion (TLC analysis shows total consumption of the starting benzylidene and the predominance of a high polarity spot). The mixture is then transferred to a pear-shaped flask and the volatiles removed *in vacuo*. The obtained crude is purified by flash chromatography using silica gel as stationary phase and EtOAc/Hex (3:7) mixtures as eluents. Alcohol **21** (0.495 g, 0.92 mmol, 70%) was isolated as colorless syrup. Compound identity was confirmed by comparison of ^{1}H and ^{13}C NMR spectra data with previously reported data.[51]
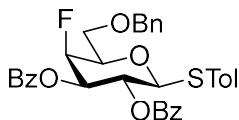
S-pTolyl-2,3-O-benzoyl-6-O-benzyl-4-fluorogalactoside (22): To a solution of compound **11** (175 mg, 0.30 mmol) in DCM (870 μL) was added pyridine (40 μL). The resulting solution was cooled (-78°C) and stirred under argon, and Tf$_2$O (73 μL, 0.448 mmol) was added. The reaction mixture was warmed to room temperature and, after 40 min, TLC analysis (ethyl acetate–hexane, 2 : 3 v/v) showed complete conversion of starting material into triflate intermediate (R$_f$ 0.88). The reaction mixture was diluted with DCM (10 ml) and was washed successively with saturated aq. sodium hydrogen carbonate (2 × 10 ml) and brine (2 × 10 ml). The organic phase was dried using sodium sulphate and concentrated to dryness in vacuum to yield a sticky yellow

solid. This compound was immediately dissolved in THF (900 μL) stirred under argon, and TBAF solution (1.1 M in THF, dried over molecular sieves 4 Å; 250 μL, mmol) was added. A color change from yellow to deep red was observed and immediate TLC analysis (ethyl acetate–cyclohexane, 2 : 3 v/v) showed complete conversion of the intermediate (Rf 0.88) into a major product (Rf 0.67). The reaction mixture was concentrated to dryness in vacuo, the resulting brown solid was dissolved in DCM (10 ml), and the solution was washed with brine (2 × 10 ml). The organic phase was dried (MgSO₄) and concentrated to dryness in vacuo to yield a sticky yellow brown solid. Crude fluorinated analog **22** was purified by flash chromatography with silica gel as stationary phase and EtOAc/Hex mixtures (1:1) as eluents. Compound **22** (100.3 mg, 0.216 mmol, 57.3%) was isolated as a white solid. ^1H NMR (CDCl₃, 400 MHz) δ 7.97 - 7.07 (m, Aromatic H's), 5.70 (dd, J = 9.9 Hz and 9.9 Hz, H-2), 5.36 (ddd, J = 2.1, 9.9 Hz and 27.6 ($^3J_{HF}$) Hz, H-3), 5.12 (dd, J = 2.1 and 50.1 ($^2J_{HF}$) Hz, H-4), 4.88 (d, J = 9.9 Hz, H-1), 4.58 (s, 2H, PhC$\underline{H}_2$O), 3.94 (ddd, J = 6.5, 6.5 and 26.7 ($^3J_{HF}$) Hz, H-5), 3.79 (m, H-6 and H-6'), δ 2.32 (s, 3H). ^{13}C NMR (100 MHz, CDCl₃) δ 206.9, 165.8, 165.1, 138.5, 137.7, 133.5, 133.4, 133.3, 129.9, 129.8, 129.7, 129.4, 128.9, 128.5, 128.5, 128.4, 128.3, 127.9, 127.7, 87.3, 86.8, 85.5, 77.3, 77.0, 76.7, 76.3, 76.1, 73.7, 73.6, 73.4, 67.9, 67.5, 30.9, 21.2.
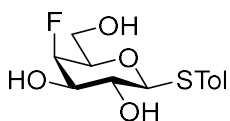
S-pTolyl-4-fluorogalactoside (26): Thioglycoside **22** (47.5 mg, 0.081 mmol) was dissolved in methanol (0.5 mL) and sodium methoxide (0.1 mg) was added. The suspension was stirred at r.t. for 24 hours which is enough time for the trans-esterification reaction to be completed (shown by TLC analysis). The system was then neutralized with Amberlyst IR-120+ resin followed by filtration. Methanol was

removed *in vacuo* with rotary evaporator and the crude dried under high vacuum in a Schlenk line for 24 hours prior to use. Structure of deprotected fluorinated compound **30** was confirmed by comparison of its ^{1}H and ^{13}C NMR spectra with previously reported data. ^{1}H NMR (400 MHz, CDCl$_3$) δ 8.05 -7.11 (m, Aromatic H's, 4H), 4.86 (d, *J* = 49.0 Hz, H-4), 4.46 (d, *J* = 9.2 Hz, H-1), 3.80 – 3.68 (m, 3H), 3.65 (d, *J* = 9.2 Hz, 2H), 1.25 (s, 3H). ^{13}C NMR (100 MHz, CDCl$_3$) δ 133.3, 132.9, 129.9, 129.6, 128.5, 128.4, 127.9, 127.7, 89.2, 88.5, 87.4, 77.3, 77.0, 76.7, 76.4, 76.2, 73.7, 73.7, 73.6, 69.8, 67.8, 67.7, 60.4, 52.1, 31.6, 22.7, 21.2, 14.2, 14.1.
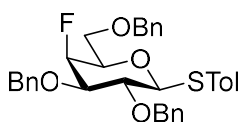
S-pTolyl-2,3,6-O-benzyl-4-fluorogalactoside (27): Alcohol **30** (30.1 mg, 0.182 mmol) is dissolved in dry DMF (1.0 mL) and cooled to 0°C with an ice-bath. NaH (13.1 mg, 0.546 mmol, 60% suspension in mineral oil) was added portion-wise and the resulting suspension was kept under vigorous stirring at 0°C for 20 minutes. Benzyl bromide (26 μL, 0.21 mmol) was then added and the system allowed warming to r.t. After 4 hours TLC analysis shows total consumption of the starting alcohol and the predominance of one single spot. The mixture was cooled again to 0°C, quenched by MeOH (0.5 mL) addition and transferred to a pear-shaped flask for solvent removal with rotary evaporator. The crude was then purified by flash chromatography over SiO$_2$ and using EtOAc/Hexanes (1:9) mixture as eluent. Benzylated adduct **31** (22.5 mg, 0.051 mmol, 75%) was isolated as a waxy white solid. ^{1}H NMR (400 MHz, CDCl$_3$) δ 7.36 (dd, *J* = 12.6, 7.8 Hz, 4H), 7.31 – 7.15 (m, 13H), 7.00 (d, *J* = 7.8 Hz, 2H), 4.81 (d, *J* = 49.1 Hz, H-4), 4.71 (d, *J* = 10.0 Hz, 1H), 4.69 – 4.57 (m, 1H), 4.51 (d, *J* = 9. Hz 1H), 3.74 – 3.62 (m, 1H), 3.59 – 3.43 (m, 1H), 2.24 (s, 3H), 1.29 (d, *J* = 22.6 Hz, 2H), 0.85 – 0.60 (m, 4H). ^{13}C NMR

(100 MHz, CDCl$_3$) δ 138.2, 137.8, 137.8, 137.6, 132.7, 129.7, 129.4, 128.6, 128.5, 128.4, 128.3, 127.9, 127.8, 127.8, 87.9, 86.7, 84.9, 81.2, 80.9, 77.3, 77.0, 76.9, 76.7, 75.9, 75.8, 75.7, 73.7, 72.2, 67.8, 67.8, 36.6, 33.7, 31.9, 30.2, 29.7, 29.4, 26.7, 22.7, 21.1, 14.1.
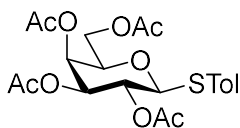
S-pTolyl-2,3,4,6-tetra-O-acetylgalactoside (28): Galactose pentaacetate **18** (13.6 g, 34.8 mmol) and tolylmercaptan (4.76 g, 38.3 mmol) were dissolved in dry DCM (70.0 mL) and cooled to 0°C. BF$_3$Et$_2$O (1.3 mL, 10.4 mmol) was added dropwise and the solution was allowed to warm to r.t. under stirring. After 5 hours of TLC shows total consumption of the starting material and the reaction was cooled to 0°C and quenched with triethylamine (5.0 mL). After 15 minutes of stirring at 0°C, the volatiles were removed *in vacuo* and the crude purified by flash chromatography using SiO$_2$ as stationary phase and EtOAc/Hexanes mixture (3:7) as eluent. Thioglycoside **28** (14.4 g, 31.7 mmol, 91%) was isolated as a waxy white solid. Compound identity was confirmed by comparison of ^{1}H and ^{13}C NMR spectra data with previously reported data.[10]
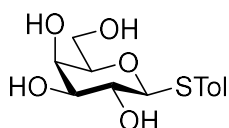
S-pTolylgalactoside (29): Thioglycoside **28** (12.1 g, 26.6 mmol) was dissolved in methanol (50.0 mL) and sodium methoxide (300.1 mg) was added. The suspension was stirred at r.t. for 24 hours which is enough time for the trans-esterification reaction to be completed (shown by TLC analysis). The system was then neutralized with Amberlyst IR-120+ resin followed by filtration. Methanol was removed *in vacuo* with rotary evaporator and the crude dried under high vacuum in a Schlenk line for 24 hours prior to use. Structure of tetraol **29** was confirmed by comparison of its ^{1}H and ^{13}C NMR spectra with previously reported data.[53]
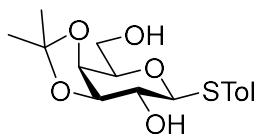
S-pTolyl-3,4-acetonidegalactoside (30): Tetraol **29** (4.70 g, 17.3 mmol) was dissolved in 2,2-dimethoxypropane (100.0 mL) at r.t. and camphor sulfonic acid (160.0 mg, 0.68 mmol) was added to the solution. After 48 hours of stirring at r.t. TLC shows total consumption of the starting material and the predominance of 2 spots corresponding to the desired 3,4-acetonide and 3,4-acetonide-6-hemiketal byproduct. Reaction was quenched by addition of Et_3N (5.0 mL), the volatiles were removed *in vacuo* and the residue re-dissolved in EtOAc and percolated through a bed of silica gel. The mixture was then re-dissolved in a $MeOH/H_2O$ mixture (10:1, 50 mL) and refluxed until 6-hemiketal (top TLC spot) hydrolysis was complete (usually after 4 hours of reflux). Acetonide was then purified by flash chromatography using SiO_2 as stationary phase and EtOAc/Hexanes mixture (3:2) as eluent. The respective diol **30** (4.0 g, 12.3 mmol, 71%) was isolated as a white solid. Compound identity was confirmed by comparison of ^{1}H and ^{13}C NMR spectra data with previously reported data.[54]
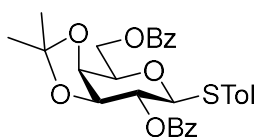
S-pTolyl-3,4-acetonide-2,6-benzoylgalactoside (31): Diol **30** (4.0 g, 12.3 mmol) was dissolved in pyridine (20.0 mL) and benzoyl chloride (4.3 mL, 37.0 mmol) was added to the solution at r.t. After 8 hours of stirring TLC analysis shows total consumption of the starting material and the volatiles were removed *in vacuo*. Dibenzoylated adduct was then purified by flash silica gel chromatography using EtOAc/Hexanes mixture (3:7) as eluents. Compound **31** (6.26 g, 11.7 mmol 95%) was isolated as a white solid. Compound identity was confirmed by comparison of ^{1}H and ^{13}C NMR spectra with previously reported data.[10]
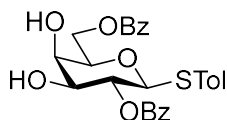
S-pTolyl-2,6-benzoylgalactoside (32): Acetonide **31** (10.2 g, 19.1 mmol) was dissolved in a mixture of TFA/H_2O (9:1, 20.0 mL) at r.t. and stirred for 10 minutes. After that period TLC analysis shows complete consumption of the starting material. Then TFA and water were removed *in vacuo* with rotary evaporator and the crude diol was purified by flash chromatography with silica gel as stationary phase and EtOAc/Hexane mixtures (1:1) as eluents. Compound **32** (8.70 g, 17.6 mmol, 92%) was isolated as a white solid. [10]
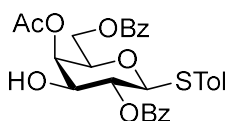
S-pTolyl-4-acetyl-2,6-benzoylgalactoside (33): 3,4-Diol **32** (4.68 g, 9.5 mmol), triethylorthoacetate (5.4 mL, 29.5 mmol) and camphorsulfonic acid were dissolved in dry $CHCl_3$ (45.0 mL) and stirred at r.t. until the *trans*-esterification reaction was complete (TLC analysis). The galactose orthoester product was then partially hydrolyzed *in situ* by addition of MeCN/H_2O (5:1, 5.0 mL) and stirring at r.t. After the reaction was complete, purification was performed by flash chromatography using SiO_2 as stationary phase and EtOAc/Hexanes mixture (2:4) as eluent. 4-*O*-acetate **7** (4.8 g, 8.9 mmol, 94%) was obtained as a white solid. Compound identity was confirmed by comparison of ^{1}H and ^{13}C NMR spectra with previously reported data.[10]
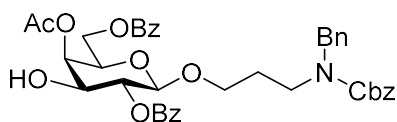
**O-[3-(N-benzyl-N-carboxybenzyl)propyl]-4-acetyl-2,6-benzoylgalactoside (34):** Monosaccharide **33** (885 mg, 1.65 mmol) and Alcohol **25** (0.988 g, 3.3 mmol) were dissolved in Acetonitrile (6.6 mL) in the presence of 4 Å molecular sieves (200.0 mg). The suspension was stirred at r.t. for 15 mins and then cooled to -20 - -30°C using dry ice. NIS (408.3 mg, 1.815 mmol) was then

added followed by TMSOTf (29.8 μL, 0.165 mmol) and vigorous stirring was continued

until total consumption of the donor was observed (TLC, 3 hours). Reaction was then

diluted with ethyl acetate (5.0 mL), quenched with Et₃N (1.0 mL), allowed to warm to r.t.,

filtered over a Celite® bed, transferred to a separation funnel and washed with NaS_2O_3.

The organic fraction was dried over Na_2SO_4, the volatiles removed *in vacuo* and the crude

purified by flash chromatography using silica gel as stationary phase and EtOAc/Hexanes

(1:2) gradient as eluent solutions. Glycosylated monosaccharide **26** (787.3 mg, 1.08

mmol,88.93%) was isolated as a white solid.
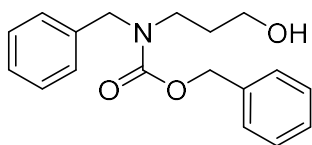
3-(N-benzyl-N-carboxybenzyl)propanol (37): To a solution of 3-amino-1-propanol **35** (14.73 g, 196 mmol) in MeOH (49 mL)

at 0°C were added $HC(OMe)_3$ (21.50 mL, 196 mmol) and benzaldehyde (20 mL, 196 mmol).

The reaction mixture was warmed to room temperature under an argon atmosphere.

After stirring at the same temperature for 3.5 h, $NaBH_4$ (7.41 g, 196 mmol) as added at

0°C. Then, the reaction mixture was stirred for 10 h at room temperature. After quenching

the reaction mixture by adding H_2O at 0°C, the resulting mixture was concentrated under

reduced pressure and then diluted with $CHCl_3$. The organic phase was separated, and the

aqueous phase was extracted three times with $CHCl_3$. The combined organic extracts

were washed with brine, dried over $MgSO_4$, filtered, and concentrated under reduced

pressure. The crude material was used in the next reaction without further purification.

To a solution of the crude material in CH_2Cl_2 (196 mL) and H_2O (137.2 mL) was added

K_2CO_3 (23.02 g, 166.6 mmol) at 0 °C. After the reaction mixture was stirred vigorously at

room temperature for 10 min under an argon atmosphere, CbzCl (28.0 mL, 196 mmol)

was added at 0 °C over 60 min. After stirring at room temperature for 12 h under an argon atmosphere, the reaction mixture was diluted with CH_2Cl_2 and H_2O. The organic phase was separated, and the aqueous phase was extracted three times with CH_2Cl_2. The combined organic extracts were washed with brine, dried over $MgSO_4$, filtered, and concentrated under reduced pressure. The crude material was purified by silica gel flash column chromatography(EtOAc/n-hexane = 50 : 50) to afford N-(benzyl)benzyloxycarbonyl 3-amino-1-propanol 25 (14.40 g, 98% in two steps) as a colorless oil. ^{1}H NMR (400 MHz, $CDCl_3$) δ 7.38-7.28 (m, 8H), 7.19 - 7.18 (m, 2H), 5.19 (s, 2H), 4.47 (s, 2H), 3.55 (dd, *J* = 5.2 and 5.2, 2H), 3.45 (dd, *J* = 5.7 and 5.7, 2H), 1.65 (m, 2H). ^{13}C NMR (100 MHz, $CDCl_3$) δ 204.8, 155.3, 135.2, 134.2, 126.4, 126.3, 125.9, 125.8, 125.3, 125.2, 75.1, 75.0, 74.8, 74.5, 65.5, 58.2, 56.3, 48.0, 40.7, 28.7, 27.9, 12.0.

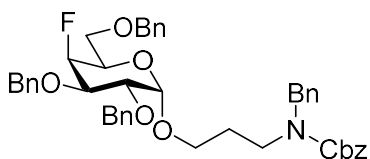**O-[3-(N-benzyl-N-carboxybenzyl)propyl]-2,3,6-benzyl-4-fluorogalactoside (38):** Monosaccharide **31** (9.1 mg, 0.0162 mmol) and Alcohol **25** (9.7 mg, 3.3 mmol) were dissolved in diethylether (65.12 μL) in the presence of 4 Å molecular sieves (1.0 mg). The suspension was stirred at r.t. for 15 mins and then cooled to -20 - -30°C using dry ice. NIS (4.0 mg, 0.0172 mmol) was then added followed by TMSOTf (0.3 μL, 1.6 μmol) and vigorous stirring was continued until total consumption of the donor was observed (TLC 2 hours). Reaction was then diluted with ethyl acetate (5.0 mL), quenched with Et_3N (0.5 mL), allowed to warm to rt, filtered over a Celite® bed, transferred to a separation funnel and washed with NaS_2O_3. The organic fraction was dried over Na_2SO_4, the volatiles removed *in vacuo* and the crude purified by flash chromatography using silica gel as

stationary phase and EtOAc/Hexanes (1:2) gradient as eluent solutions. Glycosylated monosaccharide **38** (8.2 mg, 0.011 mmol, 90 %) was isolated as a yellow solid. * Compound identity is pending to be confirmed by NMR. TLC analysis showed that this product has a lower R_f value respect to the donor **27** and higher R_f respect to alcohol **37**. In addition, compound **38** stains strongly with H_2SO_4 and Ninhydrin (donor **27** stains with H_2SO_4 only) providing evidence of the successful installation of the aglycone.
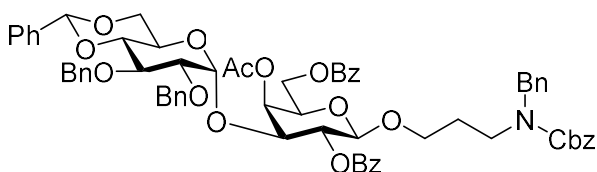
S-pTolyl-2,3-O-dibenzyl-4,6-O-benzylideneglucoside-1→4-O-[3-(N-benzyl-N-carboxybenzyl)propyl]-2,6-O-dibenzoyl-4-O-acetylgalactoside (42): Monosacharide acceptor **26** (571.5 mg, 0.785 mmol) and donor **27** (653.3 mg, 1.17 mmol) were dissolved in Diethylether (3.2 mL) in the presence of 4Å molecular sieves (200.0 mg). The suspension was stirred at r.t. for 15 mins and then cooled to -20 - 30°C using dry ice. NIS (353.3 mg, 1.57 mmol) was then added followed by TMSOTf (14.2 μL, 0.0785 mmol) and vigorous stirring was continued until total consumption of the donor was observed (TLC, 3 hours). Reaction was then diluted with ethyl acetate (5.0 mL), quenched with Et_3N (1.0 mL), allowed to warm to r.t., filtered over a Celite® bed, transferred to a separation funnel and washed with NaS_2O_3. The organic fraction was dried over Na_2SO_4, the volatiles removed *in vacuo* and the crude purified by flash chromatography using silica gel as stationary phase and EtOAc/Hexanes (3:7) gradient as eluent solutions. Glycosylated disaccharide **28** (508.8 mg, 0.699 mmol, 89%) was isolated as a white solid. * The presence of the signature signals of the two anomeric

and benzylidene hydrogens in the ^{1}H NMR spectra, provide evidence that this compound

was formed and isolated. However, confirmation of compound identity is pending.
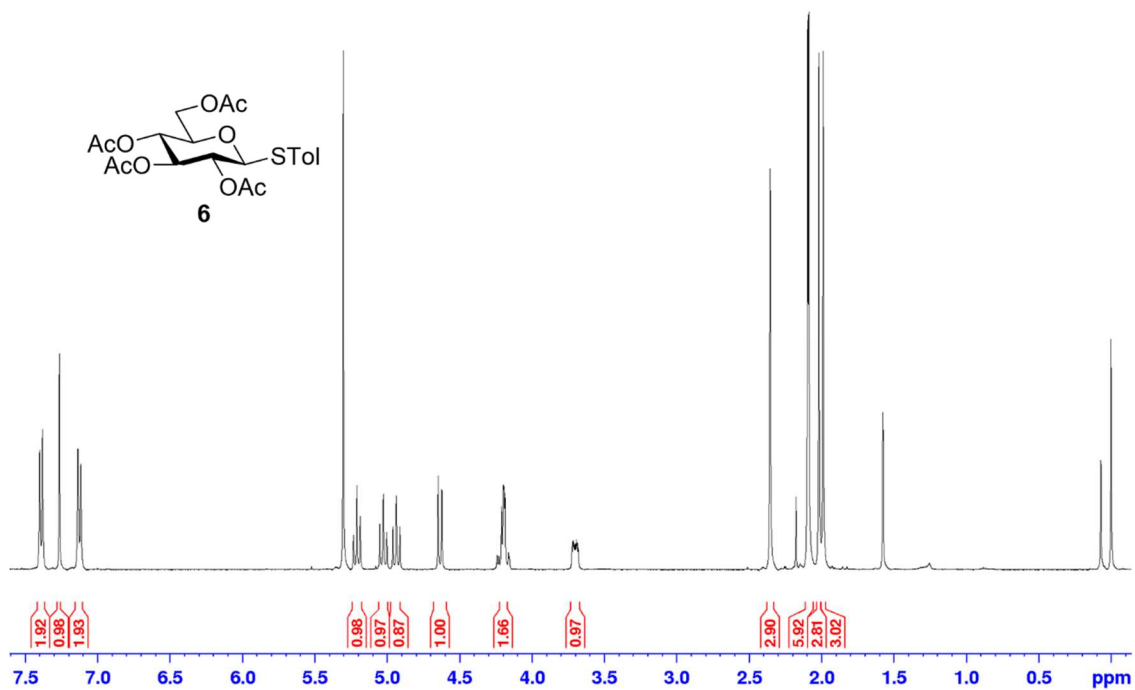
Figure 1.15. ^{1}H NMR (CDCl$_3$, 400 MHz) spectra of compound **6.**
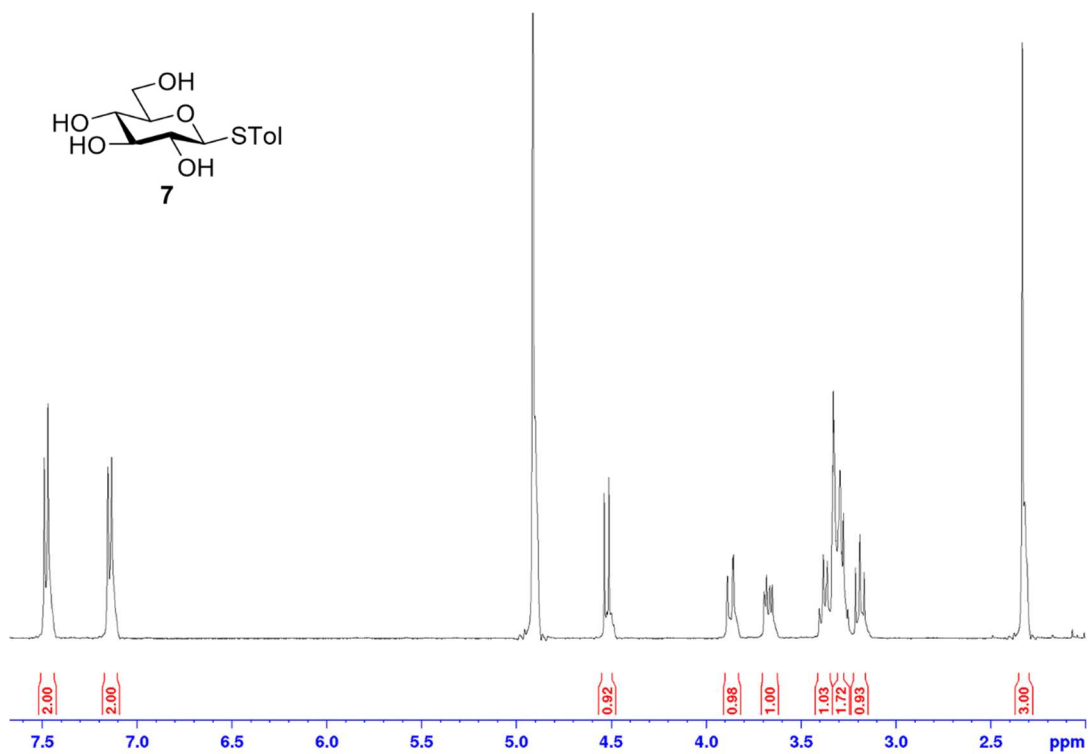
Figure 1.16. ^{1}H NMR (D$_2$O, 400 MHz) spectra of compound **7.**
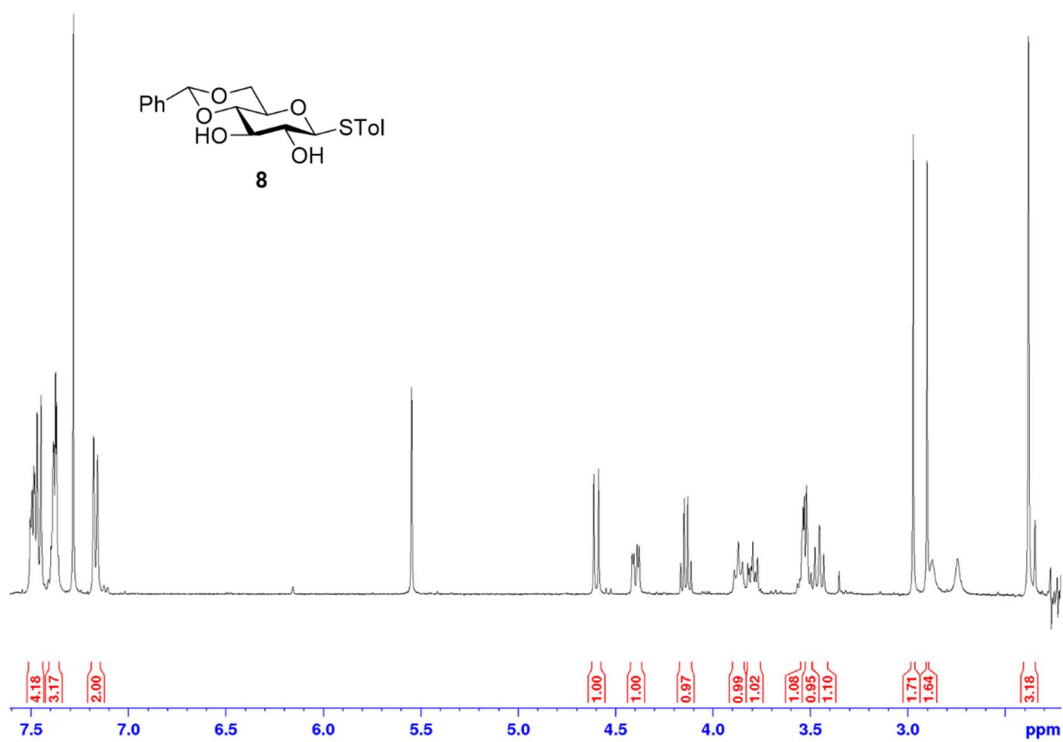
Figure 1.17. ^1H NMR (CDCl$_3$, 400 MHz) spectra of compound **8.**
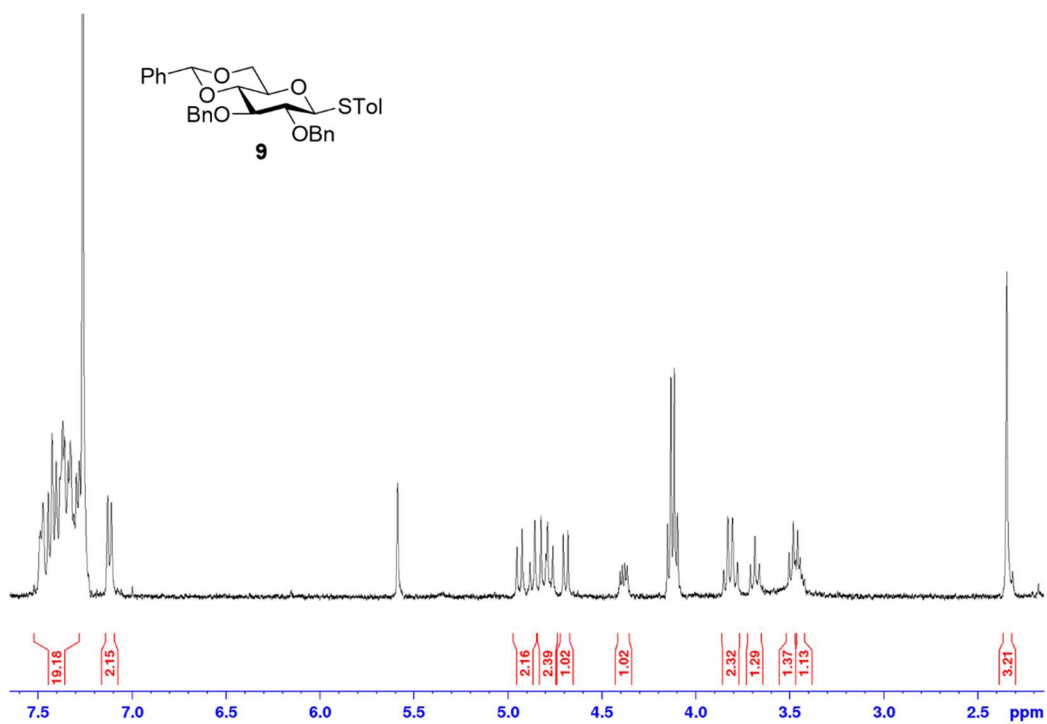
Figure 1.18. ^1H NMR (CDCl$_3$, 400 MHz) spectra of compound **9.**
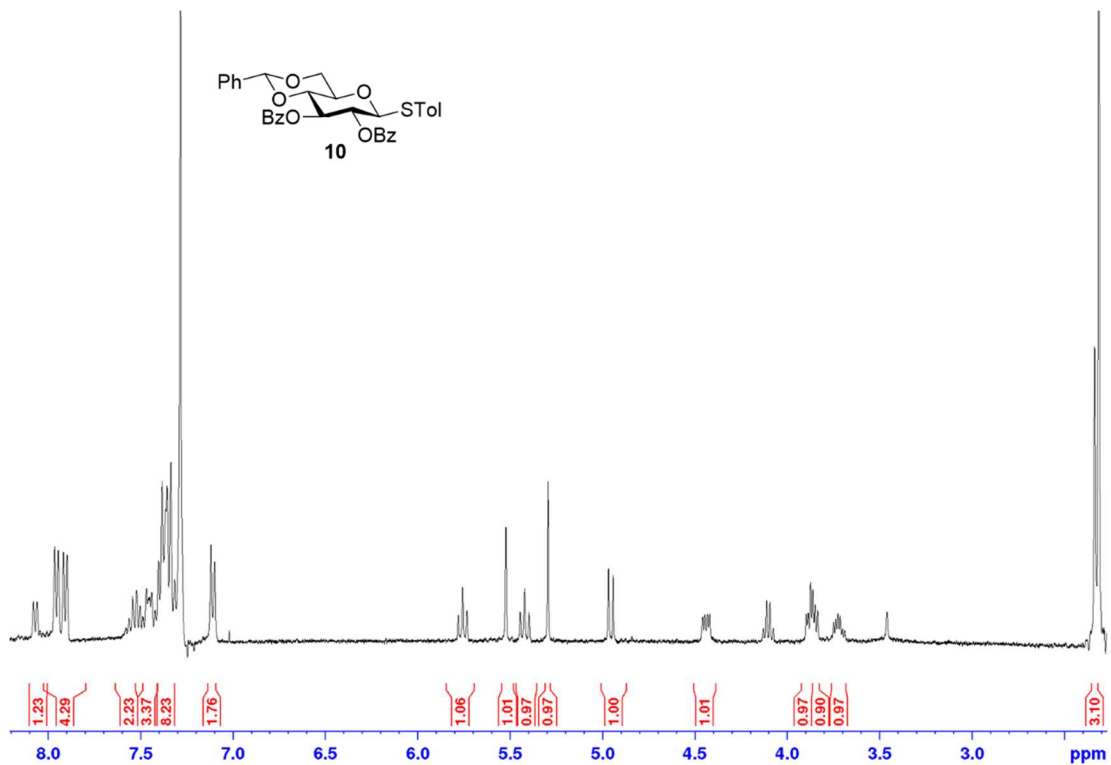
Figure 1.19. ^{1}H NMR (CDCl$_3$, 400 MHz) spectra of compound **10.**
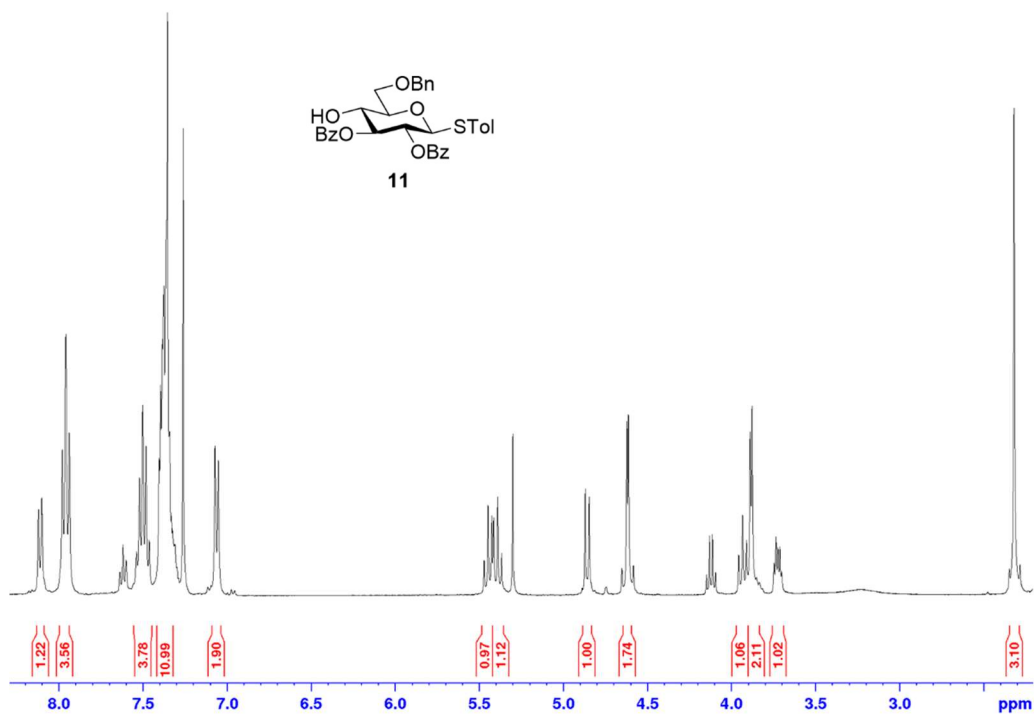
Figure 1.20. ^{1}H NMR (CDCl$_3$, 400 MHz) spectra of compound **11.**

62
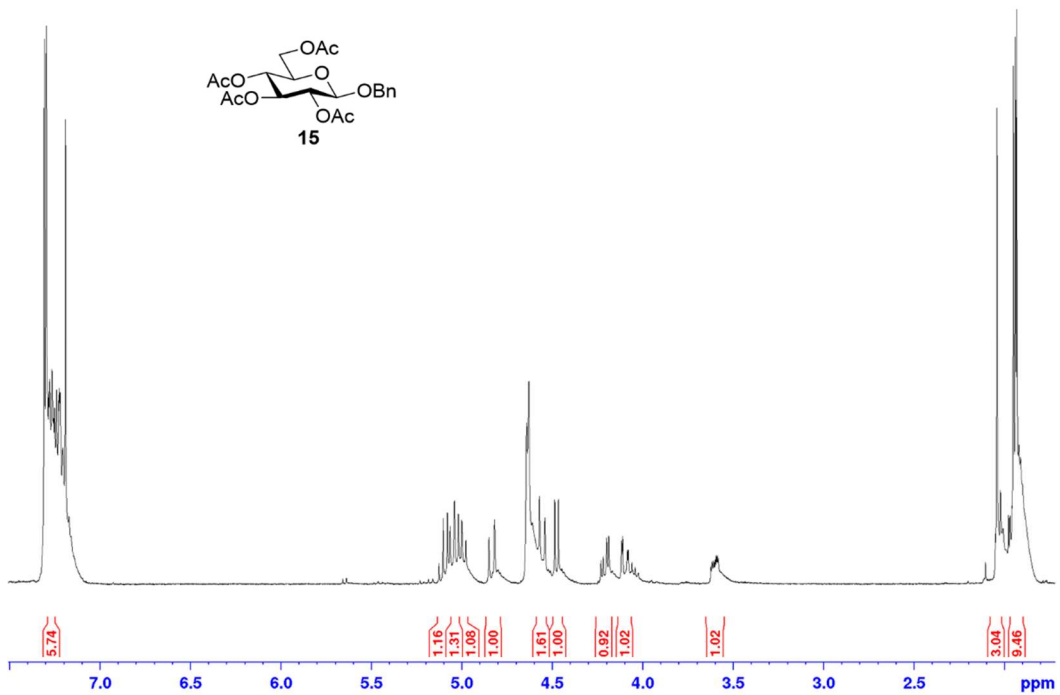
Figure 1.21. ^{1}H NMR (CDCl$_3$, 400 MHz) spectra of compound **15.**
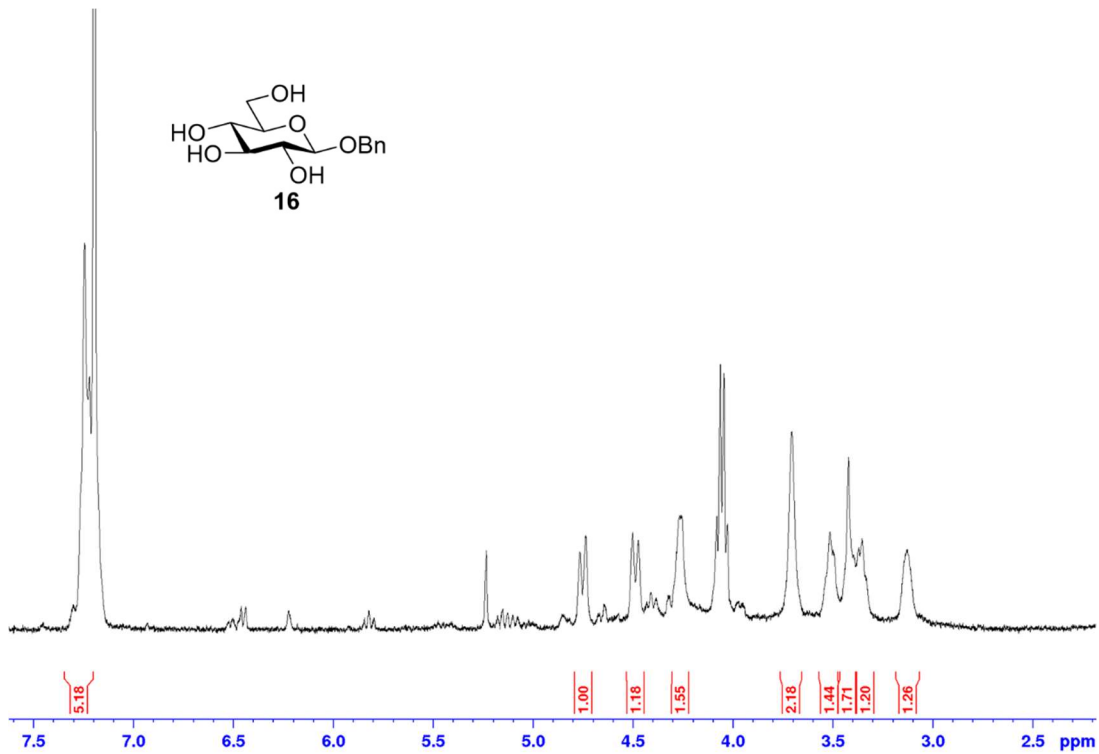
Figure 1.22. ^{1}H NMR (CD$_3$OD, 400 MHz) spectra of compound **16.**
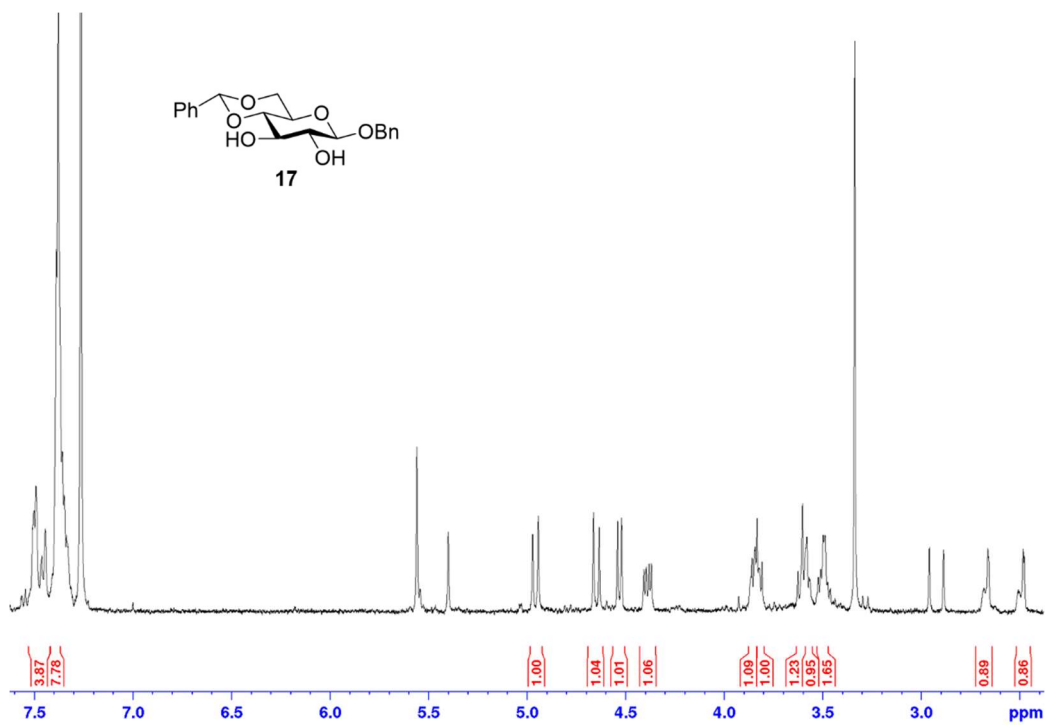
Figure 1.23. ^{1}H NMR (CDCl₃, 400 MHz) spectra of compound **17.**
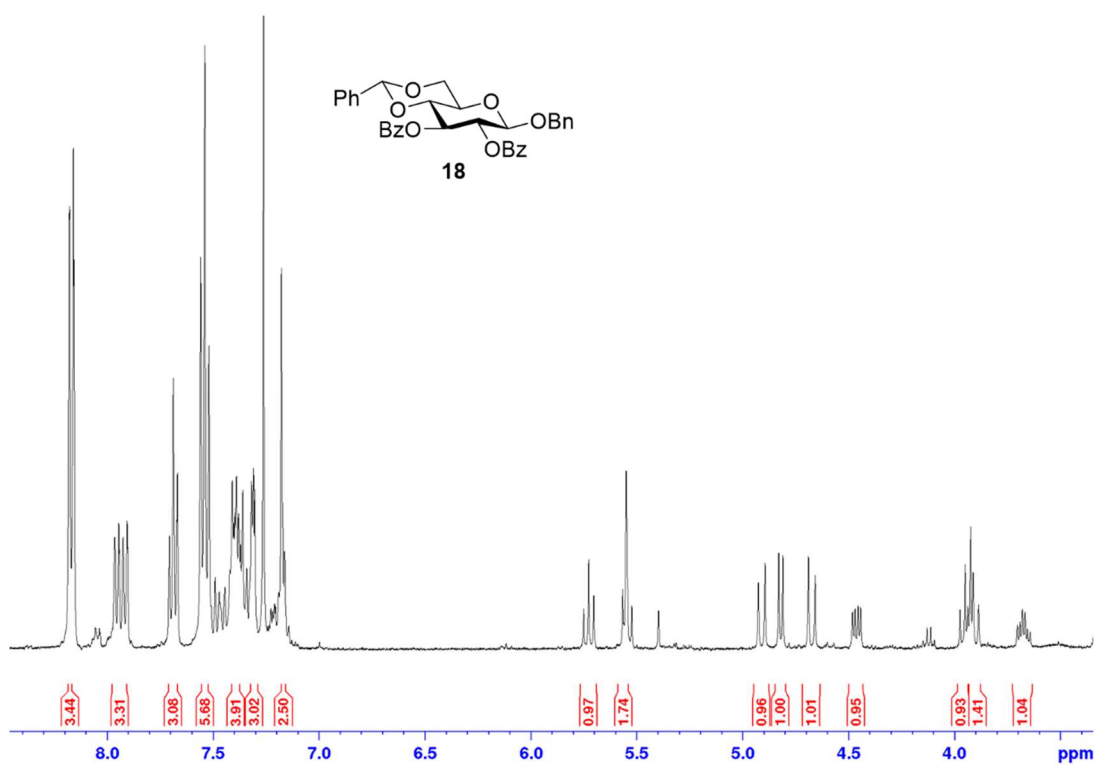
Figure 1.24. ^{1}H NMR (CDCl₃, 400 MHz) spectra of compound **18.**
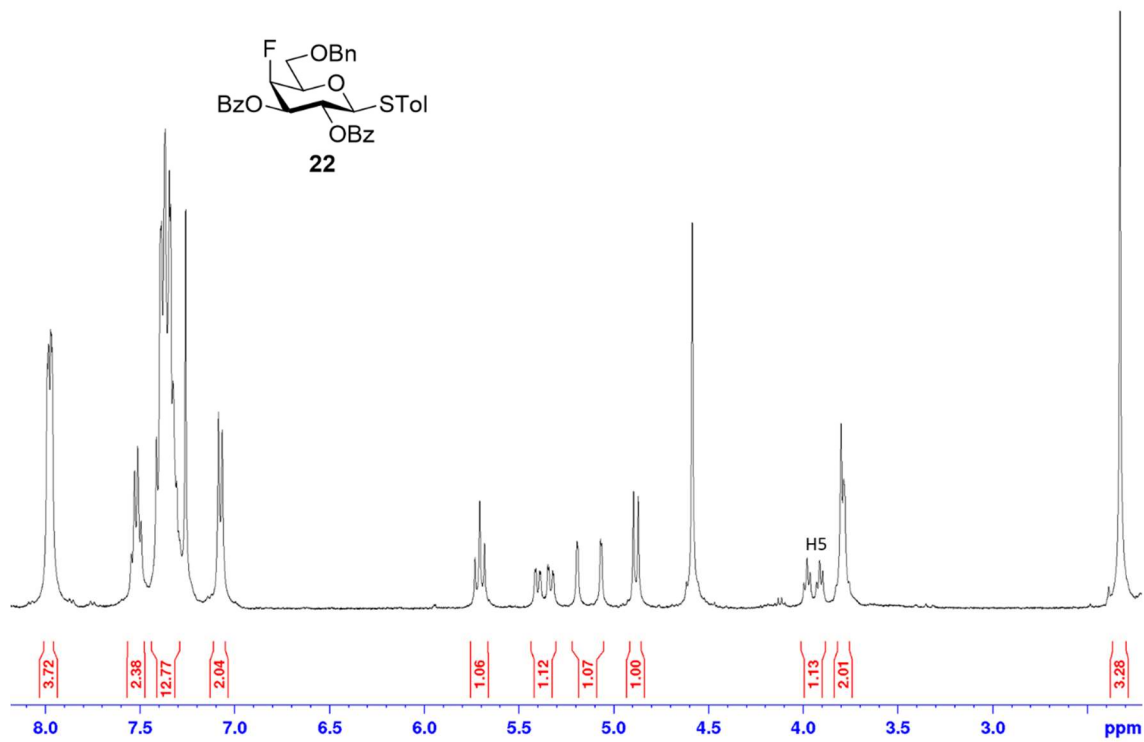
Figure 1.25. ^{1}H NMR (CDCl$_3$, 400 MHz) spectra of compound **22.**
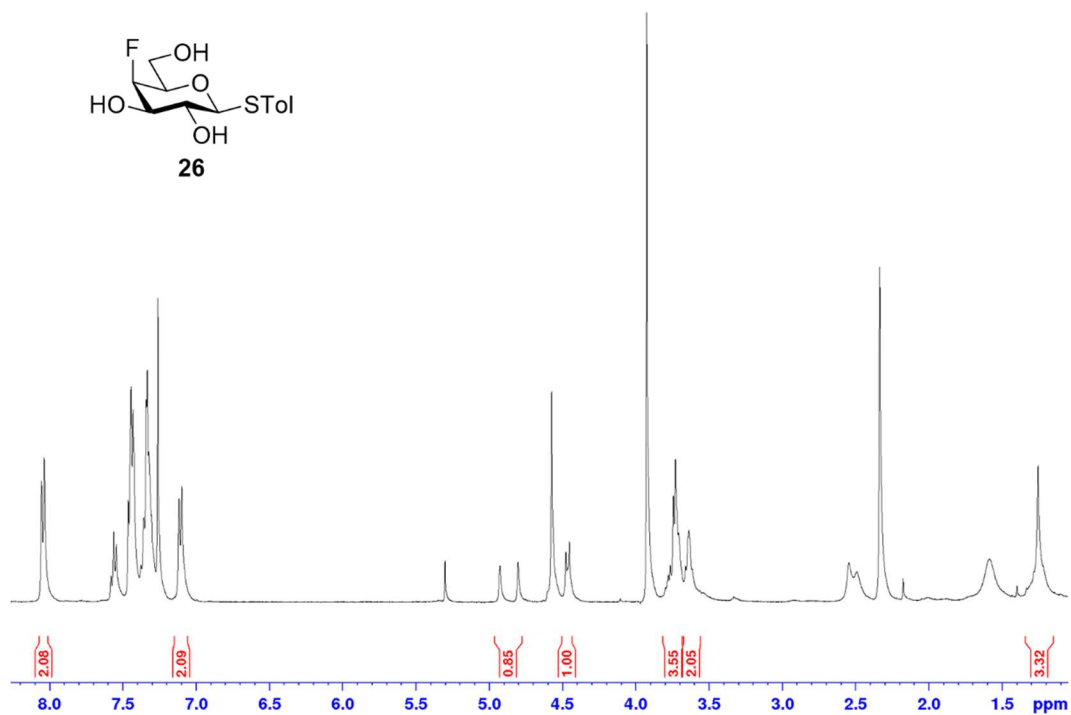
Figure 1.26. ^{1}H NMR (CD$_3$OD, 400 MHz) spectra of compound **26.**
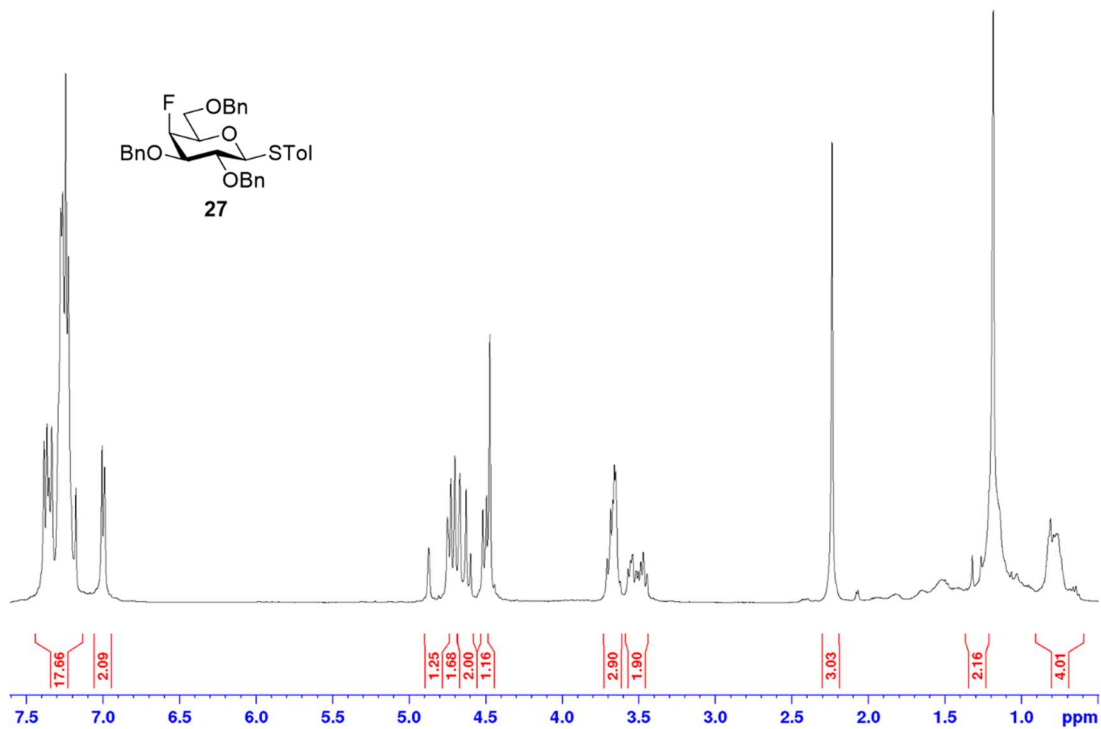
Figure 1.27. ^{1}H NMR (CDCl$_3$, 400 MHz) spectra of compound **27.**
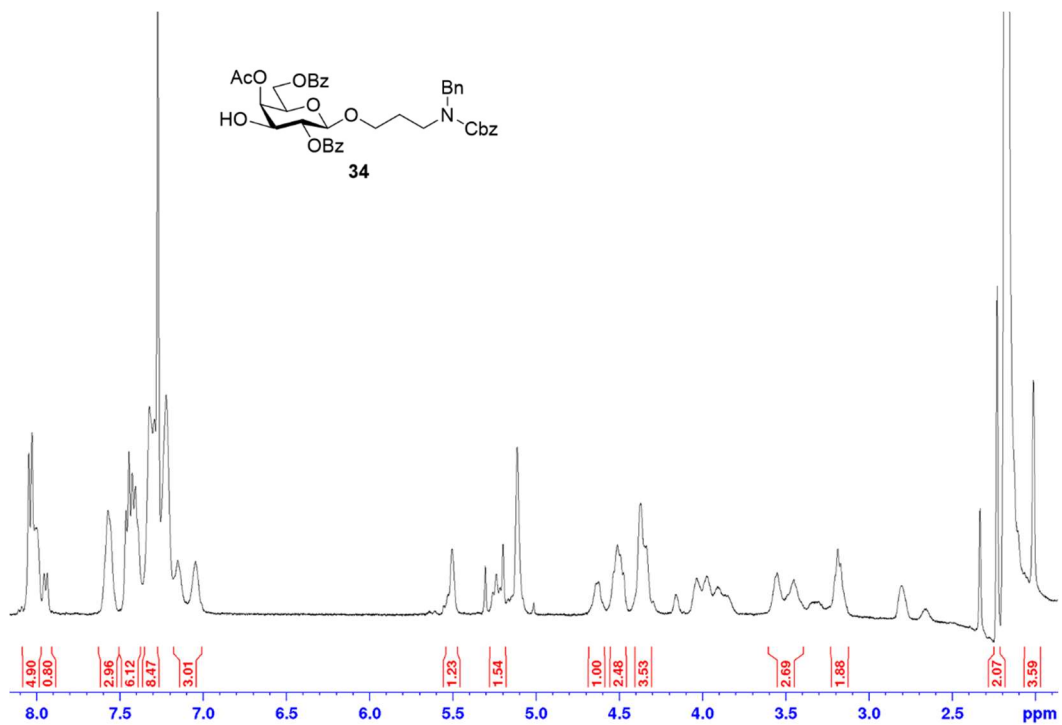
Figure 1.28. ^{1}H NMR (CDCl$_3$, 400 MHz) spectra of compound **34.**
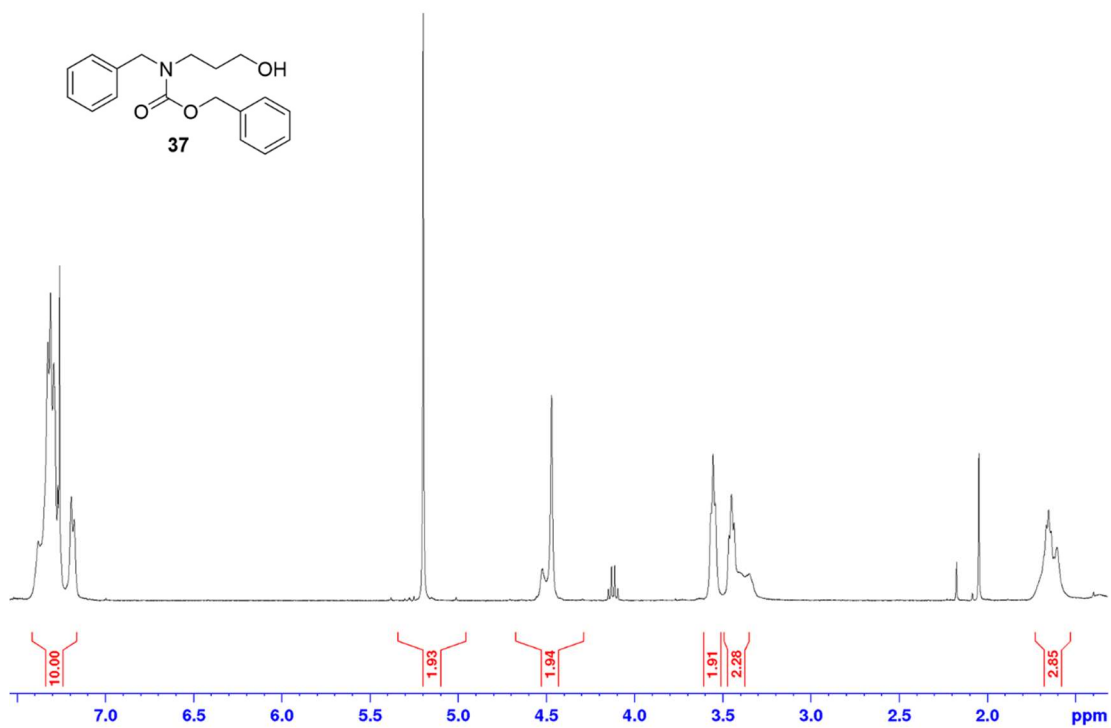
Figure 1.29. ^{1}H NMR (CDCl$_3$, 400 MHz) spectra of compound **37.**
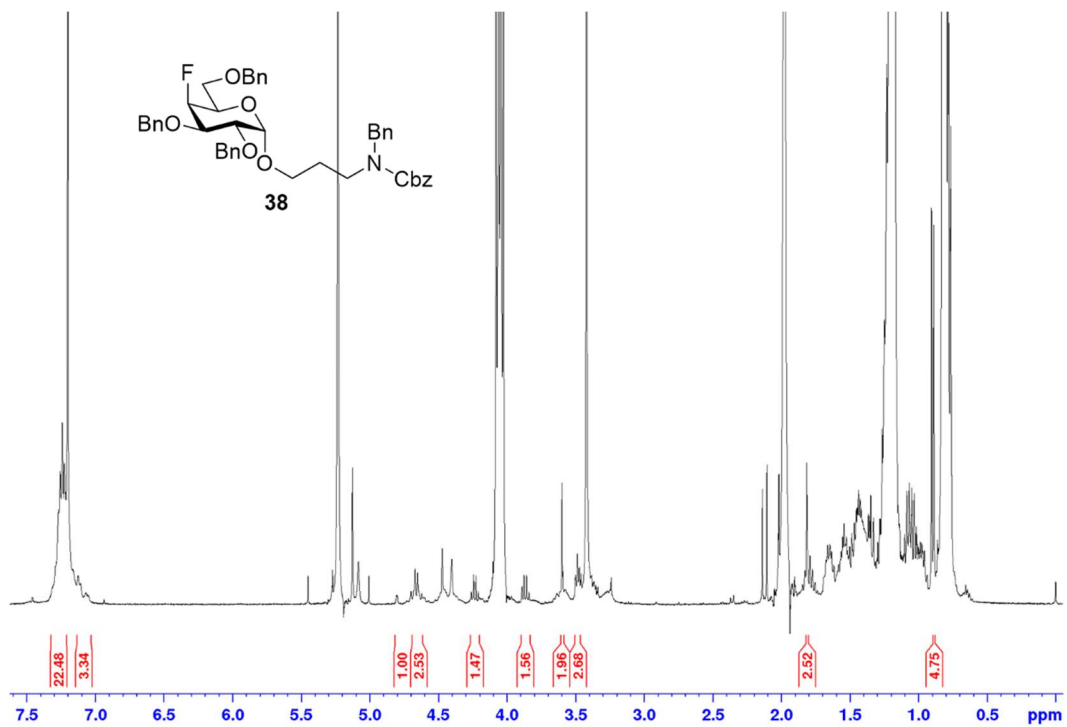
Figure 1.30. ^{1}H NMR (CDCl$_3$, 400 MHz) spectra of compound **38.**
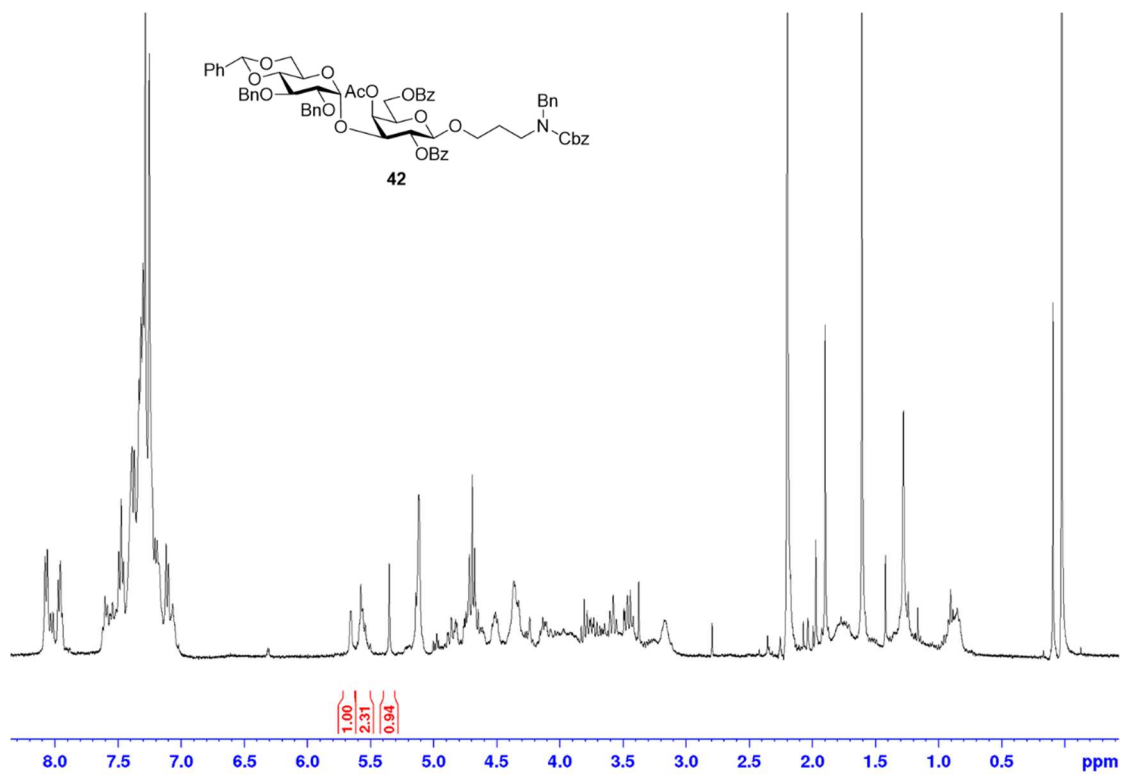
Figure 1.31. ^{1}H NMR (CDCl$_3$, 400 MHz) spectra of compound **42.**

CHAPTER 2

CONFORMATIONAL ANALYSIS OF RUTINOSE GLYCOSIDES

1. Introduction

The biological activity of carbohydrates extends far beyond their classical roles as energy sources or structural building blocks. Many biological processes such as cell differentiation, fertilization, cell-cell communication, infection, etc. involve the recognition of carbohydrate ligands by protein receptors as part of the signaling cascade. [55] The specificity, and success, of these molecular recognition events depend on the fulfillment of well-defined geometric and conformational requirements in both receptor and ligand. In the case of carbohydrates, given their inherent flexibility, the conformational properties claim a higher share, in comparison with other classes of molecules, in determining the specificity and the affinity of the interaction. Hence, the study of the conformational properties of sugars is paramount for understanding receptor-ligand interactions and can provide key information for the design of effective glycomimetic drugs.

The degree of flexibility of saccharides depends to a greater extent on the free rotation around the inter-glycosidic bonds. In the case of the (1→6) disaccharide shown in figure 2.1, the relative orientation of the two monosaccharides is described by the torsion angles ϕ (H1-C1-O-C6'), ψ (C1-O-C6'-C5'), and ω (O-C6'-C5'-H5'). Equivalent definitions are used for describing saccharides with different connections.
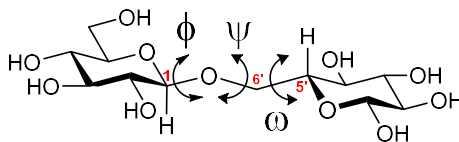
Figure 2.1. Torsional angles in (1→6) disaccharides

The conformation of the rings depends on the spatial distribution of the substituents. In sugars, two chair conformations are possible and the chair displaying a higher number of equatorial groups is typically preferred. In the case of natural saccharides made of common pyranoses (glucose, mannose, galactose, glucosamine, etc.) the predominant conformation of the ring is designated as $^4C_1$ chair conformation.
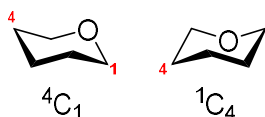
Figure 2.2. Chair conformations of pyranose rings

Given the possibility to rotate around three consecutives σ bonds, pyranose saccharides with (1→6) linkages are usually more flexible compared with saccharides connected *via* (1→1), (1→2), (1→3), and (1→4) linkages. The conformation around C5-C6 (ω) can exist in three staggered conformations denoted *gauche-gauche* (*gg*), *gauche-trans* (*gt*), *and trans-gauche* (*tg*) and the contribution of each rotamer to the equilibrium is influenced by the configuration of the stereocenter C4, the nature of the substituents on C4 and C6, the polarity of the solvent, the configuration of the anomeric carbon, and the nature of the aglycone substituent.
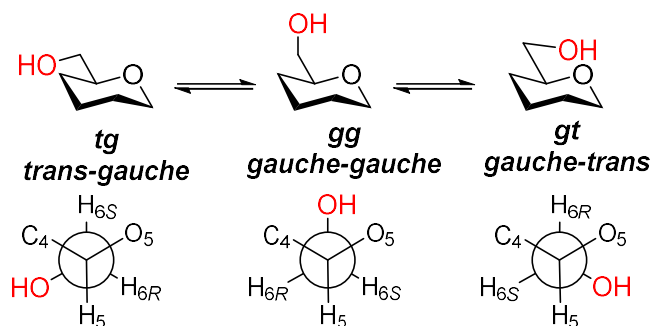
Figure 2.3. Staggered conformations around C5-C6 bonds

Previous studies on protected *O-*, *S-* and *C-*glucosides showed that, in organic media, the rotamers with major contributions to the conformational equilibrium are *gg* and *gt* and this equilibrium can progressively be displaced to a greater *gt* population by increasing the bulkiness of the aglycone substituent. In fact, Vazquez et. al showed that exists a linear correlation between the percent contribution of *gt* with the Taft's steric parameter of the aglycone substituent (figure 2.4). [56-58]
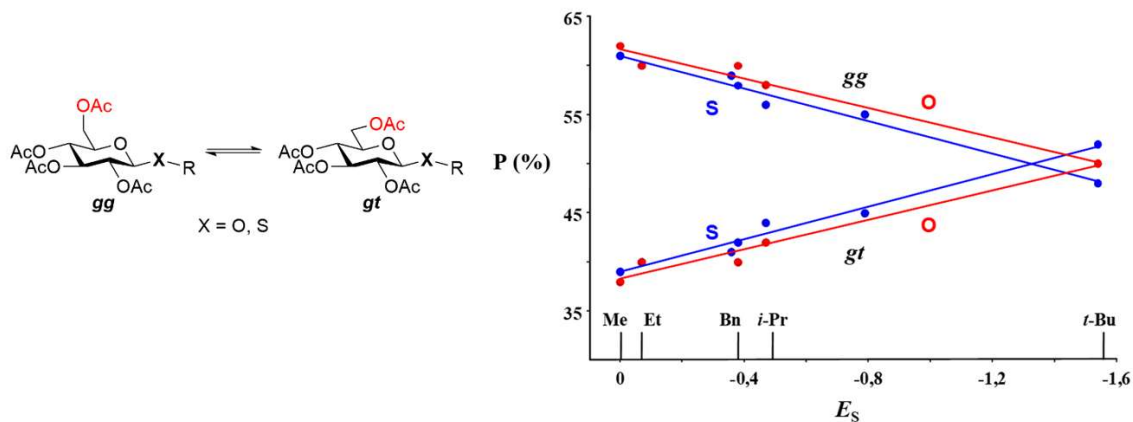
Figure 2.4. Relationship of the percent contributions of *gg* and *gt* rotamers with the steric properties of *O-* and *S-*aglycones.
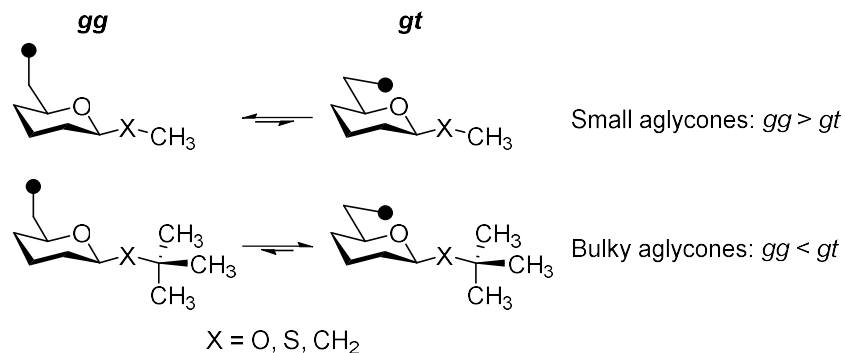
Figure 2.5. Summary of the influence of the steric properties of the aglycone on the conformational equilibrium around C5-C6

The remote conformational control described above can be observed in ether- and ester-protected glucosides, mannosides, and galactosides. The polarity of the media also has an influence over the rotamer populations by changing the slope of the trends.

A different behavior is observed in the case of unprotected glycosides where there is not an observable influence of C1 substituents over the hydroxymethyl (C5-C6) conformation. Plausible explanations of this finding can be a more significant influence of the solvent polarity and the possibility of free hydroxyls to make intramolecular hydrogen bonds adding rigidity to the system.

The study of how the steric properties of the aglycone affects the rotational equilibrium around the C5-C6 bond have extensively been performed in protected monosaccharides as well as in protected glycosides of gentiobiose (Glcβ(1→6)GlcOR). To the best of our knowledge, this type of studies has not been extended to other classes of saccharides neither unprotected glycosides.

In order to explore the presence of this effect in complex saccharides and deepen our understanding about their conformational properties, we centered our attention in rutinose, a disaccharide made of L-rhamnose and D-glucose, as a model compound for carrying out the conformational studies. Rutinose contains the linkage of interest (1→6) and includes a relatively hydrophobic 6-*O* substituent, rhamnose, that might contribute to diminish the conformational control exercised by polar protic solvents such as water.

We foresee that the conformational study of unprotected β-*O*-rutinosides will reveal clues about to what extent the nature of the aglycone can modulate the conformational properties of saccharides. The results from this study may provide valuable tools for the design of conformational glycomimetics in a near future. The study can also be useful and can be applied for conformational analysis of αGal Glycomimetics.
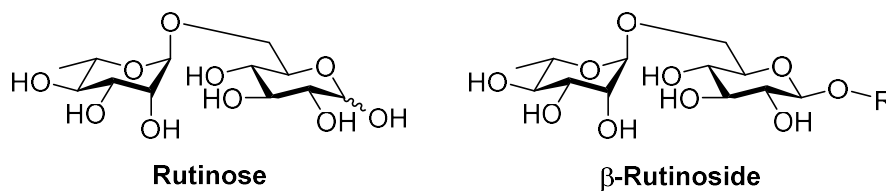
Figure 2.6. Structure of rutinose (L-Rhaα(1→6)-D-Glc) and general structure of the β-rutinosides to be studied in this thesis

2. Discussion

The synthesis of the target β-*O*-rutinosides **14(a-d)** started with the preparation of the L-rhamnose donor **4** and the D-glucose acceptor **10**.

The rhamnose trichloro-acetimidate donor **4** was prepared in three steps from commercially available L-rhamnose **1**. Treatment of **1** with Ac_2O in pyridine afforded the respective *per*-acetylated donor **2** which was then subjected to the regioselective removal of the anomeric acetate by treatment with NH_2NH_2 and AcOH in DMF. The resulting anomeric alcohol **3** was reacted with Cl_3CCN and DBU in DCM for generating the target rhamnose donor **4** in 78% overall yield.
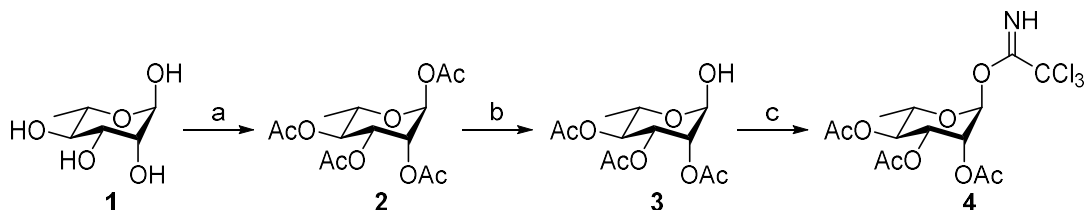
Scheme 2.1. Synthesis of L-rhamnose donor **4**. a) Ac_2O, Py, CH_2Cl_2, rt. 60 mins, b) NH_2NH_2, HOAc, DMF, rt. 24h, c) Cl_3CCN, DBU, DCM, rt. 12h.

The preparation of the glucose-derived acceptor **10** (scheme 2.2) started from β-penta-*O*-acetyl glucose. The glycosylation reaction of benzyl alcohol with the acetate donor **5** was performed in MeCN using BF_3Et_2O as catalyst and the desired glycoside **6** was isolated in 75% yield. The removal of the acetyl protecting groups of **6** was achieved in quantitative yield by treatment with NaOMe in MeOH. The regioselective protection of the hydroxyl group on C6 was accomplished by making the respective trityl-protected glycoside **8**

derived from the reaction of **7** with (Ph)₃CCl in pyridine. The free hydroxyl groups on C2,

C3 and C4 in **8** were then protected as benzoyl esters by BzCl/pyridine treatment. This

procedure afforded the fully protected intermediate **9** in 60% yield. The final removal of

the trityl group on C6, performed by dissolving **9** in neat TFA, yielded the target acceptor

10 in quantitative yield.
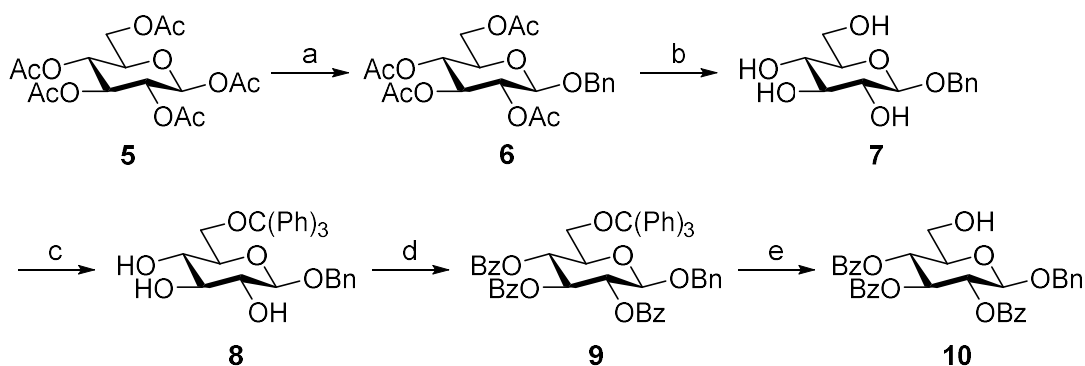
Scheme 2.2. Synthesis of glucose acceptor **10**. a) BnOH, BF₃Et₂O, MeCN, b) NaOMe, MeOH, c) (Ph)₃CCl, Py, 2hrs d) BzCl, Py, 8hrs e) TFA/DCM

The activation of **4** with TMSOTf in the presence of the acceptor **10**, lead to the

stereoselective formation of the desired α-(1→6) linkage with the glucose moiety. The

anchimeric participation of the axial acetyl group over C2 in the rhamnose ring accounts

responsible for the selective formation of the 1,2-*trans* linkage and formation of the β-

(1→6) stereoisomer was not observed. Thus, the assembly of the *O*-benzyl rutinoside **11**

was accomplished in 85% yield.
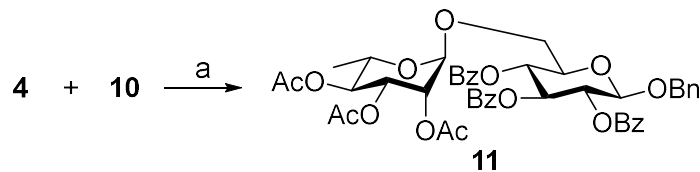
Scheme 2.3. Assembly of rutinose glycoside **11**. a) TMSOTf, DCM, 0°C, 20 min.

The ^{13}C NMR spectra of **11** shows two anomeric carbons at 99.2 ppm and 98.3 ppm and the anomeric protons were identified by their respective cross peaks with C1 in the HSQC spectra. The two anomeric protons appear, as expected, as doublets in the ^{1}H NMR spectra at 4.94 ppm and 4.82 ppm with $^{3}J_{H1\text{-}H2}$ coupling constants of < 1.0 Hz and 7.9 Hz respectively. The signal with the large J value (7.9 Hz) is assigned to the β-glucose ring since coupling constants between 7 and 10 Hz can only be generated by *trans*-diaxial systems with dihedral angles close to 180°, a configuration that, in the case of rutinose, only the β-glucose can fulfil given the axial disposition of both H1 and H2. The situation for rhamnose is different and the $^{3}J_{H1\text{-}H2}$ coupling constants in both α and β anomers are predicted to vary from 1 to 4 Hz, given that the dihedral angles for both α and β isomers are close to 60° which is associated with small J values according to Karplus equations.[59, 60] Therefore, the analysis of $^{3}J_{H1\text{-}H2}$ is an ambiguous criterion for assigning the anomeric configuration in rhamnosides and the confirmation of the configuration of the Rha-(1→6)-Glc glycosidic linkage must be done by an alternative method such as the analysis of spatial couplings of H1. Alternatively, it is safe to assume that the major compound is expected to be the α adduct considering the structure of the glycosyl donor that includes a stereo-directing group on C-2, next to the reaction center.
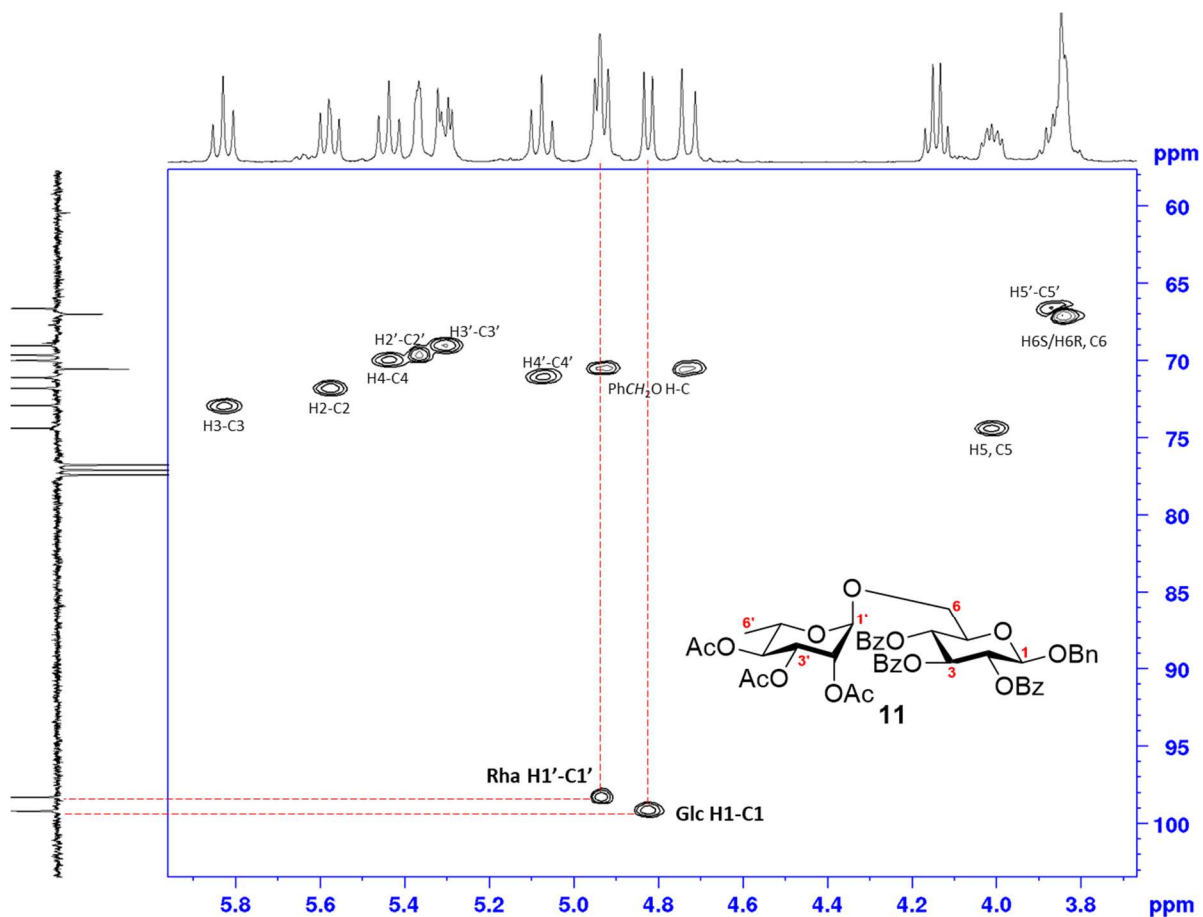
Figure 2.7. HSQC spectra of benzyl-*O*-rutinoside **11**.

In pyranose rings, the axial hydrogens appear, in general, more de-shielded *versus* equatorial protons. From the comparison of the anomeric hydrogens of glucose (4.82 ppm) and rhamnose (4.94 ppm) we can speculate that the rhamnose H1 could be occupying an axial position. In the same approach, the ^{13}C NMR spectra show the anomeric carbon assigned to rhamnose (98.3 pm) more shielded compared with the C1 of glucose (99.2 ppm). This analysis provides additional information for assigning the anomeric configuration of the rhamnose moiety since, normally, α-anomeric carbons are more shielded than β.

To study the conformational properties of rutinose glycosides and determine to what extent the nature of the alcohol substituents controls it, we propose the synthesis of a series of rutinose glycosides of aliphatic alcohols with representative steric properties. Benzyl rutinose glycoside **11** was envisaged as a key intermediate for preparing, on a multigram scale, the convenient rutinose trichloro-acetimidate donor **13**. Palladium-catalyzed hydrogenolysis of the anomeric benzyl group in **11** lead to the quantitative formation of the anomeric alcohol **12** which was immediately converted into the trichloro-acetimidate donor **13** by treatment with Cl_3CCN and DBU in DCM. The rutinose donor **13** was obtained in 81% overall yield from **11**.
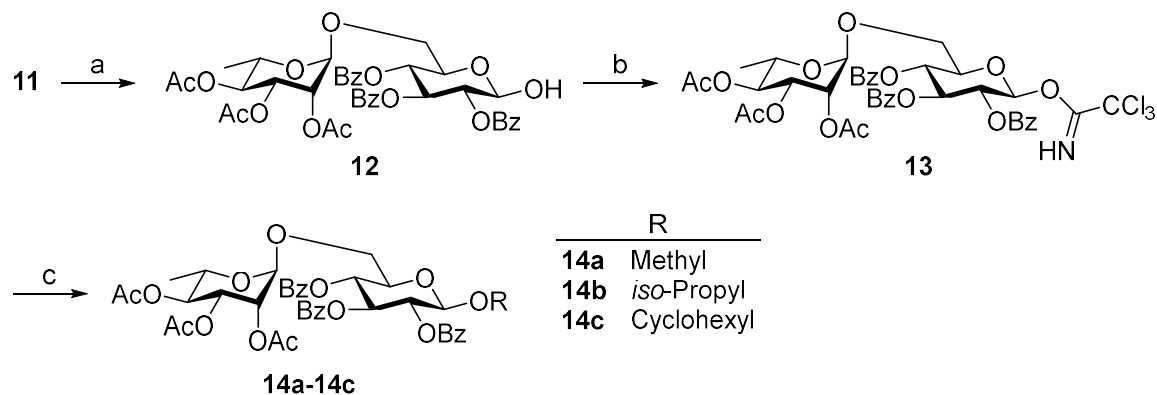
Scheme 2.4. Synthesis of rutinose imidate **13** and generation of aliphatic rutinose glycosides **14a-14d**. a) H_2, Pd/C, EtOH, rt, 48h. b) Cl_3CCN, DBU, CH_2Cl_2, rt, 12h. c) R-OH, TMSOTf, MeCN, 0°C to rt. 30 min.

Rutinose glycosides **14(a-c)** were prepared by glycosylation of the respective aliphatic alcohols with donor **13**. The reactions were carried out in MeCN and the donor was activated with a catalytic amount of TMSOTf. MeCN was selected as a solvent because of its effect in favoring the formation of equatorial adducts which, combined with the presence of a participating group on C2 in **13**, lead to the formation of β-glycosides as

major products. This procedure afforded the desired glycosides **14(a-c)** in excellent yields (85-99%).

The NMR characterization of the products was carried out in $CDCl_3$ at 25°C and selected ^1H and ^{13}C NMR data for rutinosides **11** and **14(a-c)** is summarized in table 2.1. From the analysis of the data for aliphatic rutinose glycosides **14(a-c)**, a trend on ^1H chemical shifts for the glucose anomeric proton can be observed where δH1 moves to lower field as the degree of substitution of the aglycone increases. Similar behavior is observed for δC1 of glucose. In the case of rhamnose both anomeric proton and carbon remains practically invariable along the series.

Table 2.1. Selected NMR ($CDCl_3$, 300 MHz) data for rutinosides **14(a-c)**
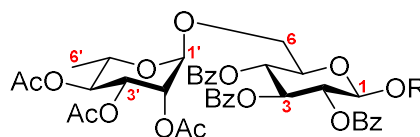
Compound	R	δH1	δH1'	δH5	δH5'	δH6R	δH6S	δC1	δC1'
11	Benzyl	4.94	4.83	4.01	3.86	-*	-	99.2	98.3
14a	Methyl	4.65	4.78	3.95	3.76	-*	-	101.9	98.2
14b	iso-Propyl	4.87	4.89	4.03	3.99	-	-	99.9	98.2
14c	Cyclohexyl	4.88	4.86	4.01	3.81	-	-	99.6	98.2

* "−" = overlapped signal, no chemical shifts can be read from spectra

The values of $^3J_{\text{H5-H6}R}$ and $^3J_{\text{H5-H6}S}$ were extracted from the splitting pattern of H5 since a direct measurement from H6$_{\text{pro-}R}$ and H6$_{\text{pro-}S}$ was not possible due to the overlapping of both signals. Fortunately, H5 appeared well isolated and allowed the reading of $^3J_{\text{H5-H6}R}$ and $^3J_{\text{H5-H6}S}$ in the four rutinosides presented. Table 2.2 shows the measured values of $^3J_{\text{H5-H6}R}$ and $^3J_{\text{H5-H6}S}$ for compounds **14(a-c)** and their respective calculated populations for the rotamers *gg*, *gt*, and *tg*.

Table 2.2. $^3J_{\text{H5-H6}R}$ and $^3J_{\text{H5-H6}S}$ values (CDCl$_3$, 300 MHz, 21°C) for rutinosides **14(a-c)**.

		$^3J_{\text{H5-H6}S}$	$^3J_{\text{H5-H6}R}$	*Pgg*	*Pgt*	*Ptg*
11	Benzyl	4.0	5.5	34	37	29
14a	Methyl	2.6	7.0	37	61	2
14b	*iso*-Propyl	4.2	5.6	39	41	20
14c	Cyclohexyl	5.0	5.0	39	32	29

*Pgg, Pgt, Ptg in Percentage (%)

The percent contribution of each rotamer to the conformational equilibrium was calculated from the $^3J_{\text{H5-H6}R}$ and $^3J_{\text{H5-H6}S}$ values using Karplus-like equations. Several equation systems are available for calculating rotamer populations about C5-C6.[59, 61-65] We opted for the system proposed by Serianni[66] in 2004 since this system has been demonstrated to provide accurate results in addition to positive values for the *tg* rotamer which is typically low populated in glucose-derived saccharides.

$$2.8 \; Pgg + 2.2 \; Pgt + 11.1 \; Ptg = {}^{3}J_{H5H6S}$$

$$0.9 \; Pgg + 10.8 \; Pgt + 4.2 \; Ptg = {}^{3}J_{H5H6R}$$

$$Pgg + Pgt + Ptg = 1$$

Equations 2.1. Serianni's equations used in this work for calculation rotational populations in rutinose glycosides

The analysis of the calculated populations for rutinosides **14(a-c)** and **11** shows the three rotamers, *gg*, *gt*, and *tg* contributing to the equilibrium and the percent contribution of the *gg* rotamer exhibits minor variations along the series remaining practically constant. However, populations of *gt* and *tg* exhibit significant variation through the series. In particular, the contribution of *tg* increases at *gt* expense as the bulkiness of the aglycone increases. In compound **14a**, the rutinose glycoside substituted with the smallest alkyl group (methyl), the conformational equilibria about C5-C6 is predominated by the *gt* rotamer with a contribution of 61%, followed by *gg* with 37%, and *tg* with 2%. For cyclohexyl glycoside **14c**, substituted with the bulkiest group of the series, the conformation is predominated by the *gg* rotamer with 39% contribution, followed by *gt* and *tg* with 32% and 29% respectively. The influence of the steric properties of the aglycone over the conformation about C5-C6 is more evident when comparing the *Pgt* and *Ptg* differences between **14a** and **14c**, being ΔPgt and ΔPtg 29% and 27% respectively. These results are consistent with reported data regarding the remote conformational influence of the aglycone over the ω torsion.[67]

The figures 2.10 and 2.11 show the relationship between the calculated rotamer populations and the Taft steric parameter (E_S), a molecular descriptor of the steric properties of alkyl groups. In figure 2.10 the calculated *gt*, *gg*, and *tg* populations of aliphatic rutinose glycosides **14(a-c)** are represented as a function of E_S. The data shows a clear linear relationship between the contributions of g*t* and *tg* rotamers with E_S. In particular, the percent contribution of the *tg* rotamer increases, at the cost of the *gt* contribution, as E_S of the aglycone substituent is more negative. In other words, the rotamer equilibrium is progressively displaced towards *tg* predominance as the bulkiness of the aglycone increase. The percent population of the *gg* rotamer does not vary as a function of E_S and remains constant along the series.
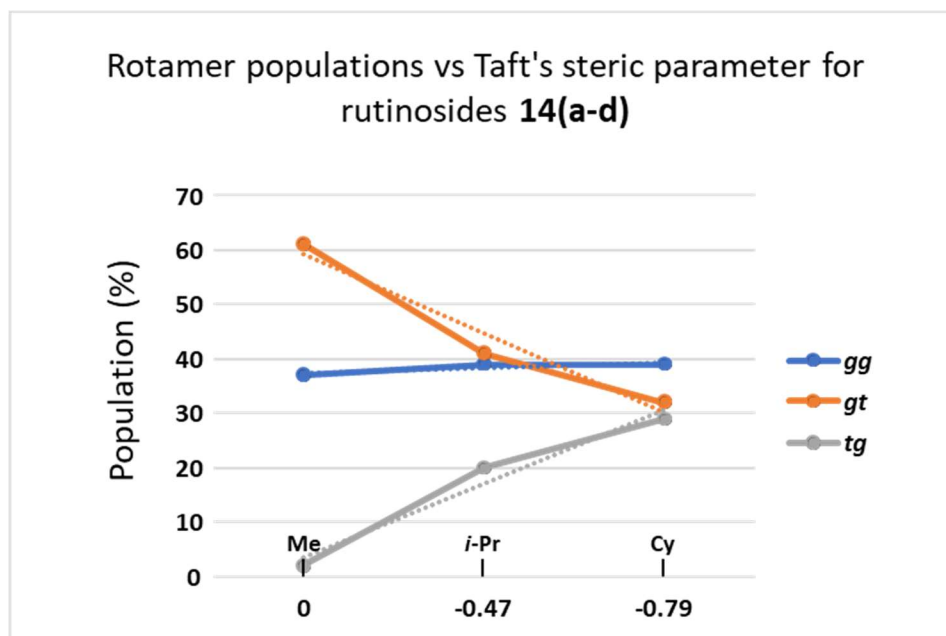
Figure 2.8. Relationship between *gg*, *gt* and *tg* rotamer populations with Taft's steric parameter of the aglycone substituent.

The variations of *tg* and *gt* populations among the glycosides studied provide evidence of a remote conformational control exerted by the substituent group of the aglycone where the conformational equilibrium around C5-C6, an inter-glycosidic linkage in our model compounds, can be influenced by groups attached at a three bond distance. The linear dependency of *Pgt* and *Ptg* with E_S provides an insight about the significance of the steric properties of the aglycone substituent on this effect. However, steric properties cannot be regarded as the only variable exerting the observed conformational control and other factors, such as electronic and polar attributes, should also be considered. This becomes evident when including the rutinose glycoside of benzyl alcohol **11**, with non-aliphatic aglycone substituent, in the representation of the rotamer populations *versus* E_S (figure 2.11). The inclusion of **11** in the series leads to a loss of linearity indicating that electronic factors also play a role in the modulation of the conformational properties of rutinose glycosides.

The conformational behavior of the studied rutinosides differ from the behavior observed for other types of glucose-derived saccharides. In the case of *per*-acetylated *O*-glucosides,[68] *O*-mannosides,[69] and *S*-gentiobiosides (Glcβ(1$\rightarrow$6)GlcSR)[70] the conformation about C5-C6 is also influenced by the steric properties of the aglycone being *gt* the rotamer that increases its contribution, at the expense of *gg*, as the bulkiness of the aglycone increase. In addition, the contribution of *tg* in these classes of glycosides is negligible and independent of the anomeric substitution. A hypothetical explanation for
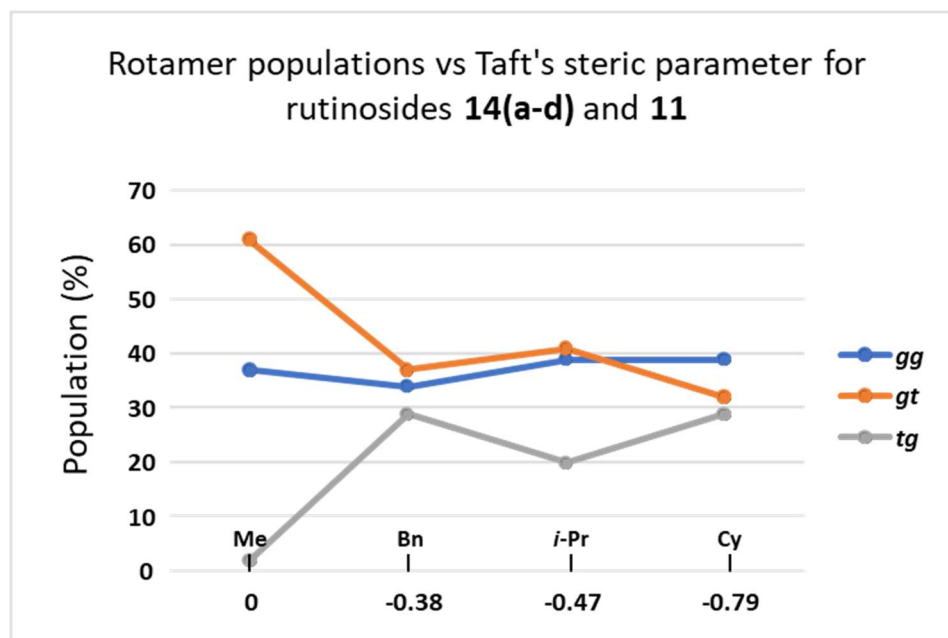
Figure 2.9. Relationship between *gg*, *gt* and *tg* rotamer populations with Taft's steric parameter of the aglycone substituent.

the atypical high *tg* population observed in rutinosides **11** and **14(a-c)** could be the stabilizing effect of the CH-π interaction between the methyl group of rhamnose (C-6') and the aromatic ring of the benzoyl group on C-4 of glucose (figure 2.12**.**). Using methyl *O*-rutinoside **14a** as a model, the optimized structure (MMFF94) of its *tg* conformer shows a 3.6 Å distance between the C-6' hydrogen and the center of the C-4 benzoyl ring, a value that falls within the range (< 4.0 Å) for CH-π interaction to take place.[71-73]
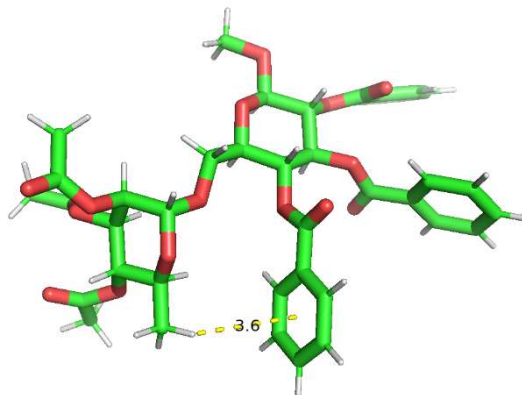
Figure 2.10. Proposed stabilization of the *tg* rotamer via CH-π interaction between the methyl group C-6' of rhamnose and the aromatic ring of the benzoyl group over C-4 of glucose.

Although there is not a conclusive explanation for the dependency of *Pgg*, *Pgt* and *Ptg* with the aglycone's E_S, a hypothesis based on stereoelectronic effects seems plausible. In carbohydrate chemistry it is postulated that the preference of electronegative C1 substituents for the axial position (α anomers) can be explained based on the combined stabilization of two stereoelectronic interactions between a lone electron pair of the electronegative heteroatom X (n_X) with the sigma antibonding orbital of the C1-O5 bond ($\sigma^*_{C1\text{-}O5}$) and the interaction of the axial lone electron pair of O5 (n_{O5}) with the sigma antibonding orbital of the C1-X bond ($\sigma^*_{C1\text{-}X}$). These interactions are named the *exo*-anomeric and the *endo*-anomeric effects, respectively. In the case of β-glycosides, the geometry of the anomeric carbon fulfills the requirements for the *exo*-anomeric effect to take place whereas both *exo*- and *endo*-anomeric effects are possible in the α-glycosides (figure 2.12).
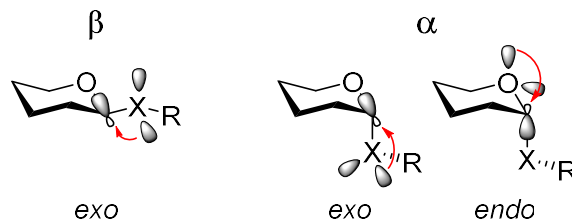
Figure 2.11. Stereoelectronic interactions

A consequence of hyperconjugation interactions is the shortening of the bond where the donor atom is connected and the subsequent enlargement of the bond that holds the antibonding orbital. In the case of β-glycosides, the C1-O5 bond is longer because of the C1-O(R) bond shortening. We hypothesize that the variations in the bond lengths may have an effect in de-stabilizing the *gg* rotamer resulting in a displacement of the equilibrium towards a higher contribution of *gt* and/or *tg* as a result of the geometrical change in the molecular neighborhood. Stereoelectronic interactions also can be proposed in the stabilization of the *gg* and *gt* conformers. The donation of the C5-H5 sigma bond to the C6-O6 sigma antibonding orbital ($\sigma_{C5-H5} \rightarrow \sigma^*_{C6-O6}$) can stabilize *gg* rotamer whereas the interaction C6-H6*S*/C5-O5 ($\sigma_{C6-H6S} \rightarrow \sigma^*_{C5-O5}$) can stabilize *gt*. A similar analysis for *tg* involves the donation of the C6-H6*R* to C4-C5 ($\sigma_{C6-H6R} \rightarrow \sigma^*_{C4-C5}$), however, this type of interaction is less likely to take place given the poor acceptor character of the C-C bonds. Hence, the results observed for the rutinosides studied herein, i.e. an increment of *tg* population along the series, cannot be explained based on the $\sigma_{C6-H6R} \rightarrow \sigma^*_{C4-C5}$ interaction and the stabilization by CH-π interaction seems more reasonable. On the other hand, the general tendency of the rotational populations to linearly change

with respect to the steric properties of the aglycone is a phenomenon that remains to be

explained.
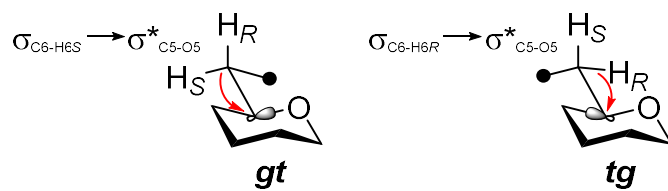
Figure 2.12. *gt* and *tg*-stabilizing stereoelectronic interactions

3. Future work

The aim of this work is to determine the conformational properties of fully deprotected saccharides in solution and we have chosen rutinose glycosides as model compounds for carrying out this study. The data obtained from the conformational analysis of protected rutinosides **14(a-c)** showed an unexpected behavior for this class of compounds and further studies will be carried out on homogeneously protected derivatives (i.e. *per*-acetylated compounds) for a direct comparison with previous data and test the hypothesis of *tg* stabilization via CH-π interaction. We consider including other types of saccharides into this study depending on the results observed for the *per*-acetylated series.
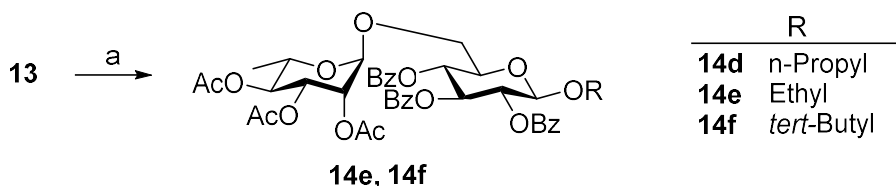
Scheme 2.5. Synthesis of rutinose glycoside **14e** and **14f**. a) R-OH, TMSOTf, MeCN, 0°C to rt. 30 min.

The studies of the deprotected model compounds will be carried out after completing the synthesis of two remaining compounds, substituted with ethyl and *tert*-butyl *O*-aglycones, for increasing the number of collected data points and making the analysis statistically more significant.

	R
15a	Methyl
15b	*iso*-Propyl
15c	Cyclohexyl
15d	n-Propyl
15e	Ethyl
15f	*tert*-Butyl
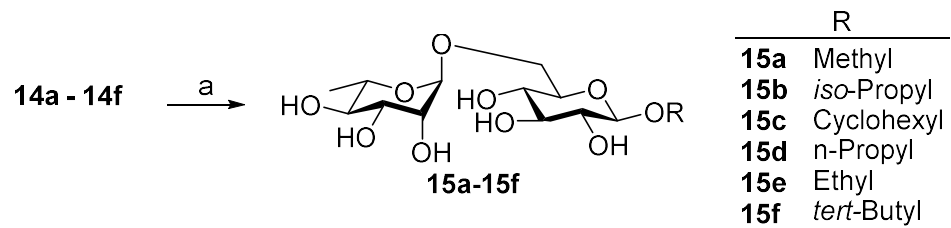
Scheme 2.6. Synthesis of rutinose glycoside **15a-15f** a) NaOMe, MeOH, r.t.

4. Experimental Section
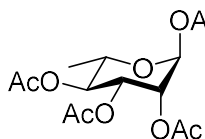
1,2,3,4-tetra-O-acetyl L-rhamnose (2): Rhamnose **1** (5g, 3.45 mmol) was dissolved in pyridine (11.05 mL) and cooled to 0°C. Acetic anhydride (25.8mL, 273.15 mmol) was then added was added to the solution and the solution was allowed warming to r.t. After 2 hours of stirring TLC analysis shows total consumption of the starting material and the volatiles were removed *in vacuo*. Acetylated product was then purified by flash silica gel chromatography using EtOAc/Hexanes mixture (1:1) as eluents. Compound **2** (1.68 g, 2.97 mmol 99%, Rf 0.7) was isolated as a white solid. Compound identity was confirmed by comparison of ^{1}H and ^{13}C NMR spectra with previously reported data.[74]
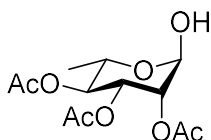
2,3,4-tri-O-acetyl L-rhamnose (3): A solution of (90.9 g, 274 mmol) of peracylated sugar **2** in of tetrahydrofuran (150 mL) was added to an ammonical solution of (1500 mL) of tetrahydrofuran-methanol (2.3:1, prepared by bubbling ammonia into the solvent for 30 min) cooled in an ice-water bath. The cooling bath was removed, and the solution warmed to rt. After 5.5 h, thin layer chromatography (silica gel; dichloromethane-methanol, 9:1) showed consumption of **2**, and the solvent removed in vacuo. The residue was triturated with approximately 150 mL of diethyl ether to afford 61 g (77%) of rhamnose triacetate **3** as a white solid.[75]
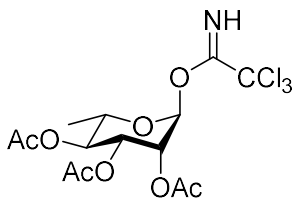
O-(2-trichloroethanimine)-2,3,4-tri-O-acetyl L-rhamnose (4):

Rhamnose-1-OH **3** is dissolved in DCM. Trichloroacetonitrile is then added to the solution with stirring. DBU is then added and the solution is allowed to stir at room temperature for 12 hrs. After 12 hrs TLC analysis shows complete conversion to product. Volatiles are removed *in vacuo.* The crude so obtained is purified by flash chromatography using SiO_2 as stationary phase and EtOAc/Hexanes mixture (3:7) as eluent. glycoside **4** (7.55 g, 17.2 mmol, 75.15%) was isolated as a waxy white solid. Compound identity was confirmed by comparison of ^{1}H and ^{13}C NMR spectra data. [75]
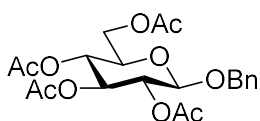
O-benzyl-2,3,4,6-tetra-O-acetylglucoside (6): Glucose pentaacetate **5** (10.07 g, 25.7 mmol) and Benzyl alcohol (5.34 ml, 51.4 mmol) were dissolved in dry Acetonitrile (77.1 mL) and BF_3Et_2O (1.58 mL, 12.85 mmol) was added dropwise and the solution was refluxed at $50 – 80^0C$ under stirring. After 6 hours of TLC shows total consumption of the starting material and the reaction was cooled to 0°C and quenched with triethylamine (4.0 mL). After 15 minutes of stirring at 0°C, the volatiles were removed in vacuum and the crude purified by flash chromatography using SiO_2 as stationary phase and EtOAc/Hexanes mixture (3:7) as eluent. *O*-benzylglycoside **6** (7.55 g, 17.2 mmol, 75.15%) was isolated as a waxy white solid. Compound identity was confirmed by comparison of ^{1}H and ^{13}C NMR spectra data with previously reported data. ^{1}H NMR (400 MHz, CDCl$_3$) δ 7.35 – 7.26 (m, Aromatic H's, 6H), 5.09 (dd, *J* = 9.3 Hz and 6.06 Hz, H-4), 5.03 (dd, *J* = 8.5 Hz and 9.5 Hz, H-3), 4.99 (dd, *J* = 9.3 Hz and 7.7 Hz, H-2), 4.82 (d, *J* = 12.3 Hz, 1H), 4.56 (d, *J* = 12.3 Hz, 1H), 4.48 (d, *J* = 7.9

Hz, H-1), 4.21 (dd, J = 12.3, 4.7 Hz, H-6), 4.10 (dd, J = 12.3, 2.4 Hz, H-6'), 3.60 (ddd, J = 9.6, 4.6, 2.4 Hz, H-5), 2.04 (s, 3H), 1.95 (s, 3H), 1.94 (s, 3H), 1.93 (s, 3H). ^{13}C NMR (100 MHz, CDCl$_3$) δ 170.7, 170.3, 169.4, 169.3, 140.9, 136.6, 128.6, 128.5, 128.1, 127.8, 127.7, 127.0, 99.3, 77.3, 77.0, 76.7, 72.8, 71.9, 71.3, 70.8, 68.4, 65.4, 61.9, 20.8, 20.6, 1.0.[51]
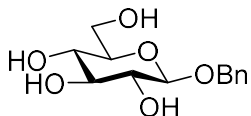
O-benzylglucoside (7): *O*-benzyl-2,3,4,6-tetra-*O*-acetylglucoside **6** (7.24 g, 15.9 mmol) was dissolved in methanol (30.0 mL) and sodium methoxide (100 mg) was added. The suspension was stirred at r.t. for 24 hours which is enough time for the trans-esterification reaction to be completed (shown by TLC analysis). The system was then neutralized with Amberlyst IR-120+ resin followed by filtration. Methanol was removed *in vacuo* with rotary evaporator and the crude dried under high vacuum in a Schlenk line for 24 hours prior to use. Structure of 1-benzyloxy-ß-D-glucopyranoside **7** was confirmed by comparison of its ^{1}H and ^{13}C NMR spectra with previously reported data. ^{1}H NMR (400 MHz, CDCl$_3$) δ 7.32 – 7.18 (m, Aromatic H's, 5H), 4.75 (d, J = 12.0 Hz, 1H), 4.49 (d, J = 11.4 Hz, 1H), 4.29 (d, J = 5.6 Hz, 1H), 3.71 (s, 2H), 3.51 (s, 1H), 3.35 (s, 2H), 3.13 (s, 1H). ^{13}C NMR (100 MHz, CDCl$_3$) δ 136.1, 127.4, 127.1, 76.3, 76.2, 75.9, 75.7, 70.3, 59.4, 20.0, 13.2.[51]
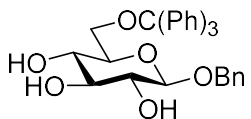
O-benzyl-6-O-(triphenylmethyl)glucoside (8) *O*-benzylglucoside **7** (3.65g, 13.5 mmol) was dissolved in Pyridine (21 ml) and Triphenyl chloride (3.76 g, 13.5 mmol) was added to the solution. The solution was heated at 70^{0}C and stirred for 2 hours. After 2 hours of stirring TLC analysis shows total consumption of the starting material. The reaction was then diluted with distilled water and with water and ethyl acetate. The volatiles were then removed *in vacuo*. 2,3,4-Diol **9** was then

purified by flash silica gel chromatography using EtOAc/Hexanes mixture (2:3) as eluents. Compound **8** (3.5 g, 6.82 mmol 60%) was isolated as a yellowish white solid. Compound identity was confirmed by comparison of ^{1}H and ^{13}C NMR spectra with previously reported data.[76]
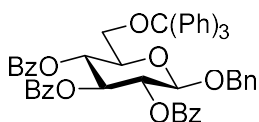
O-benzyl-2,3,4-tribenzoyl-6-O-(triphenylmethyl)glucoside (9): O-benzyl-6-O-(triphenylmethyl)glucoside **8** (6.83 g, 3.5 mmol) was dissolved in pyridine (5.25 mL) and benzoyl chloride (2.9 mL, 24.58 mmol) was added to the solution at r.t. After 3 hours of stirring TLC analysis shows total consumption of the starting material and the volatiles were removed *in vacuo*. Tribenzoylated adduct was then purified by flash silica gel chromatography using EtOAc/Hexanes mixture (2:3) as eluents. Compound **9** (1.68 g, 2.97 mmol 99%) was isolated as a yellowish white solid. Compound identity was confirmed by comparison of ^{1}H and ^{13}C NMR spectra with previously reported data. ^{1}H NMR (400 MHz, CDCl$_3$) δ 7.92 – 7.10 (m, Aromatic H's, 35H), 5.72 (dd, J = 9.4 and 9.4 Hz, H-3), 5.61 (d, J = 7.9 and 7.9 Hz, H-2), 5.59 (d, J = 9.4 and 9.4 Hz, H-4), 4.99 (d, J = 11.9 Hz, 1H), 4.81 (d, J = 11.9 Hz, 1H), 4.78 (d, J = 8.7 Hz, H-1), 3.80 (m, H-5), 3.32 (m, 2H, H-6 and H-6'). ^{13}C NMR (100 MHz, CDCl$_3$) δ 130.8, 129.7, 129.1, 128.6, 128.4, 127.7, 126.9, 77.3, 77.2, 77.0, 76.7, 30.9.
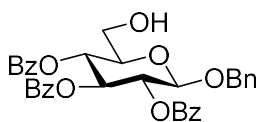
O-benzyl-2,3,4-tribenzoylglucoside (10): O-benzyl-2,3,4-tribenzoyl-6-O-(triphenylmethyl)glucoside **9** (1.3g, 1.57 mmol) was dissolved in a mixture of TFA/DCM (2:8, 10.0 mL) at r.t. and stirred for 30 minutes. After that period TLC analysis shows complete consumption of the starting material. Then TFA and water were removed *in vacuo* with rotary evaporator and the crude diol was purified

by flash chromatography with silica gel as stationary phase and EtOAc/Hex mixtures (1:1) as eluents. Compound **10** (8.70 g, 17.6 mmol, 92%) was isolated as a white solid. ^{1}H NMR (400 MHz, CDCl$_3$) δ 7.92 (d, J = 7.7 Hz, 4H), 7.83 (d, J = 7.6 Hz, 2H), 7.54 (m, 2H), 7.46 – 7.38 (m, 5H), 7.30-7.20 (m, 7H), 5.88 (dd, J = 9.8, 9.8 Hz, H-4), 5.58 (dd, J = 7.9 and 9.5 Hz, H-2), 5.49 58 (dd, J = 9.3 and 9.3 Hz, H-3), 4.92 (d, J = 12.6 Hz, 1H, O$\underline{CH_2}$ Ph), 4.84 (d, J = 8.0 Hz, H1), 4.74 (d, J = 12.7 Hz, 1H, O$\underline{CH_2}$ Ph), 3.87 (dd, J = 4.2 and 14.3 Hz, H6), 3.74 (m, H5, H6'). ^{13}C NMR (100 MHz, CDCl$_3$) δ 207.0, 166.1, 165.8, 165.1, 136.7, 133.7, 133.2, 129.9, 129.8, 129.7, 129.3, 128.8, 128.5, 128.4, 128.3, 127.9, 127.8, 99.5, 77.3, 77.2, 77.0, 76.7, 74.6, 72.7, 71.8, 70.9, 69.6, 61.4, 30.9.[77]
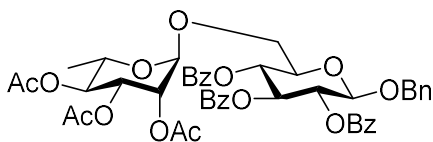
2,3,4-tetra-O-acetyl-L-rhamnose-1→6-*O*-benzyl-2,3, 4-tribenzoylglucoside (11): Monosaccharide **4** (9.1 mg, 0.0162 mmol) and Alcohol **10** (9.7 mg, 3.3 mmol) were dissolved in DCM (65.12 μL) in the presence of 4A^0 molecular sieves (1.0 mg). The suspension was stirred at r.t. for 15 mins and then cooled to -20 - 30°C using dry ice. TMSOTf (0.3 μL, 0.0016 mmol) was then added and vigorous stirring was continued until total consumption of the donor was observed (TLC 2 hours). Reaction was then diluted with ethyl acetate (5.0 mL), quenched with Et$_3$N (0.5 mL), allowed to warm to r.t., filtered over a Celite® bed, transferred to a separation funnel and washed with NaS$_2$O$_3$. The organic fraction was dried over Na$_2$SO$_4$, the volatiles removed *in vacuo* and the crude purified by flash chromatography using silica gel as stationary phase and EtOAc/Hexanes (1:2) gradient as eluent solutions. Glycosylated monosaccharide **32** (8.2 mg, 0.011 mmol, 90 %) was isolated as a yellow solid. ^{1}H NMR (400 MHz, CDCl$_3$) δ 7.94 – 7.19 (m, Aromatic H's, 20H), 5.83 (dd, J = 9.6 and

9.6Hz, H-3), 5.57 (dd, *J* = 8.1 and 9.7 Hz, H-2), 5.44 (dd, *J* = 9.7 and 9.7 Hz, H-4), 5.38-5.36

(m, 1H), 5.30 (dd, *J* = 10.0, 3.4 Hz, H-4'), 5.08 (dd, *J* = 9.9 and 9.9 Hz, H-5'), 4.93 (dd, *J* =

4.6 and 7.8 Hz, H-1', H-3'), 4.82 (d, *J* = 7.9 Hz, H-1), 4.73 (d, *J* = 12.7 Hz, H-2'), 4.03 – 3.98

(m, H-5), 3.90 – 3.80 (m, 2H, H6*R*, H6*S*), 2.14 (s, 3H), 2.06 (s, 3H), 2.02 (s, 3H), 1.16 (d, *J* =

6.2 Hz, 3H, H-6'). ^{13}C NMR (101 MHz, CDCl$_3$) δ 170.0, 165.7, 165.3, 165.1, 136.6, 133.5,

133.2, 129.9, 129.8, 129.7, 128.5, 128.4, 128.3, 128.3, 127.9, 99.2, 98.3, 77.4, 77.0, 76.7,

70.5, 66.9, 20.9, 20.8, 20.7, 17.3, 14.2, 12.9.
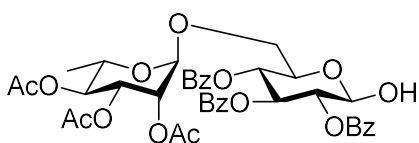
2,3,4-tetra-O-acetyl-L-rhamnose-1→6-2,3,4-tribenzo ylglucoside (12): Disaccharide **11** is first dissolved in was ethanol. Weighed quantity of the catalyst is added to the flask. Flask is evacuated and

backfilled with nitrogen gas 3 times. The flask is then evacuated and backfilled with

hydrogen gas. Hydrogen balloons are then attached to the flask and the reaction can run

at r.t. for 24 hrs. After 24 hrs TLC analysis shows complete consumption of substrate.

When the reaction is done, the contents of flask are poured into a filter funnel containing

celite to remove the palladium catalyst. Volatiles are than removed *in vacuo*. Compound

12 is isolated as white solid. The crude is then directly used to set up next reaction without

any column chromatography.
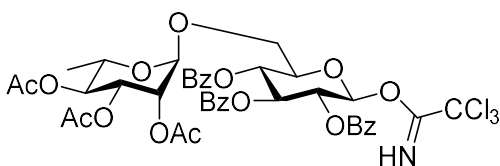
2,3,4-tetra-O-acetyl-L-rhamnose-1→6-O-(2-tri chloroethanimine)-2,3,4-tribenzoylglucoside (13):   2,3,4-tetra-O-acetyl-L-rhamnose-1→6-

2,3,4-tribenzo ylglucoside **12** is dissolved in DCM. Trichloroacetonitrile is then added to

the solution with stirring. DBU is then added and the solution is allowed to stir at room

temperature for 12 hrs. After 12 hrs TLC analysis shows complete conversion to product. Volatiles are removed *in vacuo.* The crude so obtained is purified by flash chromatography using SiO_2 as stationary phase and EtOAc/Hexanes mixture (3:7) as eluent. glycoside **4** (7.55 g, 17.2 mmol, 75.15%) was isolated as a waxy white solid. Compound identity was confirmed by comparison of ^{1}H and ^{13}C NMR spectra data. ^{1}H NMR (400 MHz, $CDCl_3$) δ 7.99 – 7.30 (m, 17H), 6.76 (d, *J* = 3.7 Hz, H1), 6.24 (t, *J* = 9.9 Hz, H3), 5.62 (t, *J* = 10.1 Hz, H2), 5.57 (dd, *J* = 10.2, 3.7 Hz, H4), 5.28 (m, H2'), 5.23 (dd, *J* = 10.0, 3.5 Hz, H3'), 5.02 (t, *J* = 9.9 Hz, H4'), 4.83 (d, H-1'), 4.50 – 4.44 (m, H5), 3.87 (m, H6*R*), 3.82 (m, H5'), 3.73 (dd, *J* = 11.8, 6.1 Hz, H6*S*), 2.14 (s, 3H), 2.04 (s, 3H), 1.97 (s, 3H), 1.15 (d, *J* = 6.2 Hz, 3H, H6'). ^{13}C NMR (100 MHz, $CDCl_3$) δ 206.9, 129.9, 129.7, 128.5, 128.4, 128.3, 98.0, 93.8, 92.9, 77.3, 77.0, 76.7, 71.1, 70.6, 70.2, 69.5, 68.9, 66.6, 30.9, 20.8, 20.7, 17.3.
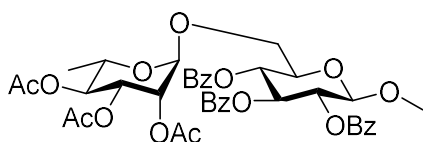
2,3,4-tetra-O-acetyl-L-rhamnose-1→6-O-methyl-2,3, 4-tribenzoylglucoside (14a): Disaccharide **13** (885 mg, 1.65 mmol) and Dry Methanol (0.988 g, 3.3 mmol) were dissolved in Acetonitrile (6.6 mL). The solution was then cooled to 0°C . TMSOTf (29.8 μL, 0.165 mmol) was then added and vigorous stirring was continued until total consumption of the donor was observed (TLC, 30 mins). The volatiles removed *in vacuo* and the crude purified by flash chromatography using silica gel as stationary phase and EtOAc/Hexanes (1:2) gradient as eluent solutions. Glycosylated disaccharide **14a** (787.3 mg, 1.08 mmol,88.93%) was isolated as a white solid. ^{1}H NMR (400 MHz, $CDCl_3$) δ 7.89 – 7.20 (m, 15H), 5.80 (t, *J* = 9.7, 9.7 Hz, H3), 5.40 (dd, *J* = 9.7, 8.0 Hz, H2), 5.33 (d, *J* = 9.7 Hz, H4), 5.20 (m, H3'), 5.17 (d, *J* = 3.5 Hz, H2'), 4.97 (dd, *J* = 17.3, 7.5 Hz, H4'), 4.79 (s, H1'), 4.65 (d, *J* = 7.9 Hz, H1), 4.00 – 3.91 (m, H5), 3.82 –

3.76 (m, H5',H6*R*), 3.76 – 3.66 (m, H6*S*), 2.06 (s, 3H), 1.99 – 1.93 (m, 3H), 1.91 (s, 3H), 1.17 (dd, *J* = 16.5, 7.6 Hz, O<u>CH₃</u>), 1.06 (d, *J* = 6.2 Hz, H6'). ^{13}C NMR (100 MHz, CDCl₃) δ 169.9, 169.9, 165.8, 165.3, 165.1, 133.5, 133.2, 129.8, 129.7, 129.3, 128.8, 128.7, 128.5, 128.4, 128.3, 101.9, 98.3, 77.3, 77.0, 76.7, 74.2, 72.9, 71.8, 71.0, 69.9, 69.6, 69.0, 67.1, 66.5, 57.2, 53.4, 29.7, 20.9, 20.8, 20.7, 17.3.
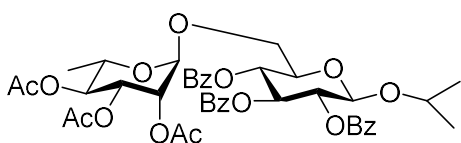
2,3,4-tetra-O-acetyl-L-rhamnose-1→6-O-isopropyl -2,3,4-tribenzoylglucoside (14b): Disaccharide **13** (885 mg, 1.65 mmol) and dry Methanol (0.988 g, 3.3 mmol) were dissolved in Acetonitrile (6.6 mL). The solution was then cooled to 0°C . TMSOTf (29.8 μL, 0.165 mmol) was then added and vigorous stirring was continued until total consumption of the donor was observed (TLC, 30 mins). The volatiles removed *in vacuo* and the crude purified by flash chromatography using silica gel as stationary phase and EtOAc/Hexanes (1:2) gradient as eluent solutions. Glycosylated disaccharide **14a** (787.3 mg, 1.08 mmol, 88.93%) was isolated as a white solid. ^{1}H NMR (400 MHz, CDCl₃) δ 7.97 – 7.31 (m, Aromatic H's, 15H), 5.88 (dd, *J* = 9.6 and 9.6 Hz, H3), 5.45 (dd, *J* = 9.8, 8.3 Hz, H2), 5.41 – 5.36 (m, H4), 5.32 – 5.29 (m, H2'), 5.26 (dd, *J* = 10.1, 3.3 Hz, H3'), 5.04 (dd, *J* = 11.4, 8.2 Hz, H4'), 4.90 (s, H1'), 4.87 (d, *J* = 8.06 Hz, H1), 4.04 (dd, *J* = 9.1, 4.8 Hz, H5), 4.00 – 3.95 (m, H5'), 3.82 – 3.79 (m, H6*S*, H6*R*), 2.14 (s, 3H), 2.05 (s, 3H), 2.00 (s, 3H), 1.22 (d, *J* = 6.2 Hz, H6'), 1.14 (s, 3H), 1.09 (d, *J* = 6.1 Hz, 2H). ^{13}C NMR (100 MHz, CDCl₃) δ 169.9, 165.8, 133.5, 129.9, 129.8, 129.7, 128.5, 128.3, 128.2, 99.8, 98.2, 77.3, 77.0, 76.7, 74.2, 73.2, 73.0, 72.0, 71.0, 70.1, 69.5, 69.1, 66.9, 66.5, 29.7, 23.2, 21.9, 20.8, 20.7, 17.1.
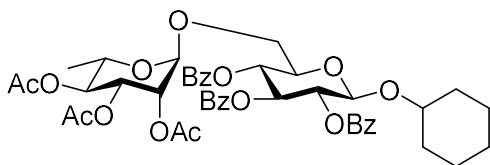
2,3,4-tetra-O-acetyl-L-rhamnose-1→6-O-cycloh exyl-2,3,4-tribenzoylglucoside **(14c):**

Disaccharide **13** (885 mg, 1.65 mmol) and Dry Methanol (0.988 g, 3.3 mmol) were dissolved in Acetonitrile (6.6 mL). The solution was then cooled to 0°C . TMSOTf (29.8 μL, 0.165 mmol) was then added and vigorous stirring was continued until total consumption of the donor was observed (TLC, 30 mins). The volatiles removed *in vacuo* and the crude purified by flash chromatography using silica gel as stationary phase and EtOAc/Hexanes (1:2) gradient as eluent solutions. Glycosylated disaccharide **14a** (787.3 mg, 1.08 mmol,88.93%) was isolated as a white solid. ^{1}H NMR (400 MHz, CDCl$_3$) δ 7.95 - 7.29 (m, 15H), 5.85 (dd, *J* = 9.7 and 9.7 Hz, H3), 5.48 – 5.42 (m, H2), 5.39 (t, *J* = 9.8 Hz, H4), 5.28 (m, H2'), 5.23 (dd, *J* = 10.0, 3.4 Hz, H3'), 5.02 (dd, *J* = 9.9 and 9.9 Hz, H5'), 4.89 (d, *J* = 7.9 Hz, H1), 4.86 (s, H1'), 4.04 (m, H5), 3.84 – 3.80 (m, H5', H6*R*), 3.79 (d, *J* = 6.4 Hz, H6*S*), 3.68 (s, 3H), 2.13 (s, 3H), 2.02 (s, 3H), 1.97 (s, 6H), 1.12 (d, *J* = 6.2 Hz, H5'). ^{13}C NMR (100 MHz, CDCl$_3$) δ 169.9, 133.5, 133.1, 133.0, 129.8, 129.7, 129.7, 128.5, 128.3, 128.2, 99.6, 98.2, 77.3, 77.0, 76.7, 74.1, 73.0, 72.0, 71.0, 70.1, 69.5, 69.1, 66.5, 31.5, 30.9, 25.4, 20.8, 20.7, 17.3.
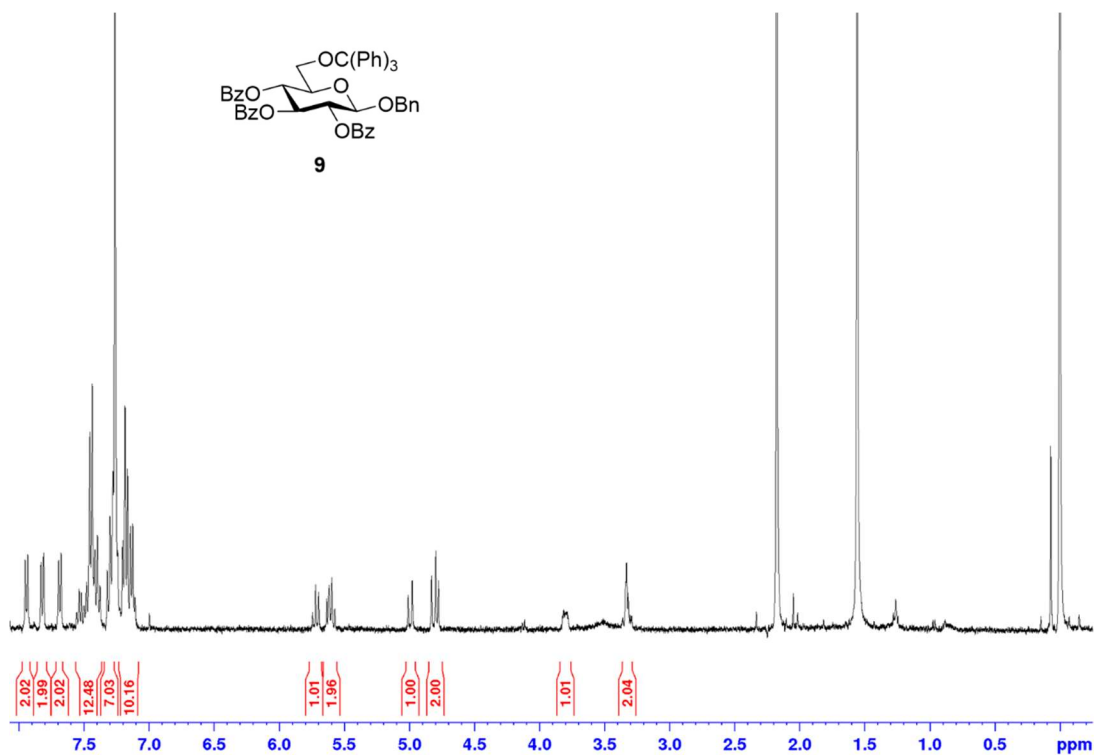
Figure 2.13. H^1 NMR spectra of compound **9**
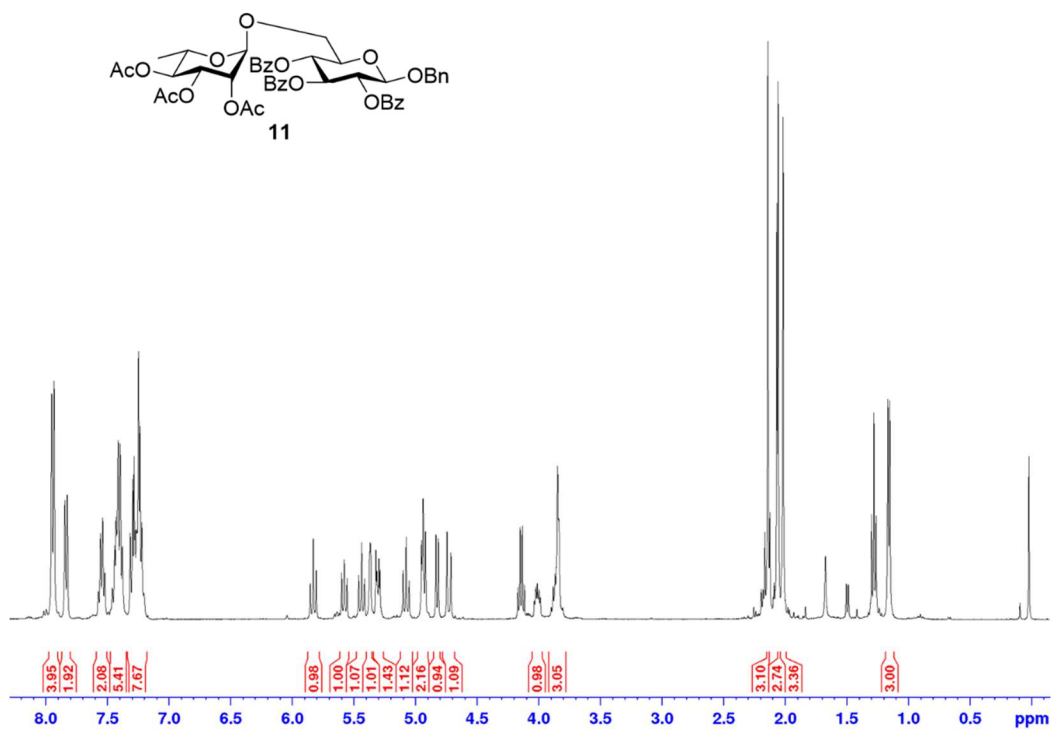
Figure 2.14. H^1 NMR spectra of compound **11**

Figure 2.15. H^1 NMR spectra of compound **13**

Figure 2.16. H^1 NMR spectra of compound **14a**

100
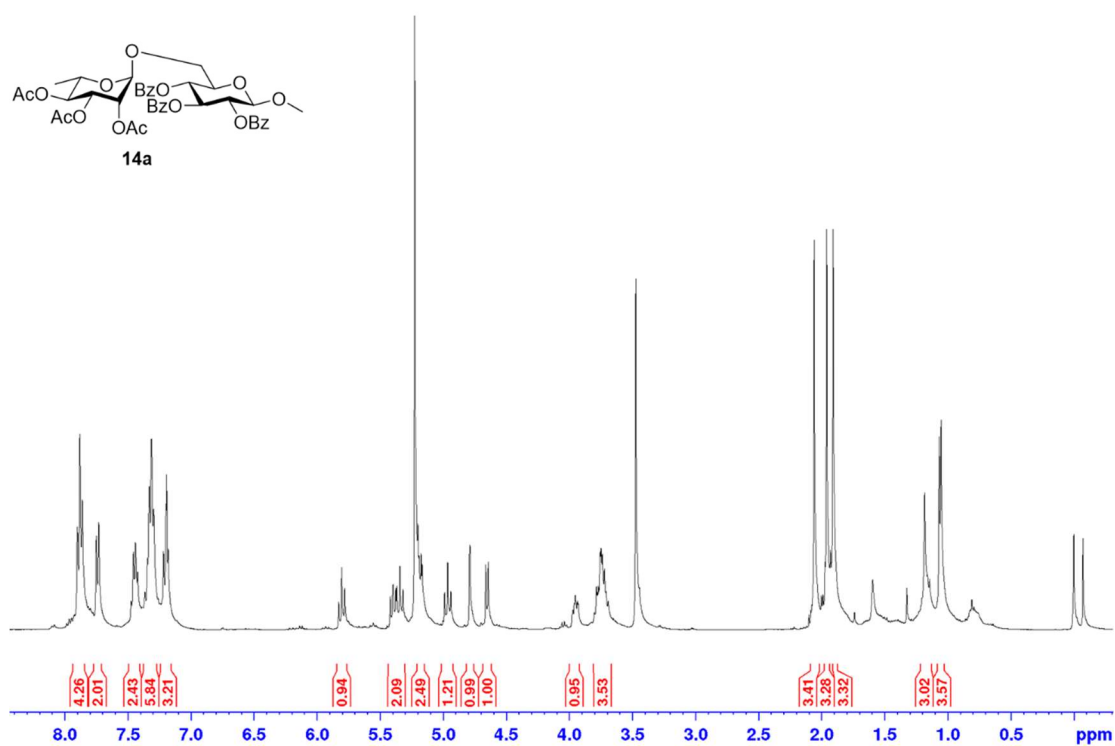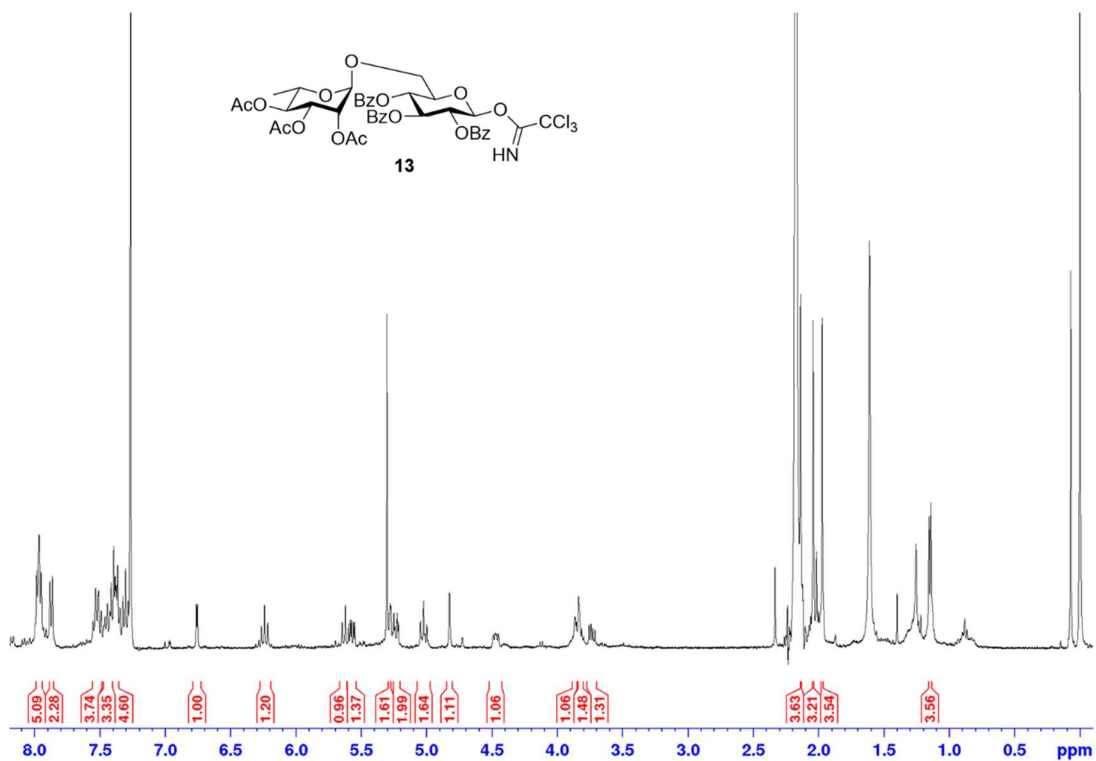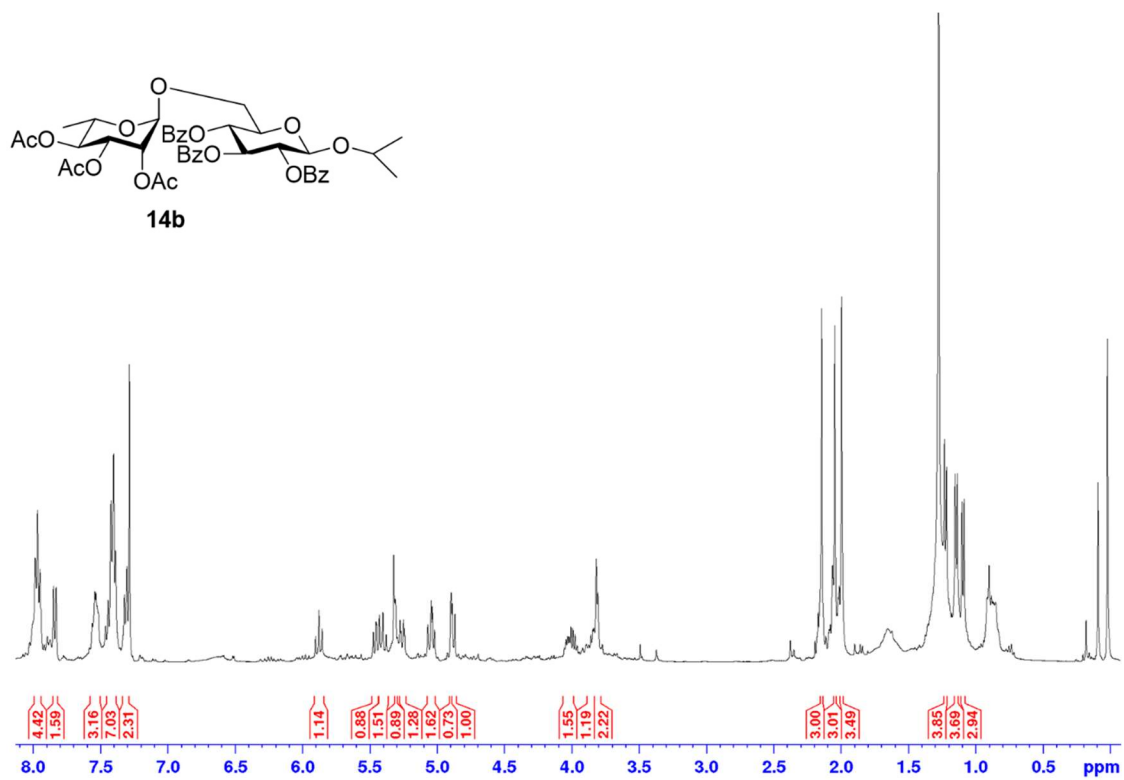
Figure 2.17. H^1 NMR spectra of compound **14b**
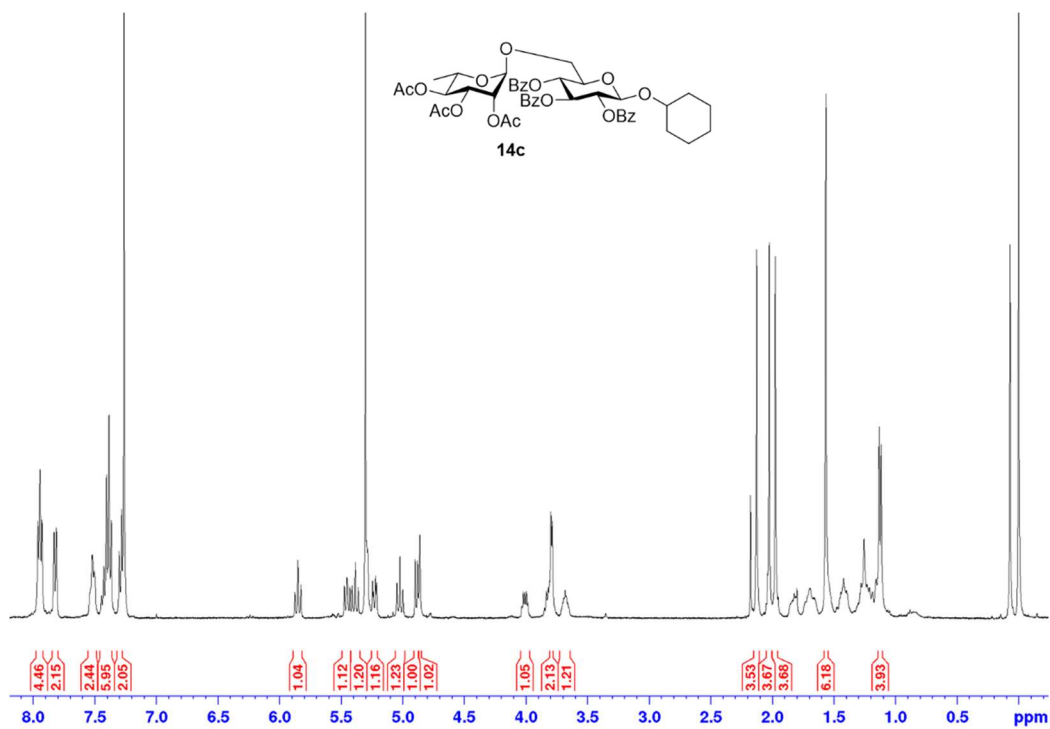
Figure 2.18. H^1 NMR spectra of compound **14c**

References

1.   Joshi, M. K. a. L., Carbohydrates in therapeutics. *Bentham Science Publishers Ltd.* **2007**.

2.   Laine, R. A., Information capacity of the carbohydrate code. *Pure and applied chemistry* **1997,** *69*.

3.   Schnaar, B. K. B. a. R. L., Cell-Surface Carbohydrates in Cell Recognition and Response. *Journal of Leukocyte biology* **1987,** *40*, 97-111.

4.   Wang, D., Carbohydrte Antigens. *Encyclopedia of Molecular Cell Biology and Molecular Medicine, 2nd Edition.* **2004**.

5.   Han Xiaoa, E. C. W., Petar Vukojicica and Carolyn R. Bertozzi, Precision glycocalyx editing as a strategy for cancer immunotherapy. *Proceedings of National academy of Sciences of United states of America* **2016,** *113*, 10304-10309.

6.   Boltje, T. J.; Buskas, T.; Boons, G. J., Opportunities and challenges in synthetic oligosaccharide and glycoconjugate research. *Nature chemistry* **2009,** *1*, 611-22.

7.   Hacker, U.; Nybakken, K.; Perrimon, N., Heparan sulphate proteoglycans: the sweet side of development. *Nature reviews. Molecular cell biology* **2005,** *6*, 530-41.

8.   Avila, J. L., α-Galactosyl-Bearing Epitopes as Potent Immunogens in Chagas' Disease and Leishmaniasis. *Subcell Biochem 1999* **1999**.

9.   Galili, U., Anti-Gal: an abundant human natural antibody of multiple pathogeneses and clinical benefits. *Immunology* **2013,** *140*, 1-11.

10.   Brito, C. R.; McKay, C. S.; Azevedo, M. A.; Santos, L. C.; Venuto, A. P.; Nunes, D. F.; D'Avila, D. A.; Rodrigues da Cunha, G. M.; Almeida, I. C.; Gazzinelli, R. T.; Galvao, L. M.;

Chiari, E.; Sanhueza, C. A.; Finn, M. G.; Marques, A. F., Virus-like Particle Display of the alpha-Gal Epitope for the Diagnostic Assessment of Chagas Disease. *ACS infectious diseases* **2016,** *2*, 917-922.

11.   Yilmaz, B.; Portugal, S.; Tran, Tuan M.; Gozzelino, R.; Ramos, S.; Gomes, J.; Regalado, A.; Cowan, Peter J.; d'Apice, Anthony J. F.; Chong, Anita S.; Doumbo, Ogobara K.; Traore, B.; Crompton, Peter D.; Silveira, H.; Soares, Miguel P., Gut Microbiota Elicits a Protective Immune Response against Malaria Transmission. *Cell* **2014,** *159*, 1277-1289.

12.   Moura, A. P. V.; Santos, L. C. B.; Brito, C. R. N.; Valencia, E.; Junqueira, C.; Filho, A. A. P.; Sant'Anna, M. R. V.; Gontijo, N. F.; Bartholomeu, D. C.; Fujiwara, R. T.; Gazzinelli, R. T.; McKay, C. S.; Sanhueza, C. A.; Finn, M. G.; Marques, A. F., Virus-like Particle Display of the alpha-Gal Carbohydrate for Vaccination against Leishmania Infection. *ACS central science* **2017,** *3*, 1026-1031.

13.   Cabezas-Cruz, A.; Mateos-Hernandez, L.; Alberdi, P.; Villar, M.; Riveau, G.; Hermann, E.; Schacht, A. M.; Khalife, J.; Correia-Neves, M.; Gortazar, C.; de la Fuente, J., Effect of blood type on anti-alpha-Gal immunity and the incidence of infectious diseases. *Experimental & molecular medicine* **2017,** *49*, e301.

14.   Hilger, C.; Fischer, J.; Wolbing, F.; Biedermann, T., Role and Mechanism of Galactose-Alpha-1,3-Galactose in the Elicitation of Delayed Anaphylactic Reactions to Red Meat. *Current allergy and asthma reports* **2019,** *19*, 3.

15.   <Carbohydrate antigen - Intro.pdf>.

16.   Wang, P. G., The synthesis of deoxy-α-Gal epitope derivatives for the evaluation of an anti-α-Gal antibody binding. *Carbohydrate Research* **2002**, 1247-1259.

17.   Kensaku Anraku, S. S., Nicholas T. Jacob, Lisa M. Eubanksa, Beverly A. Ellisa and Kim D. Janda, The design and synthesis of an α-Gal trisaccharide epitope that provides highly specific anti gal immune response.pdf. *Organic and Biomolecular chemistry* **2017**.

18.   Galili, U., Interaction of the natural anti-Gal antibody with a-galactosyl epitopes: a major obstacle for xenotransplantation in humans *Immunology today* **1993,** *14*.

19.   Huai, G.; Qi, P.; Yang, H.; Wang, Y., Characteristics of alpha-Gal epitope, anti-Gal antibody, alpha1,3 galactosyltransferase and its clinical exploitation (Review). *International journal of molecular medicine* **2016,** *37*, 11-20.

20.   URI GALILI, M. R. C., STEPHEN B. SHOHET, JOANNE BUEHLER, AND BRUCE A. MACHE, Evolutionary relationship between the natural anti-Gal antibody and the Gala1->3Gal epitope in primates. *Immunology today* **1987,** *84*, 1369-1373.

21.   Uri Galili, S. B. S., Eugenia Kobrin, Cheryl L. M. Stults, and Bruce A. Machert Man, Apes, and Old World Monkeys Differ from Other Mammals in the Expression of a-Galactosyl Epitopes on Nucleated Cells. *The Journal of Biological Chemistry* **1988,** *63*, 17755-17762.

22.   Abdel-Motal, U.; Wang, S.; Lu, S.; Wigglesworth, K.; Galili, U., Increased immunogenicity of human immunodeficiency virus gp120 engineered to express Galalpha1-3Galbeta1-4GlcNAc-R epitopes. *Journal of virology* **2006,** *80*, 6943-51.

23.   Abdel-Motal, U. M.; Wang, S.; Awad, A.; Lu, S.; Wigglesworth, K.; Galili, U., Increased immunogenicity of HIV-1 p24 and gp120 following immunization with

gp120/p24 fusion protein vaccine expressing alpha-gal epitopes. *Vaccine* **2010,** *28*, 1758-65.

24.   Galili U, M. K. T., Inhibition of anti-Gal IgG binding to porcine endothelial cells by synthetic oligosaccharides. *Transplantation* **1996,** *62*, 356-362.

25.   LaTemple, U. G. a. D. C., Natural anti-Gal antibody as a universal augmenter of autologous tumor vaccine immunogenicity *Immunology Today* **1997,** *18*.

26.   Pacheco, I.; Contreras, M.; Villar, M.; Risalde, M. A.; Alberdi, P.; Cabezas-Cruz, A.; Gortazar, C.; de la Fuente, J., Vaccination with Alpha-Gal Protects Against Mycobacterial Infection in the Zebrafish Model of Tuberculosis. *Vaccines* **2020,** *8*.

27.   Cabezas-Cruz, A.; de la Fuente, J., Immunity to alpha-Gal: The Opportunity for Malaria and Tuberculosis Control. *Frontiers in immunology* **2017,** *8*, 1733.

28.   Commins, S. P.; Platts-Mills, T. A., Delayed anaphylaxis to red meat in patients with IgE specific for galactose alpha-1,3-galactose (alpha-gal). *Current allergy and asthma reports* **2013,** *13*, 72-7.

29.   Steinke, J. W.; Platts-Mills, T. A.; Commins, S. P., The alpha-gal story: lessons learned from connecting the dots. *The Journal of allergy and clinical immunology* **2015,** *135*, 589-96; quiz 597.

30.   Wilson, J. M.; Platts-Mills, T. A. E., alpha-Gal and other recent findings that have informed our understanding of anaphylaxis. *Annals of allergy, asthma & immunology : official publication of the American College of Allergy, Asthma, & Immunology* **2020,** *124*, 135-142.

31.   Deak, P. E.; , B. K.; , A. A. Q.; , J. S.; , G. V.; , K. M. K.; Matthew J. Turner, N. S.; , W. G. S.; , T. K.; , M. H. K.; , a. B. B., Designer covalent heterobivalent inhibitors prevent IgE dependent responses to peanut allergen. *Proc. Natl. Acad. Sci. U. S. A.* **2019,** *116*, 8966–8974.

32.   Deak, P. E.; Kim, B.; Koh, B.; Qayum, A. A.; Kiziltepe, T.; Kaplan, M. H.; Bilgicer, B., Covalent Heterobivalent Inhibitor Design for Inhibition of IgE-Dependent Penicillin Allergy in a Murine Model. *J Immunol* **2019,** *203*, 21-30.

33.   Boons, G.-J., Preparation of Fluorinated galctosyl nucleoside diphosphates to study the mechanism of the enzyme galactopyranose mutase. *Journal of Chemical Society, Perkin Trans.* **1997**.

34.   Johannes, M.; Reindl, M.; Gerlitzki, B.; Schmitt, E.; Hoffmann-Roder, A., Synthesis and biological evaluation of a novel MUC1 glycopeptide conjugate vaccine candidate comprising a 4'-deoxy-4'-fluoro-Thomsen-Friedenreich epitope. *Beilstein journal of organic chemistry* **2015,** *11*, 155-161.

35.   Wang, Y.; Yan, Q.; Wu, J.; Zhang, L.-H.; Ye, X.-S., A new one-pot synthesis of α-Gal epitope derivatives involved in the hyperacute rejection response in xenotransplantation. *Tetrahedron* **2005,** *61*, 4313-4321.

36.   Card, P. J., Synthesis of Fluorinated Carbohydrates. *Journal of Carbohydrate Chemistry* **2007,** *4*, 451-487.

37.   Dong, H., Efficient Carbohydrate Synthesis by Controlled inversion strategies. **2006**, 46.

38.   Hai Dong, Z. P., and Olof Ramstro¨m*, Stereospecific Ester Activation in nitrite mediated carbohydrate in epimerization. *The Journal of Organic Chemistry* **2006**.

39.   Hai Dong, Z. P., Marcus Angelin, Styrbjo¨rn Bystro and Olof Ramstro, Efficient Synthesis of â-D-Mannosides and â-D-Talosides by Double parallel or double serial inversion. **2006**.

40.   Gucchait, A.; Ghosh, A.; Misra, A. K., Convergent synthesis of the pentasaccharide repeating unit of the biofilms produced by Klebsiella pneumoniae. *Beilstein journal of organic chemistry* **2019,** *15*, 431-436.

41.   Janssens, J.; Risseeuw, M.; Van der Eycken, J.; Calenbergh, S., Regioselective Ring Opening of 1,3-Dioxane-Type Acetals in Carbohydrates. *European Journal of Organic Chemistry* **2018**.

42.   Po-Chiao Lin, A. K. A., Shau-Hua Ueng, Li-De Huang, Kuo-Ting Huang, Ja-an Annie Ho, and Chun-Cheng Lin, DAST-Mediated Regioselective Anomeric Group Migration in Saccharides. *Journal of Organic Chemistry* **2009**.

43.   Misra, A.; Sau, A., Odorless Eco-Friendly Synthesis of Thio- and Selenoglycosides in Ionic Liquid. *Synlett* **2011,** *2011*, 1905-1911.

44.   Richtmyer, A. L. C. a. N. K., Aryl Thioglycopyranosides, Aryl Glycopyranosyl Sulfones, and the Novel Oxidation-Acetylation of Aryl 1 -Thio-β-D-glucopyranosides to 6-0-Acetyl-β-D-glucopyranosyl Aryl Sulfones. *The Journal of Organic Chemistry* **1964,** *29*, 1782–1787.

45.   Bevan, J. G. M.; Lourenço, E. C.; Chaves-Ferreira, M.; Rodrigues, J. A.; Rita Ventura, M., Immobilization of UDP-Galactose on an Amphiphilic Resin. *European Journal of Organic Chemistry* **2018,** *2018*, 908-914.

46.   Chang, C. W.; Wu, C. H.; Lin, M. H.; Liao, P. H.; Chang, C. C.; Chuang, H. H.; Lin, S. C.; Lam, S.; Verma, V. P.; Hsu, C. P.; Wang, C. C., Establishment of Guidelines for the Control of Glycosylation Reactions and Intermediates by Quantitative Assessment of Reactivity. *Angew Chem Int Ed Engl* **2019,** *58*, 16775-16779.

47.   Liao, G.; Burgula, S.; Zhou, Z.; Guo, Z., A Convergent Synthesis of 6-O-Branched beta-Glucan Oligosaccharides. *European J Org Chem* **2015,** *2015*, 2942-2951.

48.   Xiong, C.; Feng, S.; Qiao, Y.; Guo, Z.; Gu, G., Synthesis and Immunological Studies of Oligosaccharides that Consist of the Repeating Unit of Streptococcus pneumoniae Serotype 3 Capsular Polysaccharide. *Chemistry* **2018,** *24*, 8205-8216.

49.   Chen, J.-H.; Ruei, J.-H.; Mong, K.-K. T., Iterative α-Glycosylation Strategy for 2-Deoxy- and 2,6-Dideoxysugars: Application to the One-Pot Synthesis of Deoxysugar-Containing Oligosaccharides. *European Journal of Organic Chemistry* **2014,** *2014*, 1827-1831.

50.   Chun-Cheng Lma , T.-S. H., Kuo-Cheng Lua and I-Ting Huanga, Synthesis of ß-D-Glucopyranosyl(1->3)-1-thiol-ß-glucosamine Disaccharide Derivative as Building Block for the Synthesis of Hyaluronic Acid *Journal of Chinese Chemical Society* **2000,** *47*, 921-928.

51.   Degenstein, J. C.; Murria, P.; Easton, M.; Sheng, H.; Hurt, M.; Dow, A. R.; Gao, J.; Nash, J. J.; Agrawal, R.; Delgass, W. N.; Ribeiro, F. H.; Kenttamaa, H. I., Fast pyrolysis of

13C-labeled cellobioses: gaining insights into the mechanisms of fast pyrolysis of carbohydrates. *J Org Chem* **2015,** *80*, 1909-14.

52.   Chun-Cheng Lma, T.-S. H., Kuo-Cheng Lua and I-Ting Huanga, Synthesis of ß-D-Glucopyranosyl(1->3)-1-thiol-ß-glucosamine Disaccharide Derivative as Building Block for the Synthesis of Hyaluronic Acid *Journal of chinese chemical society* **2000,** *47*, 921-928.

53.   Huang, C.-M.; Liu, R.-S.; Wu, T.-S.; Cheng, W.-C., Structural establishment of polygalatenosides A and B by total synthesis. *Tetrahedron Letters* **2008,** *49*, 2895-2898.

54.   McGill, N. W.; Williams, S. J., 2,6-Disubstituted benzoates as neighboring groups for enhanced diastereoselectivity in beta-galactosylation reactions: synthesis of beta-1,3-linked oligogalactosides related to arabinogalactan proteins. *J Org Chem* **2009,** *74*, 9388-98.

55.   Varki, A. C., R.; Esko, J.; Freeze, H.; Stanley, P.; Bertozzi, C.; Hart, G.; Etzler, M. , Essentials of Glycobiology. **2009**.

56.   Ezequiel Q. Morales, J. I. P., Mar Trujillo, and Jesus T. VBzquez, CD and lH NMR Study of the Rotational Population Dependence of the Hydroxymethyl Group in /3 Glucopyranosides on the Aglycon and Its Absolute Configuration. *Journal of Organic Chemistry* **1995,** *60*, 2537-2548.

57.   Juan I. Padro, E. Q. M., and Jesu´ s T. Va´zquez, Alkyl Galactopyranosides: Rotational Population Dependence of the Hydroxymethyl Group on the Aglycon and Its Absolute Configuration and on the Anomeric Configuration. *Journal of Organic Chemistry* **1998,** *63*.

58.   Padron, J. I. V., J. T, Rotational Population Dependences of the Hydroxymethyl Group in Alkyl Glucopyranosides: Anomers Comparison. *Chirality* **1997,** *9*, 626-637.

59.   Karplus, M., Vicinal Proton Coupling in Nuclear Magnetic Resonance'. *Journal of American chemical Society* **1963,** *85*, 2870-2871.

60.   Bubb, W. A., NMR spectroscopy in the study of carbohydrates: Characterizing the structural complexity. *Concepts in Magnetic Resonance* **2003,** *19A*, 1-19.

61.   M., K., *Journal of Chemical Physics 159*, 11.

62.   P.C. MANOR , W. S., D.B. DAVIES , K. JANKOWSKI and A. RABCZENKO CONFORMATION OF NUCLEOSIDES: THE COMPARISON OF AN X-RAY DIFFRACTION AND PROTON NMR STUDY OF 5 ',2-O-CYCLO, 2 ',3'-O-ISOPROPYLIDENE URIDINE *Biochimica et Biophysica Acta* **1974,** *340*, 472-483.

63.   C. A. G. HAASNOOT, F. A. A. M. D. L. a. C. A., THE RELATIONSHIP BETWEEN PROTON-PROTON NMR COUPLING CONSTANTS AND SUBSTITUENT ELECTRONEGATIVITIES-I AN EMPIRICAL GENERALIZATION OF THE KARPLUS EQUATION? *Tetrahedron* **1983,** *36*, 2783-2792.

64.   Nishida, Y.; Hori, H.; Ohrui, H.; Meguro, H., 1H NMR Analyses of Rotameric Distribution of C5-C6 bonds of D-Glucopyranoses in Solution. *Journal of Carbohydrate Chemistry* **1988,** *7*, 239-250.

65.   Roland Stenutz, I. C., Go¨ran Widmalm, and Anthony S. Serianni, Hydroxymethyl Group Conformation in Saccharides: Structural Dependencies of $^{2}J_HH$, $^{3}J_HH$, and $^{1}J_CH$ Spin-Spin Coupling Constants. *Journal Of organic chemistry* **2002,** *67*, 949-958.

66.   Christophe Thibaudeau, R. S., Brian Hertz, Thomas Klepach, Shikai Zhao, Qingquan Wu, Ian Carmichael, and Anthony S. Serianni, Correlated C-C and C-O Bond Conformations in Saccharide Hydroxymethyl Groups: Parametrization and Application of Redundant 1H-1H, 13C-1H, and 13C-13C NMR J-Couplings. *Journal of American Chemical Society* **2004,** *126*, 15668-15685.

67.   Patel, D. S.; Pendrill, R.; Mallajosyula, S. S.; Widmalm, G.; MacKerell, A. D., Jr., Conformational properties of alpha- or beta-(1-->6)-linked oligosaccharides: Hamiltonian replica exchange MD simulations and NMR experiments. *The journal of physical chemistry. B* **2014,** *118*, 2851-71.

68.   VAZQUEZ, J. I. P. A. J. T., Rotational Population Dependences of the Hydroxymethyl Group in Alkyl Glucopyranosides: Anomers Comparison. *Chirality* **1997,** *9*, 626-637.

69.   Mayato, C.; Dorta, R.; Vázquez, J., Experimental evidence on the hydroxymethyl group conformation in alkyl β-d-mannopyranosides. *Tetrahedron: Asymmetry* **2004,** *15*, 2385-2397.

70.   Sanhueza, C. A.; Dorta, R. L.; Vázquez, J. T., Conformational properties of glucosyl-thioglucosides and their S-oxides in solution. *Tetrahedron: Asymmetry* **2013,** *24*, 582-593.

71.   Nishio, M., The CH/pi hydrogen bond in chemistry. Conformation, supramolecules, optical resolution and interactions involving carbohydrates. *Physical chemistry chemical physics : PCCP* **2011,** *13*, 13873-900.

72.   Spiwok, V., CH/pi Interactions in Carbohydrate Recognition. *Molecules* **2017,** *22*.

73.	Janiak, C., A critical account on $\pi-\pi$ stacking in metal complexes with aromatic nitrogen-containing ligands. *Journal of Chemical Society, Dalton Transaction* **2000**, 3885-3896.

74.	Grayson, E. J.; Bernardes, G. J.; Chalker, J. M.; Boutureira, O.; Koeppe, J. R.; Davis, B. G., A coordinated synthesis and conjugation strategy for the preparation of homogeneous glycoconjugate vaccine candidates. *Angew Chem Int Ed Engl* **2011,** *50*, 4127-32.

75.	Donahue, M. G.; Johnston, J. N., Preparation of a protected phosphoramidon precursor via an H-phosphonate coupling strategy. *Bioorg Med Chem Lett* **2006,** *16*, 5602-4.

76.	Caridad Fernández, O. N., José Angel Fontenla, Emilia Rivas, María L. de Ceballos and Alfonso Fernández-Mayoralas, Synthesis of glycosyl derivatives as dopamine prodrugs: interaction with glucose carrier GLUT-1. *Org. Biomol. Chem.* **2003,** *1*, 767-771.

77.	PETER FUGEDI, W. B., PER J. GAREOC, AND AKE PILOT, SYNTHESIS OF A BRANCHED HEPTASACCHARIDE HAVING PHYTOALEXIN-ELICITOR ACTIVITY. *Carbohydrate Research* **1986,** *164* 297 -312.

VITA

Name	*Dhwani Ashish Mehta*
High School	*Shri Tikamdas Purushottaman Bhatia College of Science, Mumbai, India*
Date Graduated	*May 2014*
Baccalaureate Degree	*SVKM's Dr. Bhanuben Nanavati College of Pharmacy, Mumbai, India*
Date Graduated	*June 2018*